Abstract

YITBAREK, EMNET. Characterization and Analytical Applications of Dye-encapsulated Zwitterionic Liposomes. (Under the direction of Morteza G. Khaledi.)

The aim of this project was to use marker encapsulated liposomes as biomembrane mimicking entities in order to study membrane properties like permeability and to better understand the interaction of biological lipid bilayers with membrane-active molecules, like beta blocker drugs and antimicrobial peptides (AMP). The physical characteristics of liposomes, such as size, surface charge and encapsulation capacity were also studied using electrophoretic, fluorescence and light scattering techniques. In addition, marker-encapsulated and self-lysing liposomes were used to study antigen-antibody binding. The immunoassay application of these self-lysing liposomes was also investigated.

The first area of research is focused on investigating the effect of the liposome lipid composition on the size and the electrical properties of zwitterionic liposomes. The cholesterol composition of phosphatidylcholine (PC) and sphingomyelin (Sph) liposomes is varied and the effect on their size, zeta potential and electrophoretic mobility is monitored using dynamic light scattering (DLS), laser doppler velocimetry (LDV), and capillary zone electrophoresis (CZE) techniques, respectively. In addition, the permeability and the encapsulation capacity of large unilamellar vesicles (LUV), or liposomes that are made by extrusion, were compared as their lipid and cholesterol composition varied. The size and electrophoretic mobility of zwitterionic liposomes was found to increase with the cholesterol composition.

The interaction of indolicidin, a 13-mer cationic AMP, with (dye-encapsulated) liposomes that were made of different lipid and cholesterol composition was investigated by DLS, fluorescence and capillary electrophoresis (CE) methods. DLS results show a change in liposome size, and size distribution index (PI), after indolicidin interaction. Fluorescence leakage experiments show the extent of membrane perturbation caused by the AMP and the AMP's innate tryptophan fluorescence provided qualitative information regarding the type (polar/non-polar) and nature of the liposome-AMP interaction, as lipid composition of the liposomes varied. In addition, CZE and liposome electrokinetic chromatography (LEKC) techniques were also used to further probe the (polar/non-polar/electrostatic) nature of this interaction.

The immunoassay application of the marker encapsulated liposomes was investigated using a combination of fluorescence, DLS, and CE-LIF (capillary electrophoresis with laser induced fluorescence detector) techniques. The liposomes were made from a non-lamellar lipid DOPE (dioleoylphosphatidylethanolamine) that was stabilized with a 20% bilayer lipid DPPC (dipalmitoylphosphatidylcholine) and a 1% hapten-attached DPPE lipid. Small hapten molecules, like biotin and DNP (dinitrophenyl), were attached to the liposome surface via the DPPE lipid, and used to detect their conjugate molecules (avidin and anti-DNP antibody) in a homogeneous solution. The biotin-attached DOPE liposomes aggregate and leaked their marker content in standard avidin solution. The extent of liposome aggregation and the fluorescence intensity of the leaked dye are dependent on the concentration of avidin present in solution. The different parameters that affect the quality of the assay were also investigated.

Characterization and Analytical Applications of Dye-encapsulated Zwitterionic Liposomes

by
Emnet Yitbarek

A dissertation submitted to the Graduate Faculty of
North Carolina State University
in partial fulfillment of the
requirements for the Degree of
Doctor of Philosophy

Chemistry

Raleigh, North Carolina
2010

APPROVED BY:

_____	_____
Edmond F. Bowden	Tatyana I. Smirnova
_____	_____
Alexander A. Nevzorov	Morteza G. Khaledi Chair of Advisory Committee

Dedication

This dissertation is dedicated to my mother, Letebrhan Asfaw.
Your faith in God, hard work, independence and perseverance has been an inspiration in my life. You made me who I am today and I owe it all to you, mom. I love you so much.

Biography

The author, Emnet Yitbarek, was born and raised in Addis Ababa (Ethiopia). After high school, Emnet joined the chemistry department at Addis Ababa University and graduated with a BS in 1989. Following graduation, Emnet worked at the Ethiopian Geological Survey for six years and immigrated to the United States in 1995. After a year in Washington DC area, Emnet joined the chemistry graduate program at North Carolina A&T University and graduated with MS in analytical chemistry in 1998. Subsequent to the master's degree, Emnet Perused a PhD in analytical chemistry at North Carolina State University under the direction of Dr. Morteza G. Khaledi.

Acknowledgments

There are many people I would like to thank who have helped me in different ways during my graduate school years. But first and foremost, all credit and acknowledgment goes to my mother who has encouraged me to strive for higher goals, in addition to providing my different wants and needs. She had always put her children before anything, even herself. The constant motivation and support from my family has been the big factor that allowed me to pursue my curiosity in science and research.

I am very grateful to Dr. Morteza G. Khaledi for his guidance, encouragement and enduring support. I also thank the following current and former group members of the Khaledi group: Dr. Scott Burns, Dr. Hai Bui, Dr. Jason Barker, Dr. Jennifer Carrozino, Dr. Ceixiong Fu, Yang Shen, Suzy Yeh, Juan Pablo Mack, Chris Collins, and Sam Jenkins. A special thank you goes to Dr. Hai Bui for his great friendship and Sam Jenkins for his comradeship and assistance in editing most of this thesis.

Last, but not least, I would like to thank my lovely wife, Ariam Gebrehiwot. Your solid support has enabled me to focus and finish up successfully during the year of this process. One of the best things I done in life was marrying you. I am lucky to have a life partner in you.

Table of Contents

List of Tables

Chapter 1

Chapter 2

Chapter 3

Chapter 4

Chapter 5

List of Figures

Chapter 2

Chapter 4

Chapter 5

List of symbols, abbreviations, and terms

AMP ..... antimicrobial peptides

PC ..... phosphatidylcholine

Sph ..... sphingomyelin

DLS ..... dynamic light scattering

LDV ..... laser doppler velocimetry

CE ..... capillary electrophoresis

CZE ..... capillary zone electrophoresis

PI .....polydispersity index

LEKC ..... liposome electrokinetic chromatography

CE-LIF .... capillary electrophoresis with laser induced fluorescence detector

DOPE ..... dioleoylphosphatidylethanolamine

DPPC ..... dipalmitoylphosphatidylcholine

DPPE ..... dipalmitoylphosphatidylethanolamine

DNP ..... dinitrophenyl

DMPG .....Dimyristoylphosphatidylglycerol

PE..... phosphatidylethanolamine

PG ..... phosphatidylglycerol

SEC ..... size exclusion chromatography

SQF ..... self quenched fluorescence

CF ..... carboxyfluorescein

CV ..... capture volume

ELISA ..... enzyme-linked immunosorbant assay

DPPG ..... dipalmitoylphosphatidylglycerol

Trp ..... tryptophan

DMPC ..... Dimyristoylphosphatidylcholine

Indo ..... Indolicidin
MLV ..... multi lamellar vesicle
LUV ..... large unilamellar vesicles
Rh-PE ..... Rhodamine-phosphatidylethanolamine
EDL ..... electrical double layer
DSPC ..... distearoylphosphatidylcholine
ZP ..... zeta potential
EOF ..... electro-osmotic flow
SUV .....small unilamellar vesicles
GUV ..... giant unilamellar vesicles
FAT ..... freezing and thawing
CPP ..... critical packing parameter

Chapter 1

Introduction

Liposome characterization and analytical applications

Liposomes were discovered by A. Bangham [1] about 40 years ago and since then they have became very versatile tools in biology, biochemistry and medicine. Liposomes are small (30 nm-5 um) artificial vesicles of spherical shape surrounding an aqueous pool, which are made of natural non-toxic phospholipids and cholesterol. When amphiphilic phospholipids are dispersed in aqueous solutions they spontaneously form vesicular structures due to a hydrophobic effect. These spontaneously formed vesicles have multiple layers (multi-lamellar) like onions surrounding an interior aqueous pool. The application of some form of energy, sonication or high-pressure extrusion, would peel-off the layers and form unilamellar vesicles or liposomes [2]. The lipid bilayer structure and composition of liposomes is similar to biological cell membranes. Due to their resemblance to natural membranes and their non-toxic nature, liposomes have been used as in-vitro models for cell membranes, as drug delivery systems (DDS), and for signal amplification in immunoassay applications. The success of liposomes as drug carriers has been reflected in a number of liposome-based drug formulations that are commercially available and new formulations that are undergoing clinical trials [3]. Chemo therapy drugs like Doxil are encapsulated in liposomes to enhance their efficacy and reduce side effects when used to treat a wide range of cancer ailments including breast cancer [4]. These drug molecules are more easily transported through biological

membranes after they are encapsulated either in the liposome's aqueous interior or in the lipid bilayer milieu. Generally, polar compounds are encapsulated in the liposome aqueous interior, while non-polar solutes are incorporated in the lipid bilayer. Similarly, great results have been achieved in the last two decades in the area of gene delivery and cellular/tissue imaging using amphiphilic lipid mixtures, both in vivo and in-vitro [5]. Liposomes have also found wide applications in biosensors and flow based bio-analytical assays, due to their relatively large internal volume (marker encapsulation) and the ability to modify their outer-membrane with various bio-recognition elements [5;6].

Biological membranes are vital components of all living systems, forming the outer boundary of living cells and internal cell compartments (organelles). They largely consist of a lipid bilayer, which imparts the fluidic character and houses membrane proteins, receptors and other bio-molecules that facilitate communication and transport across the membrane. These features enable membranes to act as important filters keeping toxins out of the cell, but allowing nutrients and other useful metabolites to pass through to reach their cellular destination. In addition, many important biological processes are regulated at membrane surfaces, through interactions between peripheral and integral membrane proteins. The complexity of biological membranes and their interactions with intra- and extra-cellular networks make direct investigations difficult. For this reason, artificial model membranes have played an important role in unraveling the physical and chemical characteristics of biological membranes and how these contribute to permeability and other related cellular functions. The physical properties

of the phospholipid bilayer membrane in liposomes separating two aqueous phases have proven to be strikingly similar to the corresponding properties of natural membranes. So, liposomes are used as model membrane systems to study the relation between the lipid composition of natural membranes and some of the characteristics they exhibit due to their composition [1;7].

Zwitterionic lipids like, Phosphatidylcholine (PC), phosphatidylethanolamine (PE) and Sphingomyelin (Sph), together with cholesterol (Ch), constitute the major parts of many biological membranes. For example, Myelin is a lipoprotein tissue common in the human brain and is mainly composed of lipids, more than 80% by weight, as shown on table 1-1 below. Cholesterol and the zwitterionic lipids (PE, PC, Sph) constitute 75% of the total lipid in Myelin [8]. Artificial membranes like liposomes that are rich in these lipids are used to study how Multiple Sclerosis (MS), which is a severe neurological disorder, damages the lipid organization of the myelin in the brain [9-11]. In addition, high doses of steroidal drugs that treat MS have been encapsulated in liposomes to enhance therapeutic efficacy and reduce their adverse side effects [12].

Table 1-1 Lipid composition of normal brain myelin, as detected by HPLC.	
Lipid	Mass %
Cholesterol (CH) - neutral	31.9
Phosphatidylethanolamine (PE) - zwitterionic	19.2
Phosphatidylcholine (PC) - zwitterionic	14.4
Hydroxy-Galactocerebroside	10.8
Sphingomyelin (Sph) - zwitterionic	10.2
Cerebroside sulfates	6.7
Non-hydroxy Galactocerebroside	4
Phosphatidylserine (PS) - anionic	1.5
Phosphatidylinositol (PI) - anionic	trace

Zwitterionic lipids like phosphatidycholine (PC) and charged phosphatidylglycerols (PG) can be used alone or in combination with cholesterol and various other lipophilic compounds to form stable liposomes that can be used for different applications. The physical characteristics of a liposome formulation are highly influenced by its lipid composition and the preparation method. In addition to lipids, different compounds can be incorporated either inside the liposome interior or the lipid bilayer membrane. Long acyl chain phospholipids (usually C14 and above) with different head groups are mixed at certain ratios to custom design liposomes for a variety of applications with desired size, membrane property, surface moieties and charge.

There are many ways of preparing unilamellar vesicles, but sonication and extrusion are the two most widely used methods. Probe or bath sonication of

multilamellar vesicles typically produces large unilamellar vesicles with a very polydispersed size distribution, in less than five minutes. The extrusion method may take 20-30 minutes but it produces fairly homogeneous large unilamellar liposomes with a narrow size distribution. In both methods the lipids are first dissolved in neat chloroform or a cocktail of volatile organic solvents, which subsequently is removed under vacuum evaporation leaving a uniform thin lipid film on the inner flask surface. Then the dry lipid mix is hydrated with a buffer solution containing other hydrophilic solutes to be encapsulated inside the liposomes' aqueous interior. The resulting large multilamellar vesicles can either be sonicated or extruded to form smaller unilamellar vesicles. Probe sonication delivers more power than bath sonication leading to a more rapid size reduction. But unfortunately both sonication methods produce non-uniform liposomes with a wide size distribution. Extrusion of the multilamellar vesicles through a polycarbonate filter under high nitrogen pressure produces large liposomes with a more uniform size distribution [2;13;14].

The physical characterization of liposomes is of great importance to identify their suitability for a specific purpose from a variety of applications. In addition, liposome characterization also helps to better understand real biological membranes, as noted earlier. Depending on their composition and mode of preparation, liposomes show wide variability in their physical and chemical characteristics. Such characteristics include: size, size-distribution, membrane lamellarity, surface charge, permeability, and encapsulation volume. These characteristics can be studied using different techniques including microscopy, spectroscopy, chromatography, electrophoresis and

light scattering, among others. The liposomes' size is somewhat controlled by its lipid composition and the method of preparation, while their membrane surface charge is imparted from the charge of the lipid head-groups. The liposome size and size-distribution parameters are usually determined by dynamic light scattering techniques (DLS). The extrusion of an MLV suspension through double-stacked 100 nm membranes usually results in uniform LUVs with an average size of 100±20 nm and a low polydispersity index of 0.1 or less, as measured by a DLS technique [13]. The polydispersity index (PI) indicates how homogeneous the (average) size distribution of a liposome preparation is, and it is derived from the logarithmic convolution of the repeated scans of the scattered light measured [15]. Separation techniques like size exclusion chromatography (SEC) and capillary electrophoresis (CE) have also been used to fractionate liposomes based on their size. CE separates liposomes based on their charge-to-size ratio and the findings from CE, and other chromatographic methods, can be utilized to supplement the data from a DLS technique. Overall, CE is a better method, than SEC for size fractionation study since it has higher resolution with significantly smaller size requirement and sample consumption. So, we used CE, together with DLS, to characterize liposomes made by extrusion from cholesterol and zwitterionic phospholipids.

The permeability and entrapment capability of liposomes is usually studied from the fluorescence measurement of the quenched dye encapsulated inside the aqueous compartment. The Self Quenched Fluorescence (SQF) technique is commonly used in this type of characterization studies. In the SQF method, a hydrophilic marker like carboxyfluorescein (CF) is dissolved

at high concentration (about 100 mM) and entrapped inside the liposome aqueous interior during the liposome preparation [16]. The fluorescence signal from the CF at high concentrations is significantly self-quenched. The self-quenching mechanism is not clearly understood, however, the fluorescence signal increases dramatically as the entrapped CF is leaked out of liposomes (with time or as a result of physical and chemical perturbations) and subsequently diluted in the external bulk aqueous solution. The change in fluorescence signal can be used to assess the membrane permeability. Interactions of certain solutes such as some drugs or antimicrobial peptides could reduce the stability and/or change the permeability of the bilayer membrane. The extent of the leakage from an encapsulated liposome due to contact with a certain solute is determined from the relative fluorescence (%F) of the leaked marker and is calculated by

$$F = \left\lceil \frac{F_t - F_0}{F_\infty - F_0} \right\rfloor \text{X } 100\%$$

Equation (1)

F_t – Fluorescence of liposomes after incubation with solute

F_0 – Initial fluorescence due to dilution in an isomolar buffer

F_∞ – Maximal fluorescence after lysis by Triton X-100

The above equation shows that if a solute has a strong interaction with the liposome membrane then it causes an extended structural perturbation, which is measurable and the value can be used as an index to compare the membrane affinity of a group of solutes. The perturbation increases the

fluorescence intensity of the leaking dye and this increase is expected to be dependent on the concentration and nature of the solute.

It is necessary to optimize the characteristics of a liposome including its captured volume, and the retention of the entrapped material, in order to maximize the payload of a liposome formulation. These important characteristics are affected by the lipid composition and size of a liposome and they can be determined using the SQF method [16]. The encapsulated volume and efficiency are both related to the concentration of the marker trapped inside the liposome's aqueous compartment. But, the measurement of these parameters using the SQF method can be unreliable and inconsistent due to the osmotic pressure encountered as the quenched dye is encapsulated at high concentration inside the liposome. In this part of our project, liposomes are encapsulated with carboxyfluorescein at much lower concentration (<10μM) than the SQF method, and the captured (or encapsulation) volume is measured more accurately by a CE-LIF than the conventional fluorescence technique. The liposome and capture volume (V_c) is the amount of aqueous volume entrapped per amount of lipid used to make the liposome; usually expressed in units of liter per mole of lipid (L/mole) [17]. The encapsulation capacity of unilamellar liposomes, with different lipid composition, is compared from the fluorescence measurement of their encapsulated dye.

Liposomes have exhibited a potential for signal enhancement and higher sensitivities when used in immunodiagnostic applications [18]. Liposomes provide a large interior volume to encapsulate thousands of marker molecules and an outer membrane surface that offers a site to attach a large

number of ligands (antigens or antibodies). These marker-encapsulated liposomes with surface antigens are called immunoliposomes and have been used to detect the conjugate antibodies in both homogeneous and heterogeneous assay formats [6;19]. In particular, immunoliposomes that lyse upon interaction with a specific analyte then release their entrapped marker stoichiometrically are the basis for our study here. These immuno-lysis liposomes have been found to provide simple, fast and inexpensive assays with a comparable or better sensitivity for some analytes than the established techniques, like ELISA [20;21]. The liposomes that we used in our self-lysis immuno assay are similar to the (antibody) contact sensitive liposomes used by the Huang group to detect anti-theophylline and other antibodies [22;23]. The major lipid component of these liposomes is phosphatidylcholine (PC), and a small percentage (< 2 mol %) of analyte targeting molecule is also linked to the lipid head group. In homogeneous assays, the analyte in the sample forms an immuno-complex with the targeting molecule on the liposome surface and activates an attack by exogenously added complement (or other) lytic agent causing a stoichiometric marker leak from immuno-complexed liposomes [24;25]. In order to circumvent the requirement for an exogenously added membrane lytic agent, Huang & Ho used liposomes that are mostly made up of phosphatidylethanolamine (PE), which is non-bilayer phase forming lipid, together with a stabilizer lipid and a targeting molecule [22]. These PE-liposomes first aggregate then undergo a non-bilayer transition followed by content leakage when they bind to a multivalent ligand, without a need for an external lytic agent. The major component (70-90%) in Huang's contact

sensitive liposomes is the hexagonal phase forming lipid dioleoylphosphatidylethanolamine (DOPE), which is induced into forming stable liposomes due to the presence of a stabilizer lipid like DPPG, at 10-30 mole%. The packing structure of the DOPE-DPPG lipid mix allows for the formation of a stable liposome that can encapsulate marker molecules inside the aqueous compartment and link the targeting molecule, like an antigen, on its outer membrane surface (< 2%). When these antigen- attached DOPE liposomes are incubated with the antibody of interest, apposing membranes come in contact due to the cross linking multivalent antibody and they are induced into forming non-bilayer lipid structures. It is this non-bilayer structure, usually a hexagonal H2 structure, that eventually leads to the liposomes' destabilization, followed by an antibody dose dependent leakage of the encapsulated marker [22;26].

In our study DOPE is mixed with DPPC to form stable, dye-encapsulating liposomes at neutral pH and ambient temperature conditions. A biotin-attached lipid (biotin-cap-DPPE) is added at < 1% to the DOPE and PC lipid mix, as a targeting molecule, for the analysis of avidin in free solution using quantitative spectrofluorometric and CE-LIF techniques. Similarly, dinitrophenol (DNP) attached liposomes are used to detect anti-DNP antibodies in solution using the same experimental and assay conditions as the biotin analysis. In addition, a dynamic light lcattering (DLS) technique is used to monitor the liposomes' average size and size-distribution before and after their incubation with the analytes (avidin and anti-DNP).

Interaction of lipid membranes with peptides plays a very important role in cellular signaling and membrane functions. These interactions are usually

studied by using artificial lipid bilayers like liposomes. Similarly, liposomes have also been used to study the effect of short antimicrobial peptides (AMPs) on mammalian and microbial lipid membranes. The lipid composition of liposomes can be varied to mimic the surface charge and morphology of both bacterial and mammalian membranes. The membrane disrupting mechanism of AMPs and how differences in their amino acid composition affects their action is best understood from experiments using artificial membranes [27]. In addition, a thorough understanding of membrane-peptide interactions can also help design peptide antibiotic drugs that are more effective than conventional antibiotic drugs. These types of peptide antibiotics should have high specificity and potency toward bacterial (prokaryotic) membranes, without disrupting the host mammalian (eukaryotic) membranes. Hopefully in the near future, AMPs will become one of the novel classes of antibiotics that overcome the ever spreading (antibiotic) drug resistance problem worldwide. Accordingly, it is important to devise sensitive techniques to probe and better understand peptide-membrane and other related interfacial membrane interactions. Different analytical techniques have been used to study the interaction between AMPs and artificial lipid bilayers, like liposomes. From these studies, it's been observed that the peptide may affect some of the physical and structural characteristics of the liposome and vice versa. Characteristics like permeability, surface charge density, size and size-distribution of the liposomes may change due to the peptide's action. Similarly, the fluorescence behaviors of the tryptophan (Trp) moieties and the tertiary structure of the peptide may also change due to the interaction with the

liposome membrane. Different instrumental techniques including circular-dichroism, NMR and fluorescence have been used to better understand AMP's mechanism of action on biological membranes [28]

In this study, the interaction of indolicidin, a cationic 13 amino acid antimicrobial peptide, with liposomes is monitored using light scattering, fluorescence and Capillary Electrophoresis (CE) techniques. The lipid composition of the liposomes is varied between zwitterionic to anionic in order to mimic eukaryotic and prokaryotic membranes. In addition, cholesterol is mixed with the zwitterionic DMPC lipid to examine the peptide effect on the liposome's size, permeability and other physical characteristics. The liposome's average size and polydispersity index (PI) are measured before and after peptide incubation and the change in these parameters can give insight into the extent of perturbation caused by the peptide on the membrane and any fusion that might have occurred thereafter. In a similar manner, indolicidin's innate tryptophan fluorescence is compared before and after interaction with anionic and zwitterionic liposomes. The peptide's fluorescence intensity increases when it inserts deeper into the hydrophobic membrane and the emission λ_{max} is also blue shifted. An acrylamide fluorescence quenching experiment shows that the peptide's tryptophan residues insert at different depth into the liposome membrane, depending on its lipid composition [29]. Also, using a conventional fluorescence experiment, the peptide induced leakage from calcein encapsulated liposomes is compared between zwitterionic and anionic liposomes. The fluorescence of the (liposome) encapsulated dye increases when it leaks out to the extra liposomal-solution due to membrane

perturbation by the peptide's action. Finally, capillary zone electrophoresis (CZE) and liposome electrokinetic chromatography (LEKC) methods are used to compare the peptide's affinity for zwitterionic and anionic liposome membranes. The interpretation of the electropherogram peak area and retention time data, of the liposome and the peptide, are used to support what has been observed with DLS and fluorescence experiments regarding the hydrophobic and/or electrostatic nature of the interaction between the liposome and peptide.

Reference List

[1] A.D.Bangham, Membrane models with phospholipids, Prog.Biophys.Mol.Biol. 18 (1968) 29-95.

[2] M.J.Hope, M.B.Bally, L.D.Mayer, A.S.Janoff, and P.R.Cullis, Generation of multilamellar and unilamellar phospholipid vesicles, Chem Phys Lipids 40 (1986) 89-107.

[3] V.P.Torchilin, Recent advances with liposomes as pharmaceutical carriers, Nat.Rev.Drug Discov. 4 (2005) 145-160.

[4] V.P.Torchilin, Targeted pharmaceutical nanocarriers for cancer therapy and imaging, AAPS.J 9 (2007) E128-E147.

[5] V.P.Torchilin, Multifunctional nanocarriers, Adv.Drug Deliv.Rev. 58 (2006) 1532-1555.

[6] H.A.Rongen, A.Bult, and W.P.van Bennekom, Liposomes and immunoassays, J.Immunol.Methods 204 (1997) 105-133.

[7] C.Huang, L.Wheeldon and T.E.Thompson, The properties of lipid bilayer membranes separating two aqueous phases: formation of a membrane of simple composition, J Mol.Biol. 8 (1964) 148-160.

[8] B.Ohler, K.Graf, R.Bragg, T.Lemons, R.Coe, C.Genain, J.Israelachvili, and C.Husted, Role of lipid interactions in autoimmune demyelination, Biochim.Biophys.Acta 1688 (2004) 10-17.

[9] J.M.Boggs, G.Rangaraj, K.M.Koshy, C.Ackerley, D.D.Wood, and M.A.Moscarello, Highly deiminated isoform of myelin basic protein from multiple sclerosis brain causes fragmentation of lipid vesicles, J Neurosci.Res. 57 (1999) 529-535.

[10] C.Larios, M.Espina, M.A.Alsina, and I.Haro, Interaction of three beta-interferon domains with liposomes and monolayers as model membranes, Biophys.Chem 111 (2004) 123-133.

[11] P.Rispoli, R.Carzino, T.Svaldo-Lanero, A.Relini, O.Cavalleri, A.Fasano, G.M.Liuzzi, G.Carlone, P.Riccio, A.Gliozzi, and R.Rolandi, A thermodynamic and structural study of myelin basic protein in lipid membrane models, Biophys.J 93 (2007) 1999-2010.

[12] J.Schmidt, J.M.Metselaar, and R.Gold, Intravenous liposomal prednisolone downregulates in situ TNF-alpha production by T-cells in experimental autoimmune encephalomyelitis, J Histochem.Cytochem. 51 (2003) 1241-1244.

[13] M.J.Hope, R.Nayer, L.D.Mayer, P.R.Cullis, Reduction of liposome size and preparation of unilamellar vesicles by extrusion techniques, In: Gregoriadis, G. (Ed.), Liposome Technology: liposome preparation and related techniques, CRC Press Inc., Boca Raton, FL, 1993, pp. 123-139.

[14] C.Huang, Studies on phosphatidylcholine vesicles. Formation and physical characteristics, Biochemistry 8 (1969) 344-352.

[15] Malvern instruments. Dynamic Light Scattering: An Introduction in 30 Minutes. http://www.malvern.com/common/downloads/campaign/MRK656-01.pdf . 2009.

[16] J.N.Weinstein, E.Ralston, L.D.Leserman, R.D.Klausner, P.Dragsten, R.Blumenthal, Selfquenching of carboxyfluorescein fluorescence: uses in studying liposome stability and liposome-cell interaction, In: Gregoriadis, G. (Ed.), Liposome Technology, CRC Press, Boca Raton, 1984, pp. 183-204.

[17] W.R.Perkins, S.R.Minchey, P.L.Ahl, and A.S.Janoff, The determination of liposome captured volume, Chem.Phys.Lipids 64 (1993) 197-217.

[18] K.A.Edwards and A.J.Baeumner, Liposomes in analyses, Talanta 68 (2006) 1421-1431.

[19] A.K.Singh, S.J.Schoeniger, R.G.Carbonell, Liposomes as signal enhancement agents in immunodiagnostic applications, In: Victor Chi-Min Yang, That T.Ngo, and TT Ngo (Eds.), Biosensors and Their Applications, Kluwer Academics, New York, 2000, pp. 131-145.

[20] S.Y.Hwang, Y.Kumada, G.H.Seong, J.Choo, S.Katoh, and E.K.Lee, Characteristics of a liposome immunoassay on a poly(methyl methacrylate) surface, Anal.Bioanal.Chem. 389 (2007) 2251-2257.

[21] S.Miyagawa, M.Nakagawa, Y.Ito, H.Yamaji, H.Fukuda, and S.Katoh, Liposome Immune Lysis Assay of Antibodies by Liposomes Encapsulating Coenzyme â-NAD^+, J.Chem.Eng.Jpn. 34 (2001) 30-35.

[22] B.Babbitt, L.Burtis, P.Dentinger, P.Constantinides, L.Hillis, B.McGirl, and L.Huang, Contact-dependent, immunecomplex-mediated lysis of hapten-sensitized liposomes, Bioconjug.Chem. 4 (1993) 199-205.

[23] L.R.Hillis, J.D.Handly, B.P.Babbitt, Utilization of contact sensitive liposome formulations in Homogeneous immunoassays, In: Gregoriadis, G. (Ed.), Liposome Technology, CRC press, Boca Raton, FL, 1993, pp. 301-315.

[24] S.Katoh, M.Kishimura, and K.Tomioka, Immune lysis assay of antibodies by use of antigen-coupled liposomes, Colloids Surf., A 109 (1996) 195-200.

[25] S.Katoh, Y.Sohma, Y.Mori, R.Fujita, E.Sada, M.Kishimura, and H.Fukuda, Homogeneous immunoassay of polyclonal antibodies by use of antigen-coupled liposomes, Biotechnol.Bioeng. 41 (1993) 862-867.

[26] I.M.Hafez and P.R.Cullis, Roles of lipid polymorphism in intracellular delivery, Adv.Drug Deliv.Rev. 47 (2001) 139-148.

[27] K.Lohner, E.Sevcsik, G.Pabst, Liposome-Based Biomembrane Mimetic Systems: Implications for Lipid–Peptide, In: Leitmannova, L. A. (Ed.), Advances in Planar Lipid Bilayers and Liposomes, Elsevier, 2008, pp. 103-137.

[28] R.M.Epand and R.F.Epand, Liposomes as models for antimicrobial peptides, Methods Enzymol. 372 (2003) 124-133.

[29] J.R.Lakowicz, Solvent and environmental effects, Principles of Fluorescence Spectroscopy, Springer, Berlin, 2003, pp. 205-235.

Chapter 2

Electrokinetic characterization of mixed zwitterionic-cholesterol liposomes

Abstract

The size and electrical properties of zwitterionic liposomes are partially influenced by their lipid and cholesterol compositions. The zeta potential and electrophoretic mobility of different size liposomes made by extrusion from phosphatidylcholine (PC), sphingomyelin and cholesterol is measured by capillary zone electrophoresis (CZE) and laser doppler velocimetry (LDV) techniques, while their average size is measured by dynamic light scattering (DLS). Results from these experiments indicate that both dipalmitoylphosphatidylcholine (DPPC) and sphingomyelin liposomes have similar electrostatic behaviors. The DPPC/cholesterol liposome with the highest cholesterol composition (45 % by mole) had the largest size and also mobility (most negative) than lower cholesterol content liposomes (5 and 25%). The liposome mobilities measured by the LDV and CZE methods were practically the same, mostly within 2% difference. The CZE migration order of small and large liposomes was opposite to that expected from classical electrokinetic theories due to the relaxation effect of the ionic atmosphere surrounding the migrating liposomes in low ionic strength buffers. The Smoluchowski equation, with Henry's function, correctly relates the effect of particle size on its mobility in low ionic strength solutions. Together with the LDV technique, CZE can be used to fully characterize the electrostatic behavior, and the stability of liposome samples. In the absence of the expensive diffraction instruments, CZE by itself, or in

combination with chromatographic methods, can offer alternative means of characterization of charged colloid particles.

Introduction

Liposomes are artificial phospholipid vesicles that are formed by the self-assembly of lipids, and other lipophilic molecules, into a spherical structure surrounding an aqueous interior. Due to their resemblance to real membranes they have been widely used both in research and in industrial applications. The behaviors and the application of liposomes are mainly determined by their composition and physical characteristics, like size and surface charge [1;2]. The physical characterization of liposomes is important in order to monitor their stability and performance during storage and applications both in-vivo and in-vitro. Data obtained from these studies will help in formulating optimum liposome compositions and methods of their preparation for specific industrial and research applications. Also, better understanding of the natural membranes is gained through correct characterization and meaningful interpretation of the experimental results from membrane mimicking systems like liposomes [1;3].

Characterization of liposomes' size

Liposomes are often distinguished according to their number of lamellae and size. Small unilamellar vesicles (SUV), large unilamellar vesicles (LUV) and large multilamellar vesicles (MLV) have been recognized. SUVs show a diameter ranging from 20 to approximately 50 nm. LUVs and MLVs range in size from a few hundred nanometres to several micro-meters. The thickness of the membrane (phospholipid bilayer) is determined as approximately 4 to 6 nm [1;4]. Electron microscopy (EM) permits the direct observation of individual liposomes and, in principle, provides exact

information on the size of a selected few liposomes out of the whole sample. However EM is very expensive and the method is quite tedious and time consuming. Dynamic light scattering techniques (DLS) have widely been used for characterizing average size and polydispersity, while conventional size exclusion chromatography (SEC) and high performance SEC methods have been used to fractionate liposomes based on their size [1;4;5]. The DLS technique, also known as photon correlation spectroscopy (PCS), determines the diffusion coefficient of the liposomes, due to the Brownian motion in the suspension, through analysis of the time dependence of the intensity of fluctuations in scattered light. Small liposomes diffuse more rapidly than larger liposomes, and the fluctuation of the scattered light intensity varies accordingly. This method generates the translational diffusion coefficient, and the average radius of the liposome is calculated using the Stokes-Einstein equation [1;6]. However, DLS has few other limitations, beside expensive instrumentation, it offers low resolution and its accuracy is limited to a narrow particle size range. That is, it has poor accuracy for sizes smaller than 30nm and larger than 500nm. The DLS technique appears to underestimate the size of small liposomes (<30nm) in the presence of larger sized liposomes. A combined method of chromatographic fractionation followed by DLS measurement of each (eluted) fraction seems to provide better results than DLS alone [7].

SEC is an inexpensive and quick method for the fractionation and size analysis of liposomes. Using combination of TSK-G6000 (>1000Å pore) and G5000 (<1000Å) HPSEC columns, Ollivon and coworkers were able to separate liposomes with sizes ranging 20-500nm with somewhat limited

resolution. The columns are packed with cross-linked gels and retention is based on ease of permeation through the gel pores. Very large liposomes elute fast with the void volume while smaller liposomes enter the gel pores, and their retention time on the column is proportional to their size [8]. However, it is difficult to separate mixed liposomes, with a relatively narrow size distribution of less than 50nm spread, in a single elution cycle using classical or HPSEC methods. An additional step of re-chromatography of the (eluent) sub-fractions on a smaller pore-sized column might be needed to achieve the highest resolution of a polydisperse-sized liposome formulation [7]. Capillary electrophoresis may offer better resolution for liposomes and particles that carry charge.

The electrostatic behavior of liposomes

In membrane research, electrostatic phenomena play a crucial role in many biological processes taking place at the membrane surface. Generally, the electrostatic potential is important for many, if not all, types of interactions with membranes. For example, calcium ion binding has a major role in membrane processes like, signaling, endocytosis, exocytosis, and receptor binding, beside others. A change in the membrane surface potential can affect adhesion between cells as well as fusion of cell membranes through the contribution of the electrostatic force to the total adhesion process. As a further consequence, measuring and controlling the electrostatic properties of lipid vesicles is crucial for the basic understanding of real membranes and for the practical applications of liposomes. Additionally, for industrial and pharmaceutical application, the loading efficiency, the binding strength and

the release rate of encapsulated drugs are also largely affected by the electrostatic properties of the liposomes used [9;10].

The most convenient method for the electrostatic characterization of liposomes has been through determination of the zeta potential of an ensemble of charged lipid vesicles in an external electric field. The zeta potential is related to the overall particle charge in a particular medium. Historically, many of the electrophoretic studies on liposomal dispersions were done by micro-electrophoresis, which is a method of studying electrophoresis of various dispersed particles using optical microscopy. In recent times, measurement of the zeta potential of samples is done using the technique of laser doppler velocimetry. In this technique, a voltage is applied across a pair of electrodes at either end of a cell containing the particle dispersion. Charged particles are attracted to the oppositely charged electrodes and their net velocity is measured from the scattered laser light by the electrophoretically moving liposomes. The electrophoretic mobility is calculated as the ratio of the particles' velocity to the applied electric field strength [9-11].

Although, zwitterionic lipids like phosphatidylcholine, phosphatidylethanolamine and sphingomyelin, together with the neutrally charged cholesterol, make up the major portion of most biological membranes, very little work has been done in characterizing large unilamellar vesicles (LUV) made from zwitterionic lipids and cholesterol using electrophoretic methods. This might be because of the presumption that at or near the neutral pH value, these liposomes will have zero net charge and possess little or no electrophoretic mobility. But from our CE

and zeta potential determination experiments, these mixed zwitterionic-cholesterol liposomes do carry a net negative surface charge and can be characterized by light scattering and electrophoretic techniques.

Capillary electrophoretic characterization of liposomes

Capillary electrophoresis (CE) encompasses a family of related separation techniques that use narrow-bore fused-silica capillaries to separate a complex array of large and small molecules. High electric field strengths are used to separate molecules based on differences in charge, size and hydrophobicity. Sample introduction is accomplished by immersing the end of the capillary into a sample vial and applying pressure, vacuum or voltage. Depending on the types of capillary and electrolytes used, CE can be divided into several separation techniques. Capillary zone electrophoresis (CZE), also known as free-solution CE (FSCE), is the simplest form of CE. The separation mechanism is based on differences in the charge-to-size ratio of charged molecules in an applied electric field. The separation relies principally on the pH-controlled ionization of the acidic and basic functional groups of solutes [12].

In CZE, colloidal particles migrate through the capillary based on their charge density. Assuming that the liposome travels as a sphere, the electrophoretic mobility (μ) of a particle is governed by the classical electrokinetic equation:

$$\mu = \left[\frac{q}{6\pi\eta r} \right] \qquad \textit{Equation (1)}$$

Where $\boldsymbol{q}$ is the effective charge, $\boldsymbol{r}$ is the particles' hydrodynamic radius and η is the viscosity of the media. Based on this equation, for a homogeneous (sized) and uniformly charged colloidal particles, like liposomes, electrophoretic mobility is directly related to particle charge [13]. Similarly, the Smoluchwski equation relates the liposome mobility to the zeta potential when an external electric field is applied through the liposome solution. Zeta potential (ζ) is an electrostatic potential that develops at the shear surface of suspended colloidal particles, like liposomes. Smoluchowski's equation shown below is a limiting case that applies when the thickness of the electrical double layer (EDL), at the liposome interface, is much smaller than liposome size [12;14].

$$\mu = \left(\frac{\varepsilon \zeta}{\eta} \right) \qquad \textit{Equation (2)}$$

ε - Dielectric constant of media

Since the migration of the liposome through the capillary is also influenced by the bulk electro osmotic flow (EOF), due to the creation of an electrical double layer from the silica surface silanol groups at high voltage, calculation of the observed mobility (μ) will be the vector sum of the electrophoretic mobility (μ_{ep}) and the EOF-mobility (μ_{eo}).

$$\mu = \mu_{ep} \pm \mu_{eo} \qquad \textit{Equation (3)}$$

The liposome's observed mobility (μ) is also related to its total linear velocity (ν) and other parameters in the following equations:

$$\nu = \mu_{ep}E = (\mu + \mu_{eo})E$$

Equation (4)

$$\mu_{ep} = \left[\frac{l_d l_t}{V t_m}\right] and \left(E = \frac{V}{l_t}\right)$$

Equation (5)

Where E is the electric field strength (V/cm), V is the voltage applied, t_m is liposomes' migration time to the detection window, l_t and l_d are the capillary total length and its distance to the detector. The EOF mobility (μ_{eo}) is determined from the migration time of a small neutral molecule like methanol or mesityl oxide. Once the liposome's mobility is known from CZE, its mean surface charge can be calculated using equation (1), assuming each liposome is a charged sphere moving independently through a low viscosity (water) electrolyte solution [15;16].

Over the last decade, capillary electrophoresis (CE) methods have been used to characterize the size, surface and electrophoretic properties of liposomes made from charged lipids and cholesterol [14;15;17-19]. There are very few extensive published reviews related to the separation and characterization of liposomes and other sub-micron sized particles by CE [13;20-22]. Mainly, Riekkola's research group has characterized extruded liposomes made from anionic lipids like phosphatidylglycerol, phosphatidylserine, phosphatidic acid, cardiolipin (PG, PS, PA,CL) and they were able to estimate the average surface charge on the anionic liposomes [14;23]. Similar studies of charged liposomes by Roberts and others have showed that the surface charge largely determines the liposome's mobility [15;19;24]. These studies indicate that

increasing the anionic lipid mole fraction makes the liposomes more negative and leads to larger electrophoretic mobility. Also, the anionic liposomes peak width is usually broad due to a wide size distribution. For certain samples, the extent of peak broadening could be so great that would lead to indiscernible peaks from the baseline [15;19;25]. For the most part, all related published studies by others indicate that the electrophoretic migration time and peak profiles of a liposome preparation can be used to examine the electrostatic properties, which greatly affect its behavior, both in vivo and in vitro.

In this study, capillary electrophoresis and dynamic light scattering techniques have been used to characterize presumably uncharged liposomes made of the zwitterionic lipids phosphatidylcholine and sphingomyelin and cholesterol prepared by the extrusion method. The effects of liposome's lipid composition and the type of electrolyte/buffer on liposome size, stability and electrostatic behaviors were investigated. Liposomes with varying lipid/cholesterol composition were prepared by extrusion through 100 nm membrane filter, and the resulting differences in their mobility monitored. Similarly, the effect of liposome size on electrophoretic mobility was studied using liposomes made of the same lipid/cholesterol contents but extruded through 50 nm and 100 nm filters. A combination of CZE and DLS allowed rapid investigation of liposome's surface charge, average size, and size distribution.

Experimental

Materials and methods

Chemicals

1,2-Dipalmitoyl-*sn*-Glycero-3-Phosphocholine (DPPC), chicken-sphingomyelin, Rhodamine-labeled-DPPE (1,2-Dipalmitoyl-*sn*-Glycero-3-Phosphoethanolamine-N-(Lissamine Rhodamine B Sulfonyl)), and cholesterol were from Avanti Polar Lipids. 1M HEPES (pH 7.3 ± 0.1) and Tris-HCl buffers, Mesityl oxide was purchased from Fisher. Deionized 18MΩ water was obtained in-house from a reverse osmosis Millipore system. The hydrophilic marker dyes calcein, carboxyfluorescein and alexa-fluor were obtained from Probes-Invitrogen. Size exclusion gel Sephadex G-50 and Micro Spin filter columns (part # 27-5330-01) were obtained from Amersham Biosciences. Sephadex G-50 gels have an average fractionation range of 500-10,000 daltons. The molecular structures of the lipids and fluorescent dyes used in this study are given in figures 2-1 and 2-2 respectively.

Capillary Electrophoresis

The CZE-UV experiments were carried out on a laboratory-built CE instrument. A Spellman SL30 high-voltage power supply was used to apply a positive voltage over the length of the fused silica capillary (Polymicro Technologies, Phoenix, AZ, USA), with an inner diameter of 75 μm and an outer diameter of 362 μm. The temperature of the system was maintained at 25 °C using a circulating oil bath. The absorbance was measured at 254 nm and 280 nm using a SSI 500 variable-wavelength UV detector.

The CE–LIF system consisted of an argon ion laser (Omni Chrome, CA, USA) modulated by a chopper controlled by a lock-in amplifier (EG&G, Trenton, NJ, USA). The 488 nm modulated laser line was focused onto the 50 μm I.D.×362 μm O.D. bare fused-silica capillary (Polymicro Technologies, Phoenix, AZ, USA) through an upright microscope with a 40X fluorite objective which both sent the excited fluorescent beam and collected the emitted beam to/from the capillary. The laser excitation beam would pass through a dichroic filter (495 nm) and the subsequent emission beam would pass through a long pass (500 nm) and short pass (515 nm) filters and transmitted to the photomultiplier tube (Hamamatsu, Bridgewater, NJ, USA). The signal was then sent to the A/D converter and the lock-in amplifier. All data acquisition and data analysis for both CE-LIF and CE-UV experiments were performed using PC/Chrom^{+} and Lab View software's.

Liposome size, size-distribution and zeta potential

The hydrodynamic diameter and the poly-dispersity (size-distribution index) of all liposome preparations were determined by Dynamic Light Scattering (DLS) technique using the Malvern Zeta Sizer model 1000HSa. The Malvern instrument measures the time-dependent fluctuations of light scattered by the liposomes and uses it to calculate the average size and polydispersity of the liposomes [1]. We have observed that extrusion always produces liposomes with a narrower size distribution than probe-sonication and it has also been indicated by others that it does not rupture lipid chains or denature encapsulated molecules [4].

Liposome zeta potential measurement

The liposome's zeta potential, which is directly related to its net charge and affects its mobility in the buffer solution, was measured by the Malvern Zeta-nano instrument. The Zeta-nano calculates the zeta potential by first determining the electrophoretic mobility and then applies the Smoluchwski equation to calculate the potential [9;11]. The mobility is obtained by applying an external electric field (*E*) on the sample and measuring the average velocity (ν) of the liposomes with Laser Doppler Velocimetry technique.

$$\mu = \left[\frac{\nu}{E}\right] \qquad \textit{From Equation (4)}$$

The Smoluchwski equation with Henry's function, *f* (*kR),* is given as:

$$\mu = \frac{2\varepsilon\zeta}{3\eta} f(kR) \qquad \textit{Equation (6)}$$

Where

$\zeta = zeta\ \ potential$
$\mu = electophoretic\ \ mobility$
$\varepsilon = dielectric\ \ permitivity\ of\ solution$
$\eta = vis\cos ity$
$(kR) = Henry's\ \ coefficient$

The particle's radius (R) and the inverse thickness of the electrical double layer (K= 1/*k*) determine the value for Henry's function, which varies between 1.0 and 1.5. The two extreme case values are usually used as

approximations for $f(kR)$ determination, either 1.5 or 1.0. In aqueous electrolyte solutions (>10^{-3}M), where the electrical double layer (EDL) is much smaller than the particle's radius (kR>>1),the function *f(kR)* approaches 1.5, and the Smoluchwski approximation applies [10;14]. For the Smoluchwski Zeta potential, equation (6) simplifies and rearranges to:

$$\zeta = \frac{\mu\eta}{\varepsilon} \qquad \textit{Equation (7)}$$

For very weak electrolyte solutions (<10^{-3}M and kR<<1), the EDL thickness is much larger compared to the particle radius, so the particle can be treated as a point charge. Under this circumstance the value of Henry's function approaches 1.0, which is called the Huckel approximation. In the intermediate regions, between the Smoluchwski and Huckel extremes, Henry's function can have values between 1 and 1.5, based on the particles size and the nature of the electrolytic solution [10;27].

Preparation of dye encapsulating liposomes

All the liposome suspensions were prepared by the extrusion method developed by Hope, M.J, and coworkers, with a slight modification, using the Lipex 10mL thermo barrel extruder (Northern Lipids Inc., Vancouver, BC Canada) [28]. Lipids at a total concentration of 10mg/ml are first dissolved in 3-5mL of chloroform in a 50mL round bottom flask. A dried thin lipid film is formed around the flask inside walls after a 30-45 minutes of rotary evaporation on the Bushi Roto-Vap, under low pressure and >50°C. The dried lipid film is hydrated with 3-5mL of pure buffer or a buffered-dye solution with continuous shaking at a temperature above the

lipid phase transition temperature T_c (for DPPC ≥ 41°C) to form a stable multi lamellar vesicle (MLV) suspension. After vortexing and homogenizing the MLV suspension, it is first extruded about 7 times on a *single* 200nm Nucleopore Polycarbonate membrane (Whatman Inc. USA) in the 10mL Lipex extruder at 60°C and a low N_2 pressure (<100psi). Finally, the liposome suspension is extruded at least ten times through a *double* 100nm Polycarbonate membrane at a pressure of 200-400psi. During all the extrusions the temperature has to be maintained at least 10°C above the glass transition temperature (T_c) of the liposome, so as to maintain a reasonable flow at moderate extrusion pressures. All the final liposome preparations are stored in a refrigerator (4°C) until further analysis.

In some cases lipids with a dye molecule covalently attached to their head group have been used instead of a hydrophilic dye encapsulation. In this situation, a dye-attached-lipid, like Rhodamine-phosphatidylethanolamine (Rh-PE), is co-dissolved in chloroform with the other amphiphiles to form the thin lipid film, which later is hydrated with a plain buffer to form the liposomes. This way, the dye molecule is anchored to the membrane and it takes care of the random dye leakage problem, which sometimes occurs with aqueous dye encapsulated liposomes.

Separation of un-trapped marker and liposome

For the CE-LIF experiments the encapsulated liposomes have to be separated from the free un-trapped hydrophilic dye on Sephadex G-50 gel filtration micro-columns (750μL) since the fluorescence signal due to the free (untrapped) dye interferes with detection of the liposome peak. The gel

column is prepared first by boiling about 1g of Sephadex G-50 fine powder in 15-20 mL of DI-water for an hour in a covered beaker. One gram of G-50 powder swells to 7-9 mL gel volume. The gel is cooled to room temperature before it is filled into the micro-columns filling 70% of the volume. The column is equilibrated with (100μL) blank liposomes before it's used for free-dye/liposome separation. The liposome/dye mixture is gently placed on the gel micro-columns and the encapsulated-liposomes are separated from the free dye after centrifugation for 2 minutes @1000rpm. The low molecular weight dye (<5000) is trapped in the gel while the liposomes are excluded and elute first with the void-volume at almost zero dilution.

Results & discussion

Liposome composition and its effect on size

A liposome's chemical composition determines its physical characteristics including its size, encapsulation and permeability properties. Dynamic light scattering (DLS) measurements of DPPC/CH liposomes show that liposomes with more cholesterol tend to be somewhat larger, on average, than liposomes without or with less cholesterol content. Also, marker encapsulated liposomes usually are larger than the ones with only a plain aqueous buffer interior. Figure 2-3 shows the effects of cholesterol and dye contents on the liposome size. Generally, the liposomes with buffered-dye interior were larger than the ones with just a plain buffer. All the liposomes are prepared the same way and extruded through final double 100nm polycarbonate membranes. These observations are consistent with those reported in the literature [29;30]. The presence of cholesterol changes the

lipid packing structure and the orientation of the head groups along the membrane interface region. One of the reasons for the increase in size of cholesterol-rich liposomes could be due to the presence of cholesterol between the lipid molecules, which straightens the acyl chains that were tilting sideways in pure DPPC liposome membranes [1]. As illustrated in Figure 2-4(b) pure-PC bilayers adapt the tilted orientation in order to decrease the gap that is created between the lipid-acyl chains, due to the size of the lipid head groups, and maximize the hydrophobic interaction/contact between them [31;32]. This tilted packing structure might also decrease the membrane thickness and the total liposome diameter. Mixed PC-cholesterol liposomes, as shown in Figure 2-4(a), have perpendicularly oriented acyl chains since cholesterol fills the gaps between the acyl chains and this might contribute to the thickening of the bilayer membrane, thereby increasing the total liposome diameter [32]. Type of the buffer used did not have any effect on size since all the liposomes prepared in two other buffers showed the same trend of size increase with a more cholesterol composition. Comparatively, we noticed the liposomes prepared with DI water tend to be smaller, on average, than those prepared with buffers. In addition to lipid packing changes, cholesterol will also enhance the extent of hydration around the interfacial membrane region, which also might contribute to the enlargement of the liposome membrane. Generally, cholesterol enhances the orientation and order of the phospholipids thereby increasing the thickness and rigidity of the membrane [1;3;28-30]

Effect of liposome size on electrophoretic mobility

As noted in the introduction, the mobility of a charged liposome is controlled by the zeta potential at the shear surface, and is governed by Henry's equation (equation 2). The electrophoretic mobility of non-conducting spherical particles dispersed in an electrolyte solution is usually calculated by simply applying the Smoluchwski approximation with Henry's coefficients [10;11;14;16]. Under this approximation, it is implied that the mobility of a colloid particle in a dilute electrolyte solution should be essentially independent of its size and shape for all charge densities [27]. Using classical electrostatics (equation 1), it is expected that liposomes with similar charge distribution (same lipid composition) should migrate based on their charge-to-size ratio, with the smallest (negatively charged) liposome eluting last and the larger sized eluting earlier. The overlaid electropherograms on Figure 2-5 show the normal mode CZE run of a 74, 95 and 150nm DPPC/CH liposomes (extruded through 50, 100 and 200nm filters respectively) with 55/45 % mole composition. Similarly, Figure 2-6 shows the larger liposome (152nm) has a faster negative mobility (~2.2min) than the 95nm liposome (~2.0min). These liposomes are made of zwitterionic lipids but each has distinct mobility that is different from each other and the internal standard (@1.8min), the neutral marker mesityl-oxide. The liposome retention times obtained in Figure 2-6 were inconsistent to that expected by the charge-to-size mechanism (equation 1) and the Smoluchwski equation (equation 2), since the 1arge 150nm liposomes have the fastest (negative) mobility and elute later than the smaller 75 and 95nm liposomes. This indicates that liposome size plays an important role in

determining liposome CZE mobility, and therefore, Henry's equation has to be revisited in order to explain this phenomenon. The *k* term in Henry's function is the reciprocal of the Debye length ($k = 1/\mathrm{K}$), which is the electrical double layer thickness (EDL), and *R* can be approximated by the liposome radius. In the cases of small potential ($\zeta \leq 25mV$ at 25°C), Henry's function, $f(kR)$, increases in the $(1 < f(kR) < 1.5)$ range as the liposomes go from a small to a larger size [14;27]. Since EDL ($1/k$) is an explicit function of the ionic strength of the buffer, it does not change between the different sized liposome solutions. Consequently, the electrophoretic mobility of the liposomes can become a monotonic function of their size at a given ionic strength, with the larger liposome (150nm) having the fastest mobility and therefore the longest migration time under normal mode CZE [13;17;27;33]. The size difference between the 75 and 95 nm-sized liposomes was not large enough to get a CZE resolution for the liposomes that were run, in Tris buffer as shown in Figure 2-5 but the CZE runs in Hepes buffer (Figure 2-7) show better resolution, than tris buffer, with each of the 3 peaks clearly eluting at different times with the smallest 75nm liposome eluting first, followed by the 95nm one and lastly the 150nm as expected by Henry's equation. Generally, liposome run in both tris and heps buffer show similar electrokinetic migration profiles, as seen on figures 2-5, 2-6 and 2-7, with the larger 150nm liposome eluting later than both the 75 and 95nm ones. Laser Doppler Velocimetry (LDV) measurements of different sized liposomes' mobilities by Roy and Estelrich have also indicated that the absolute value of the Zeta-potential, which is directly calculated from the mobility, of mixed PS/PE liposomes is size dependent and is the highest for

the large multilamellar vesicles (MLV) followed by sonicated and extruded unilamellar vesicles [33]. Their results clearly show that the experimentally determined electrophoretic mobility was not only affected by the lipid composition, but also by the liposome preparation method and the size of the liposomes. Also, similar CE characterization of colloid particles by Radko and others have indicated that liposome mobility in low ionic strength buffers is usually smaller than from that calculated by classical electrostatic theory (*equation-1*) due to the relaxation and retardation effects of the ionic atmosphere (EDL) surrounding the liposome during electrokinetic migration [17;34;35]. In a study by Radko et al, a series of partially-resolved electropherograms of extruded liposomes show a size dependent elution order with the large sizes migrating faster than smaller liposomes in a pH~8 Tris-HCl buffer, on CZE with reverse polarity [17]. Similarly, a CZE separation of latex microspheres, ranging in size from 100 to 352nm, by Johnson and Stokes shows the large liposomes exhibiting faster mobility than small ones [34]. Generally our CZE study of zwitterionic liposomes, that have similar lipid composition and surface density, shows that mobility is primarily a function of size, with the larger liposomes migrating faster than smaller liposomes, according Henry's equation [17;27]. In addition, different studies have shown that in dilute electrolyte solutions ($<10^{-2}$M), where the EDL thickness is significant relative to the size of the liposome, the relaxation/retardation effects contribute to the dragging force which reduces electrophoretic mobility and the effect is more significant as the particle size decreases [18;27;33].

Effect of lipid and cholesterol composition

Liposomes are usually prepared from a mixture of lipids and lipophilic compounds. Cholesterol is usually added (up to 50% by mole) to increase the membrane rigidity and reduce its permeability in the liquid-crystalline state [1]. As indicated earlier, cholesterol also increases the membrane thickness and the liposome's overall size. In addition, liposomes made from pure zwitterionic phosphatidylcholine (PC) have been found to carry a negative charge at neutral pH [14;36]. This surface negative charge is manifested by the net electrophoretic mobility, which is calculated from CE and laser diffraction measurements in studies by the Riekkola group [14]. In another study by Makino and Kimiko, the DMPC (C14), DPPC (C16) and DSPC (C18) liposomes show nonzero zeta potentials when they are dispersed in Hepes buffer at pH 7.4 [37]. The charge on a liposome can be estimated using *Eq1* once its mobility is determined from *Eq5*. The viscosity (10^3 Kg/sm) and dielectric constant (80 Fm^{-1}) in *Eq1* can be substituted with that of water for these dilute liposome buffer solutions, at room temperature.

In this study we have prepared liposomes from zwitterionic lipids DPPC, Sphingomyelin (Sph), and their mixture with cholesterol in order to determine the effect of cholesterol on the liposome's surface charge and electrophoretic mobility. Table 2-1 shows that the liposome zeta potential and electrophoretic mobility increased with the increase in cholesterol content for three types of liposomes made from zwitterionic lipids DPPC and sphingomyelin, as measured by LDV. The Malvern measured mobilities on Table 2-1 were close (within 2% difference) to those calculated with *Eq5* using the retention times in Figure 2-10. Although, there are a few

publications indicating the increase in zeta potential magnitude with cholesterol content, our study is the only one (at least to our knowledge) that systematically explored the changes in surface behavior of neutral liposomes due to changes in cholesterol content, using a different technique, besides laser diffraction methods [27;30]. All the electropherograms in Figures 2-8 to 2-10 show that the liposomes have a net negative mobility since they all eluted after the neutral EOF marker Mesityl Oxide under normal mode CZE runs (+30kV voltage is applied at the anode where the sample is injected). Also, each peak in Figure 2-10, representing a liposome with a different cholesterol composition, has migrated at a different electrophoretic mobility because of differences in surface charge density. Thus, irrespective of the type of dye used, whether hydrophilic encapsulation of carboxyfluorescein or membrane anchored neutral dye Rhodamine-B, the liposome with the most cholesterol always has the longest migration time.

Since all liposome in this study were composed of zwitterionic phospholipids (DPPC or others) and neutrally charged cholesterol at the operating pH (7.0), the net negative charge on the liposomes could be due to the conformational effects of lipids in the assembly, that is a buffer dependent orientation of the phosphatidylcholine's dipole head group that creates shielding of the positive charge [37;38]. This shielding might be reinforced by the presence of cholesterol, where more of the negative side of the dipole sticks-out of the surface of the liposome and the positive side pulled more to the inside of the membrane due to hydrogen-bonding interaction with the cholesterol –OH group. This PC head-group orientation, which is responsible for imparting a negative dipole potential to the

liposome, can be represented by the schematic seen in Figure 2-11, as proposed by Makino et al [37]. Another possible explanation for the negative charge detected on the liposomes made of zwitterionic lipids could be presence of trace anionic lipid impurities.

The decrease in mobility of liposomes with lower cholesterol content could be also due to their membrane deformation during electrophoresis. Cholesterol is known to add rigidity to a lipid bilayer, and membranes without it are susceptible to deformation under physical stress, such as high voltage electrophoresis. In addition, our study also conforms to the general notion that cholesterol increases the absolute zeta potential and the electrostatic repulsion between phosphatidylcholine liposomes thereby enhancing their stability [1;29;30;39;40].

Monitoring liposome extended stability

As expected, the long-term physical stability of liposomes depends on their lipid composition. The incorporation of cholesterol in moderate amounts (up to 30%) has been found to increase the packing efficiency and reduce the surface tension (decreases aggregation) and permeability of phosphatidylcholine liposomes [39;40]. Charged lipids also reduce aggregation through electrostatic repulsion. Commonly, particle size and zeta potential measurements are performed through set intervals of time to monitor liposome stability [11]. The average size and size-distribution index (PI) increase with extended storage, while the average zeta potential decreases with time, mainly for the 45% cholesterol liposome. We have measured both the Zeta-potential and polydispersity index after 4 and 8

week intervals to examine membrane stability of PC/CH liposomes. Figure 2-12 and 2-13 illustrate that through the 8-weeks time, the polydispersity (PI) increases due to aggregation, and the zeta potential decrease as the (attractive) surface tension increases between apposing liposomes. As noted earlier, the PI is a relative comparison index which is obtained from the DLS instrument and used to qualitatively determine the width of the size distribution of colloid particles. A PI value scale ranges between 0.0 and 1.0. When PI is close to zero, it indicates a very narrow and a homogeneous size distribution of a colloid suspension, while a value close to 1.0 represents a heterogeneous and polydisperse size distribution. The same trends were also observed with sphingomyelin liposomes through a four week time period.

Conclusion

Dye-encapsulated zwitterionic liposomes composed of DPPC, Sphingomyelin and cholesterol were characterized by combined electrophoretic and DLS methods. The electrophoretic mobility calculated from CZE migration time were essentially the same and within 2% difference to those measured by the Malvern zeta LDV technique.

The amount of cholesterol in mixed DPPC/CH liposomes has an effect on both the liposome's average size and its surface charge density. The DLS measurements show that liposomes with more cholesterol are larger in size than those with less or without cholesterol. Also, the encapsulated material (buffer or dye) seems to affect liposome size as shown on Figure 2-3. For example, a marker encapsulated liposome has a larger diameter, on average, than one prepared with plain buffer, and, liposomes prepared in pure DI water tend to be smaller than those prepared in Hepes and Tris buffers.

The electrostatic behaviors are determined by the lipid and cholesterol composition of these liposomes. Both CZE and LDV experiments confirm that phosphatidylcholine and sphingomyelin liposomes do carry a net negative surface charge, and this is true irrespective of the buffer type or in plain aqueous solution. The orientation of the PC head groups could impart a negative zeta potential to the liposomes made of electrostatically neutral zwitterionic phospholipids in dilute aqueous buffers. The smallest electrophoretic mobility was observed for liposomes made with the smallest cholesterol content (5%). The fastest mobility by 45% cholesterol liposome could be due to the enhanced negative surface charge distribution of the PC

head group in the presence of cholesterol (dipole orientation) as suggested earlier. Also, since cholesterol enhances rigidity, the mixed (cholesterol+PC) liposomes might resist deformation (and retardation) during electrophoresis than pure PC liposomes thereby having faster mobility. Mobilities measured by CZE and LDV techniques were essentially the same in most cases. Incorporation of anionic lipids has been found to increase the mobility and zeta potential of phosphatidylcholine liposomes.

The size of a liposome is obviously a factor in determining its electrophoretic mobility. For a 75 and 150nm liposomes with the same lipid composition, which means similar surface charge density, the 150nm liposomes migrate faster according to Henry's equation approximation. This migration order is opposite to that expected by the charge-to-size mechanism but directly correlates well with the size of the liposomes. In addition, the migration of the smaller liposomes might be more affected by the relaxation effects of the ionic atmosphere (EDL) surrounding the liposome during electrophoresis. The long-term stability of zwitterionic-lipid/cholesterol liposomes is also monitored by measuring their Zeta potential (ZP) and polydispersity index by DLS technique. The ZP of the 45% cholesterol PC-liposomes decreased by about 50% while that of the 5%cholesterol PC-liposomes did not change by that much over the 8 weeks time. Despite the large drop in ZP, the polydispersity index of the 45% cholesterol PC-liposomes did not show a significant increase through the same period (0.094 to 0.130), which still indicates a relatively narrow size distribution. Also, the PI for the 5% cholesterol liposomes only increased by 0.051 (0.083

to 0.134), which similarly indicates a minimum aggregation. Generally, a PI value of <0.2 indicates a fairly uniform size distribution.

Table 2-1. The DLS analysis of zeta potential, mobility, size and polydispersity-index of mixed zwitterionic/cholesterol liposomes.

Zeta potential, mobility, size and polydispersity-index of mixed zwitterionic/cholesterol liposomes by DLS					
Run #	**Sample Name**	**Zeta-P (mV)**	**Mob ($cm^2/Vs)X10^{-4}$**	**Size (nm)**	**PI (dispersity)**
1	20mM DPPC: Cholesterol 5%	–2.04	–1.60	94±0.5	0.083
2	20mM DPPC: Cholesterol 25%	–3.91	–3.07	100±0.5	0.069
3	20mM DPPC: Cholesterol 45%	–5.28	–4.14	107±0.5	0.094
4	20mM total (sphingomyelin 95%: Cholesterol 5%)	–3.12	–2.45	120±1.3	0.116
5	20mM total (sphingomyelin 75%: Cholesterol 25%)	–5.68	–4.45	143±1.8	0.338
6	20mM total (sphingomyelin 55%: Cholesterol 45%)	–13.3	–10.40	245±1.7	0.273
7	20mM total (DPPC/Cholesterol 95:5) RB-labeled	–4.18	–2.18	101±0.9	0.09
8	20mM total (DPPC/Cholesterol 75:5) RB-labeled	–9.57	–5.00	103±0.6	0.063
9	20mM total (DPPC/Cholesterol 55:45) RB-labeled	–16.2	–8.47	108±1.0	0.076
10	20mM total (DPPC/Cholesterol 55:45) blank-buffer	–13.7	–7.16	105±1.3	0.014

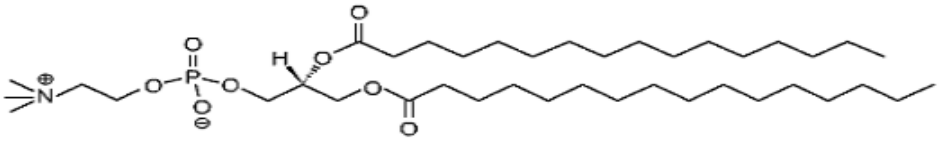

1,2-Dipalmitoyl-sn-Glycero-3-Phosphocholine (DPPC)

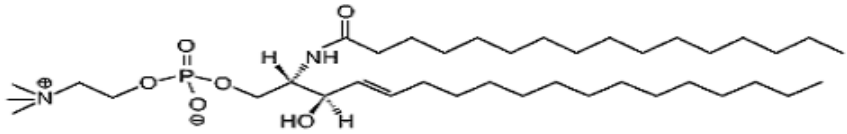

Sphingomyelin (Egg, Chicken)

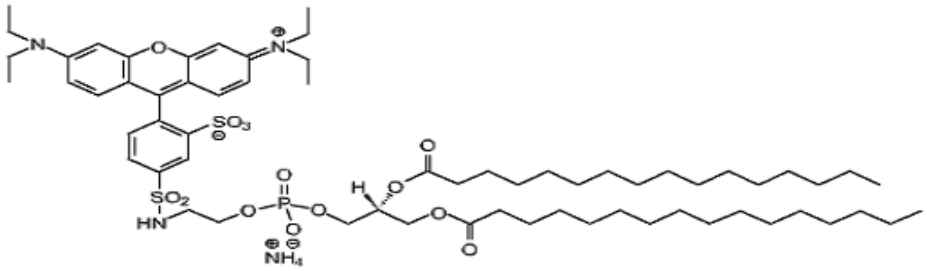

Lissamine Rhodamine DPPE

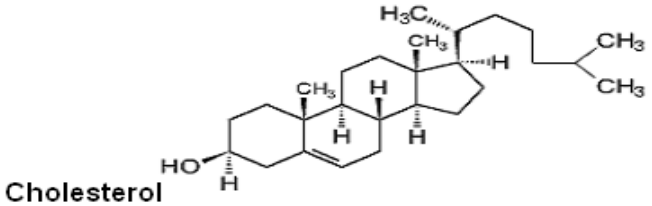

Cholesterol

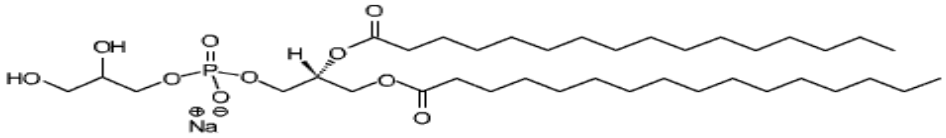

1,2-Dimyristoyl-*sn*-Glycero-3-[Phospho-rac-(1-glycerol)] (Sodium Salt)

Figure 2-1. The molecular structure of phospholipids and cholesterol. (Lipid molecular structures cited from *www.avantilipids.com*)

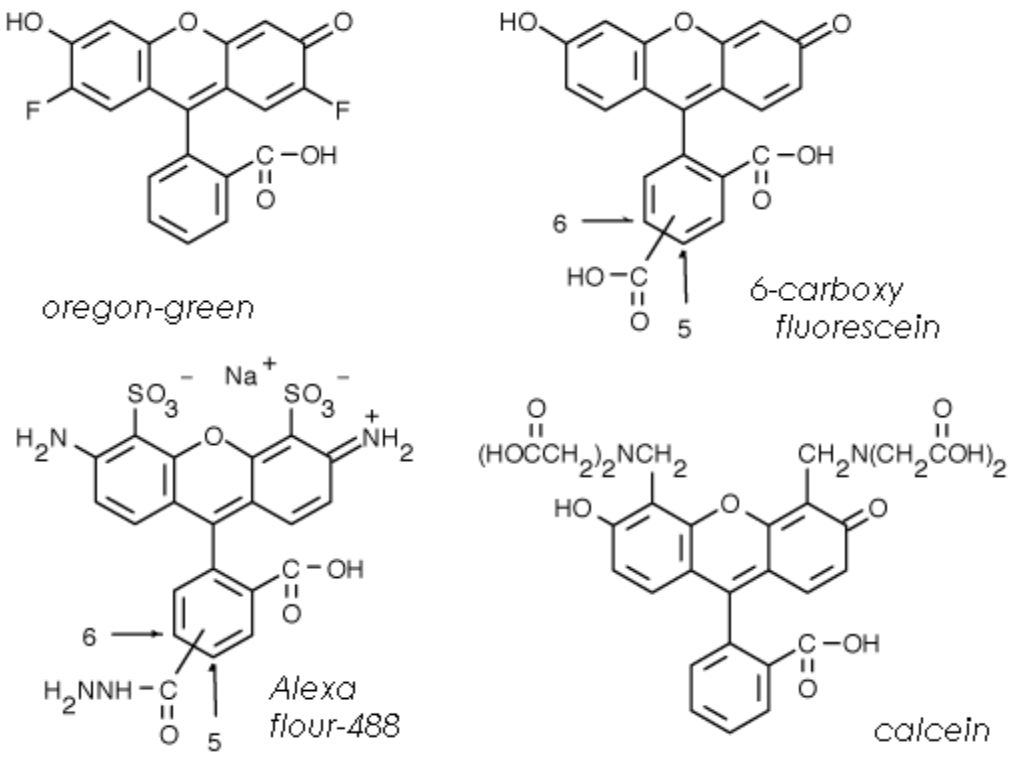

Figure 2-2. Hydrophilic dyes used for liposome encapsulation.
(Structure of dye molecules cited from *www.probes.com*)

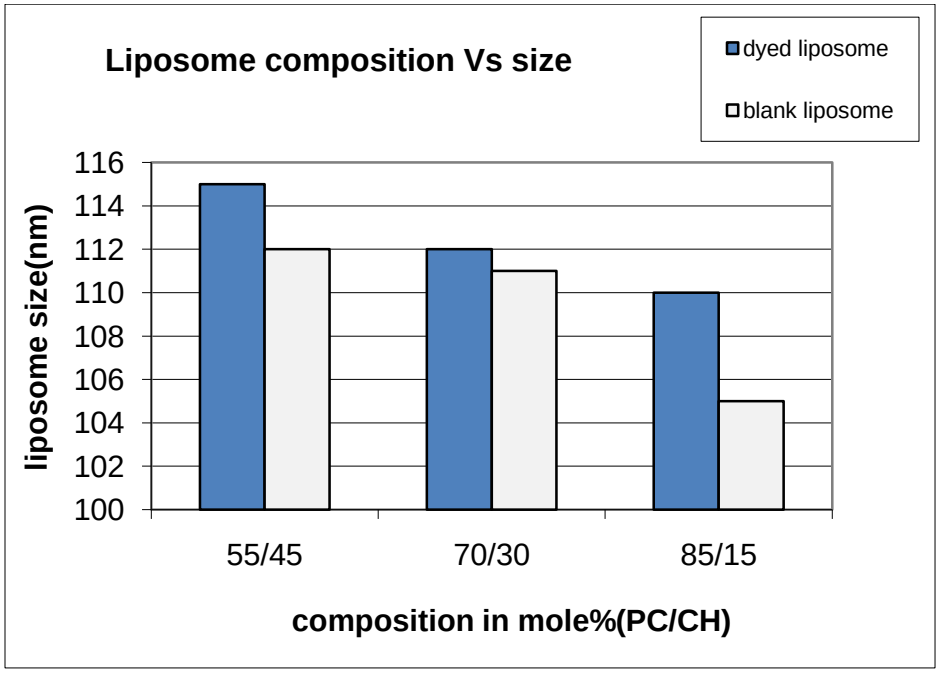

Figure 2-3. Effect of cholesterol composition and encapsulated material on liposome size. DLS size determination of 20mM DPPC/CH liposomes, encapsulated with 10μM CF dye or just a plain 20mM Hepes buffer.

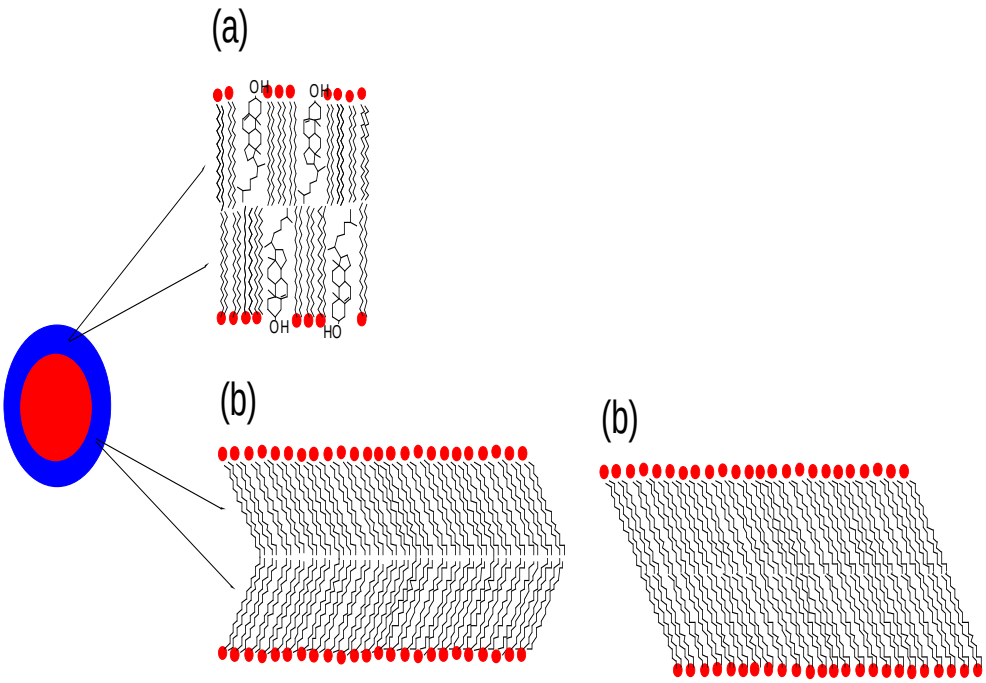

Figure 2-4. Lipid bilayer packing with and without cholesterol (a) cholesterol rich straight aligned lipid bilayer (b) cholesterol-poor tilted lipid bilayer (two hypothetical possible conformations), Reference #1*

*1. New, R. R. C. (1990) *Liposomes: a practical approach* Oxford University Press, New York, NY.

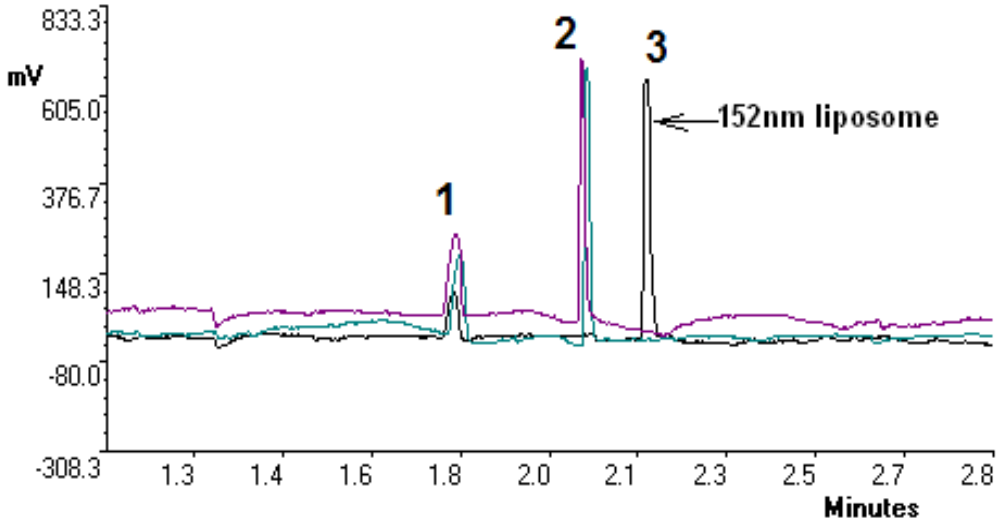

Figure 2-5. Effect of liposome size on its mobility (Tris buffer). Overlaid pherogram of 74, 95 and 152nm sized 20mM DPPC/cholesterol (45% CH) liposomes in Hepes buffer. Peaks #1 @1.8min are from uncharged internal standard mesityl oxide (t_{eo}), peaks #2 are by 74&95nm liposomes, and peak #3 is by the 152nm liposome. CZE run @30kv, 20mM Tris (pH7.3), bare fused silica capillary with 75µm ID and 65cm total length (45cm to detector). Liposomes are either encapsulated with 1mM Calcein or tagged with Rhodamine-B dyes for easy detection @ 219nm.

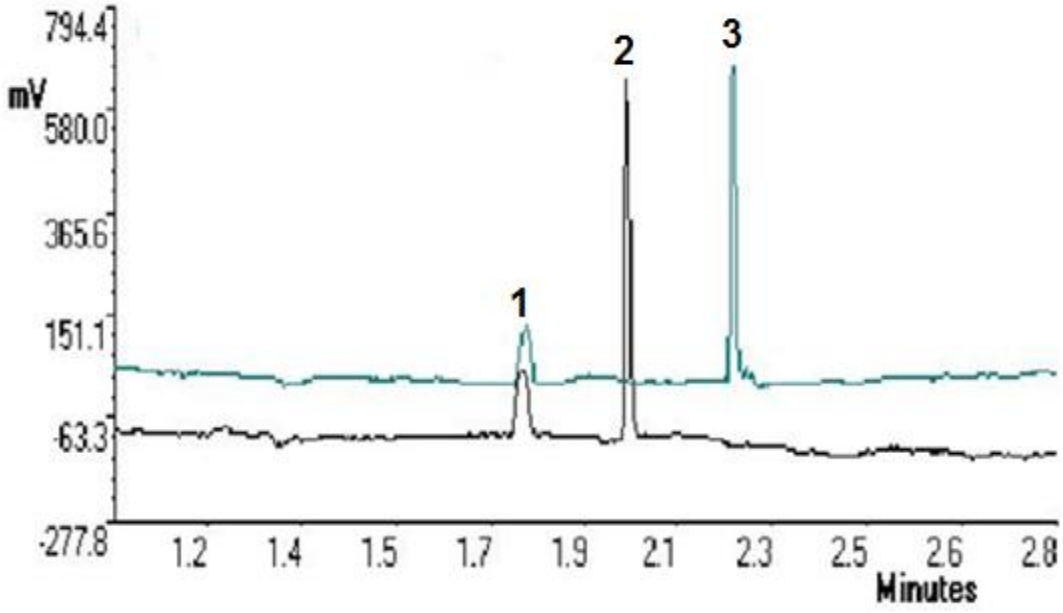

Figure 2-6. Effect of liposome size on mobility (Tris buffer). Overlaid electropherogram of 95 and 152nm sized DPPC/cholesterol liposomes in prepared in Hepes buffer. Peaks #1- t_{eo}, Peak #2 by 95nm liposome, and Peaks #3 is from the 152nm liposome (PC/CH 55/45). CZE conditions same as Figure 2-5

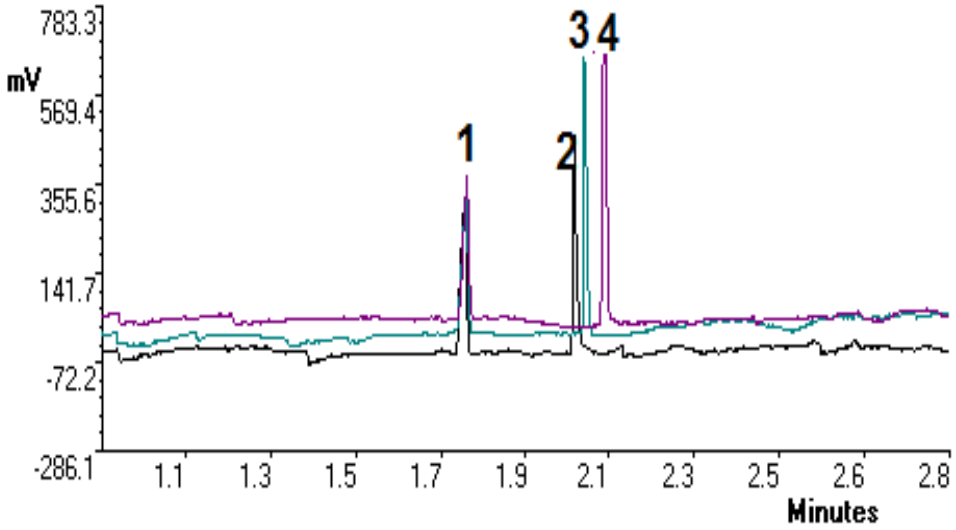

Figure 2-7. Effect of Hepes buffer and liposome size on electrophoresis (Hepes buffer). Overlaid electropheropherogram diffrent sized DPPC/cholesterol liposomes prepared in Heps buffer. Peaks #1- t_{eo}, Peaks #2, 3, and 4, are from liposomes with 76, 95nm and 152nm size, respectively. Lipid composition is DPPC/CH (55/45). Same CZE conditions as Figure 2-5.

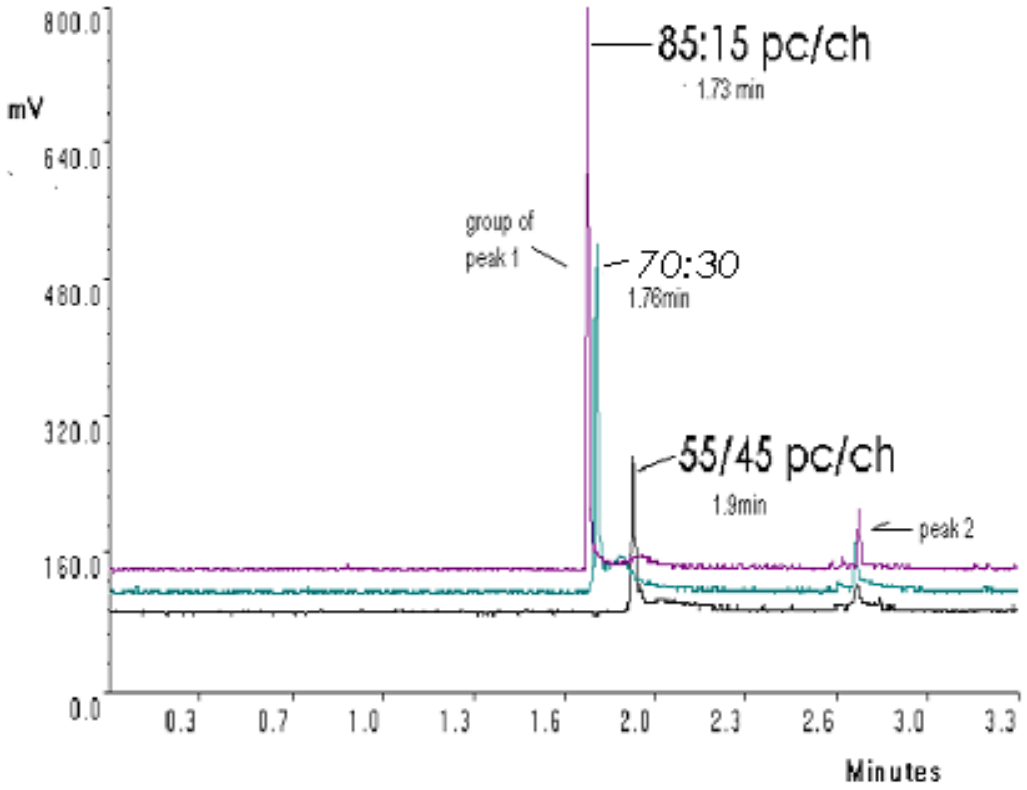

Figure 2-8. Effect of cholesterol composition on liposome migration rate. CZE-LIF run of 10μM carboxyfluorescein encapsulated DPPC/CH liposomes (85:15, 70:30, 55:45 % mole composition). Liposome suspension and CE run buffer is 20mM Hepes pH7.4. CE is run @30kV and LIF system is aligned @ 488/520nm excitation/emission wavelengths. Peak 2 is from the liposome leaked free carboxyfluorescein dye.

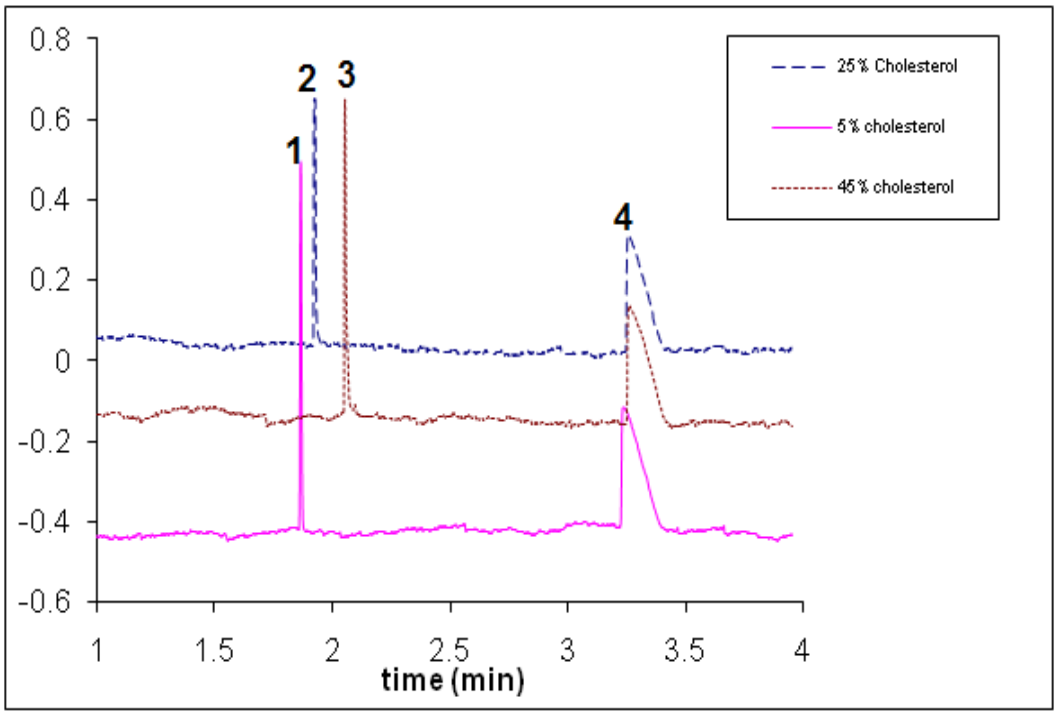

Figure 2-9. Effect of cholesterol composition on liposome migration rate. 20mM total (lipid+cholesterol) composition in 20mM Hepes buffer @pH7.3. A 10μg DPPE-RB added to each liposome composition for detection purposes. Each liposome is also spiked with 1mM carboxyfluorescein internal standard, peak #4 seen ~3.3min. Peak #1, 2, and 3 are from 5, 25 and 45% cholesterol containing PC-liposomes. All the CZE-UV conditions are same as Figure 2-5.

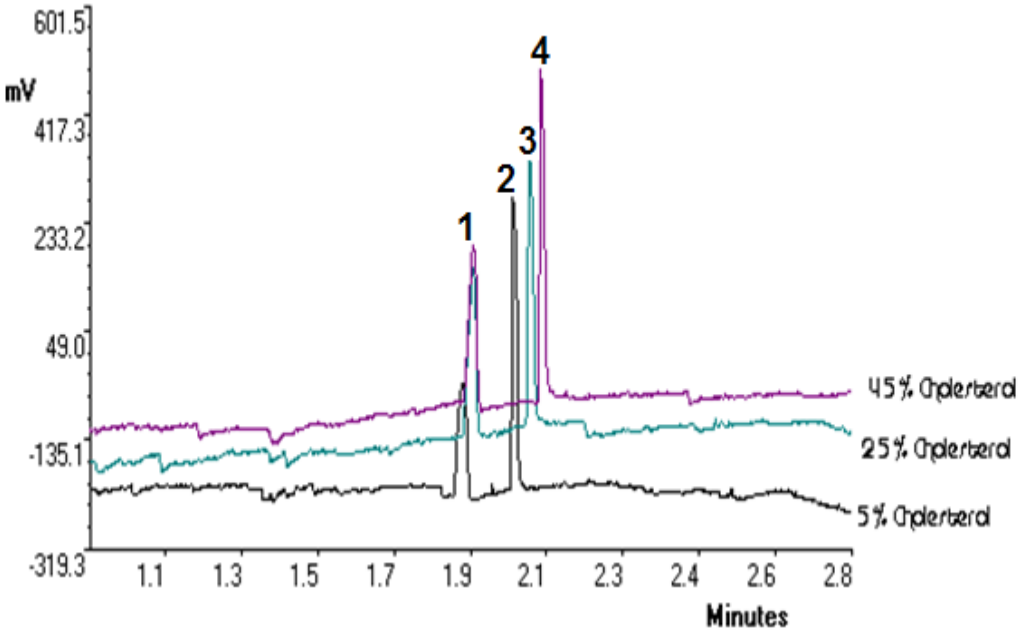

Figure 2-10. Effect of cholesterol composition on liposome electrophoretic migration rate. Overlaid electropherograms of 20mM DPPC with cholesterol liposomes (Peaks #1- t_{eo}, Peaks #2, 3, and 4, are from PC-liposomes with 5, 25, 45% mole cholesterol) run in hepes buffer. The liposomes are Rhodamine-B labeled. CZE run @30kV, UV detection @ 219nm in 20mM Heps @ pH7.3.

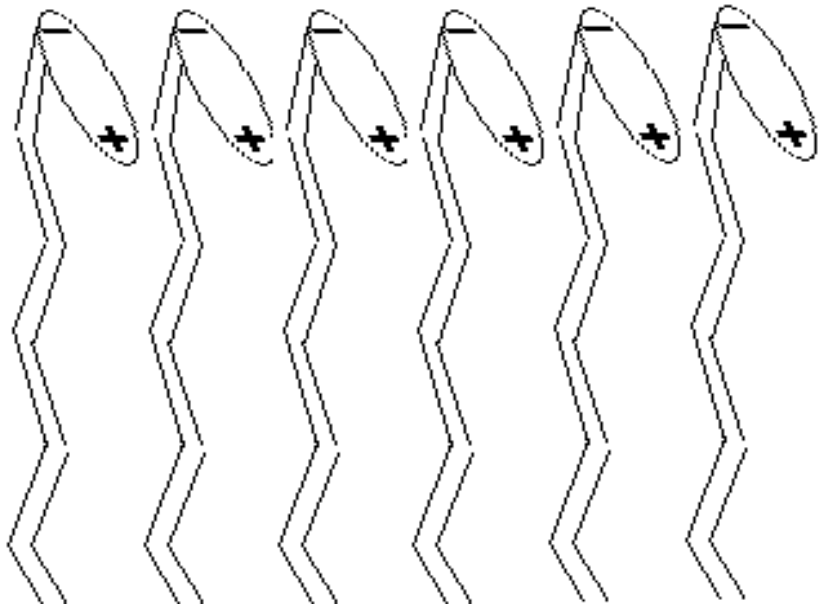

Figure 2-11. Dipole orientation of phosphatidylcholine head group dipole on membrane surfaces in a low ionic strength media. (Reference #37 and 38)

37. Makino, K., Yamada, T., Kimura, M., Oka, T., Ohshima, H., and Kondo, T. (1991) Temperature- and ionic strength-induced conformational changes in the lipid head group region of liposomes as suggested by zeta potential data, *Biophys. Chem. 41*, 175-183.

38. Jones, M. N. (1995) The surface properties of phospholipid liposome systems and their characterisation, *Adv. Colloid Interface Sci. 54*, 93-128.

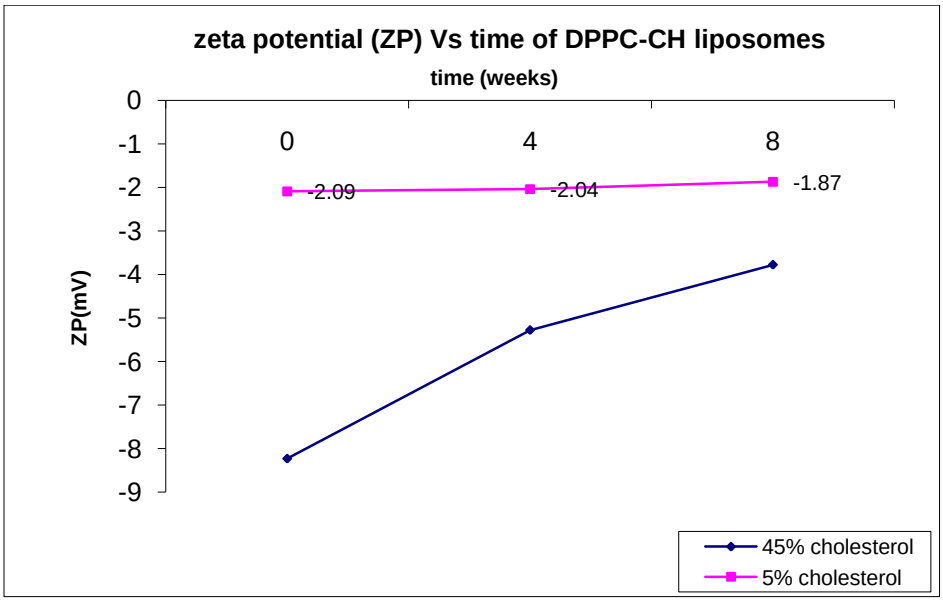

Figure 2-12. Zeta potential Vs time of storage for DPPC/Cholesterol liposomes.

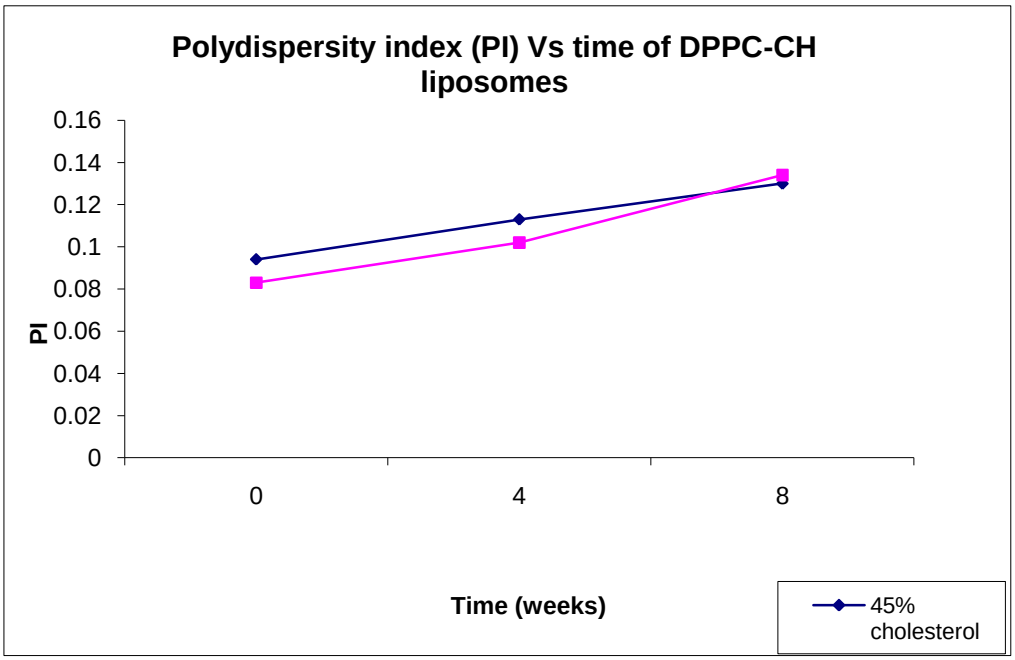

Figure 2-13. Polydispersity index (PI) Vs time of storage for DPPC/Cholesterol liposomes.

Reference list

[1] New, R. R. C. (1990) *Liposomes: a practical approach* Oxford University Press, New York, NY.

[2] New, R. R. C. (2005) Influence of Liposome Characteristics on Their Properties and Fate, in *Liposomes as tools in basic research and industry* (Philippot, J. R. and Schuber, F., Eds.) CRC Press, Boca Raton, FL.

[3] Lasic, D. D. (2005) Applications of liposomes, in *A Handbook of Bilogical Physics* (Lapowski, R. and Sackmann, E., Eds.) Elsevier, Amesterdam, The Nether.

[4] Lasic, D. D. (1993) *Liposomes : from physics to applications* Elsevier, Amesterdam, The Netherlands.

[5] Edwards, K. A. and Baumner, A. J. (2005) Analysis of liposomes, *Talanta*.

[6] Haskell, R. J. (1998) Characterization of submicron systems via optical methods, *J. Pharm. Sci. 87*, 125-129.

[7] Ingebrigtsen, L. and Brandl, M. (2002) Determination of the size distribution of liposomes by SEC fractionation, and PCS analysis and enzymatic assay of lipid content, *AAPS. PharmSciTech. 3*, E7.

[8] Grabielle-Madelmont, C., Lesieur, S., and Ollivon, M. (2003) Characterization of loaded liposomes by size exclusion chromatography, *J. Biochem. Biophys. Methods 56*, 189-217.

[9] Cohen, J. A. (2003) Electrophoretic characterization of liposomes, *Methods Enzymol. 367*, 148-176.

[10] Meulenaer, B. D., Van der Meeren, P., and Vanderdeelen, J. (2002) Electrophoresis of Liposomes , in *Encyclopedia of Surface and Colloid Science* (Somasundaran, P., Ed.) 1 ed., pp 2057-2070, Dekker, New York, NY.

[11] Malvern instruments (2001) Zeta Potential: An Introduction in 30 Minutes, Malvern instruments, London, UK.

[12] Khaledi, M. G. (1998) *High-Performance Capillary Electrophoresis: Theory, Techniques, and Applications* Wiley, New York, NY.

[13] Radko, S. P. and Chrambach, A. (2002) Separation and characterization of sub-microm- and microm-sized particles by capillary zone electrophoresis, *Electrophoresis 23*, 1957-1972.

[14] Wiedmer, S. K., Hautala, J., Holopainen, J. M., Kinnunen, P. K., and Riekkola, M. L. (2001) Study on liposomes by capillary electrophoresis, *Electrophoresis 22*, 1305-1313.

[15] Roberts, M. A., LocascioBrown, L., MacCrehan, W. A., and Durst, R. A. (1996) Liposome behavior in capillary electrophoresis, *Analytical Chemistry 68*, 3434-3440.

[16] Kawakami, K., Nishihara, Y., and Hirano, K. (1998) Compositional homogeneity of liposomal membranes investigated by capillary electrophoresis, *Journal of Colloid and Interface Science 206*, 177-180.

[17. Radko, S. P., Stastna, M., and Chrambach, A. (2000) Size-dependent electrophoretic migration and separation of liposomes by capillary zone electrophoresis in electrolyte solutions of various ionic strengths, *Anal. Chem. 72*, 5955-5960.

[18] Pysher, M. D. and Hayes, M. A. (2004) Examination of the electrophoretic behavior of liposomes, *Langmuir 20*, 4369-4375.

[19] Tsukagoshi, K., Okumura, Y., and Nakajima, R. (1998) Migration behavior of dyestuff-containing liposomes in capillary electrophoresis with chemiluminescence detection, *Journal of Chromatography A 813*, 402-407.

[20] Roberts, M. A., LocascioBrown, L., MacCrehan, W. A., and Durst, R. A. (1996) Liposome behavior in capillary electrophoresis, *Analytical Chemistry 68*, 3434-3440.

[21] Owen, R. L., Strasters, J. K., and Breyer, E. D. (2005) Lipid vesicles in capillary electrophoretic techniques: characterization of structural properties and associated membrane-molecule interactions, *Electrophoresis 26*, 735-751.

[22] Rodriguez, M. A. and Armstrong, D. W. (2004) Separation and analysis of colloidal/nano-particles including microorganisms by capillary electrophoresis: a fundamental review, *J. Chromatogr. B Analyt. Technol. Biomed. Life Sci. 800*, 7-25.

[23] Wiedmer, S. K., Jussila, M. S., Holopainen, J. M., Alakoskela, J. M., Kinnunen, P. J., and Riekkola, M. L. (2002) Cholesterol-containing phosphatidylcholine liposomes: Characterization and use as dispersed phase in electrokinetic capillary chromatography, *Journal of Separation Science 25*, 427-437.

[24] Duffy, C. F., Gafoor, S., Richards, D. P., Admadzadeh, H., O'Kennedy, R., and Arriaga, E. A. (2001) Determination of properties of individual liposomes by capillary electrophoresis with postocolumn laser-induced fluorescence detection, *Anal. Chem. 73*, 1855-1861.

[25] Radko, S. P., Stastna, M., and Chrambach, A. (2001) Polydispersity of liposome preparations as a likely source of peak width in capillary zone electrophoresis, *J. Chromatogr. B Biomed. Sci. Appl. 761*, 69-75.

[26] Burns, S. T. and Khaledi, M. G. (2002) Rapid determination of liposome-water partition coefficients (Klw) using liposome electrokinetic chromatography (LEKC), *J Pharm Sci. 91*, 1601-1612.

[27] Radko, S. P., Stastna, M., and Chrambach, A. (2000) Capillary zone electrophoresis of sub-microm-sized particles in electrolyte solutions of various ionic strengths: size-dependent electrophoretic migration and separation efficiency, *Electrophoresis 21*, 3583-3592.

[28] Hope, M. J., Nayer, R., Mayer, L. D., and Cullis, P. R. (1993) Reduction of liposome size and preparation of unilamellar vesicles by extrusion techniques, in *Liposome Technology: liposome preparation and related techniques* (Gregoriadis, G., Ed.) 2 ed., pp 123-139, CRC Press Inc., Boca Raton, FL.

[29] Liang, X., Mao, G., and Ng, K. Y. (2004) Mechanical properties and stability measurement of cholesterol-containing liposome on mica by atomic force microscopy, *J. Colloid Interface Sci. 278*, 53-62.

[30] Liu, D. Z., Chen, W. Y., Tasi, L. M., and Yang, S. P. (2000) Microcalorimetric and Shear Studies on the Effects of Cholesterol on the Physical Stability of Lipid Vesicles, *Colloids and surfaces A 172*, 57-67.

[31] Nagle, J. F. and Tristram-Nagle, S. (2000) Structure of lipid bilayers 9, *Biochim. Biophys. Acta 1469*, 159-195.

[32] McIntosh, T. J. (1980) Differences in hydrocarbon chain tilt between hydrated phosphatidylethanolamine and phosphatidylcholine bilayers. A molecular packing model
3, *Biophys. J 29*, 237-245.

[33] Roy, M. T., Gallardo, M., and Estelrich, J. (1998) Influence of Size on Electrokinetic Behavior of Phosphatidylserine and Phosphatidylethanolamine Lipid Vesicles, *J. Colloid Interface Sci. 206*, 512-517.

[34] Johnson, M. E. and Stokes, J. C. (2004) Resolution in sub-micrometer particle separations by capillary electrophoresis , *Microchemical Journal 76*, 121-129.

[35] Wiersema, P. H., Loeb, A. L., and Overbeek, J. Th. G. (1966) Calculation of the Electrophoretic Mobility of a Spherical colloid particles, *Journal of Colloid and Interface Science 22*, 78-99.

[36] Pincet, F., Cribier, S., and Perez, E. (1999) Bilayers of neutral lipids bear a small but significant charge, *The European Physical Journal B 11*, 127-130.

[37] Makino, K., Yamada, T., Kimura, M., Oka, T., Ohshima, H., and Kondo, T. (1991) Temperature- and ionic strength-induced conformational changes in the lipid head group region of liposomes as suggested by zeta potential data, *Biophys. Chem. 41*, 175-183.

[38] Jones, M. N. (1995) The surface properties of phospholipid liposome systems and their characterisation, *Adv. Colloid Interface Sci. 54*, 93-128.

[39] Ohvo-Rekila, H., Ramstedt, B., Leppimaki, P., and Slotte, J. P. (2002) Cholesterol interactions with phospholipids in membranes, *Prog. Lipid Res. 41*, 66-97.

[40] Vargha-Butler, E. I. and Hurst, E. L. (1995) Study of liposomal drug delivery systems 1. Surface characterization of steroid loaded MLV liposomes , *Colloids and surfaces B 761*, 69-75.

Chapter 3

Characterization of liposome permeability and encapsulation behaviors using CE-LIF and DLS techniques

Abstract

Understanding the permeability and encapsulation behavior of liposomes is vital since they have been used as membrane mimicking entities, drug delivery vehicles and analytical method development tools. In this study, we used capillary electrophoresis, with laser induced fluorescence detector (CE-LIF), together with dynamic light scattering (DLS), to study the permeability and encapsulation behavior of zwitterionic and anionic liposomes. Liposomes with different lipid, and cholesterol composition were encapsulated with 5um carboxyfluorescein dye and the fluorescence values were used to determine the captured volume (CV), also to understand the effect of a beta blocker drug (propranolol) on the liposome's permeability. The encapsulation of liposomes made from different composition of DPPC, DPPG and cholesterol was compared using a CE-LIF method. Increasing the cholesterol content of decreased the encapsulation capacity of PC liposomes. In addition, our CE-LIF results show that freezing and thawing (FAT) of the lipid suspension, prior to the extrusion step, produces liposomes with better encapsulation (CV) than non-FAT liposomes, as so indicated by others. In addition, the interaction of a beta-blocker drug, propranolol, with liposomes was monitored using DLS and CE techniques. The CE and DLS results show that propranolol perturbs cholesterol rich liposomes more than pure PC liposomes.

Introduction

Liposomes are widely used as biocompatible vehicles for the delivery of drugs and gene based therapy [1]. Liposomes are also used to encapsulate reporter molecules for signal enhancement purposes in bio-analytical assay development. The effectiveness of liposomes as delivery entities, and reporter molecule carriers depend on the nature and concentration of the encapsulated material, the liposome lipid composition and the method used to form the liposomes. The encapsulation efficiency, which is a measure of the total compound entrapped within the liposome, is an important parameter in liposomal characterization [2;3]. Encapsulation efficiency (EE) has been related to

- The captured aqueous volume per mole of lipid used (L/mole)
- The concentration of entrapped compound per mole of lipid used
- The ratio of concentration of the compound inside the liposome over its concentration in the loading solution.

The encapsulation efficiency and the degree of retention of the encapsulated material over a longer period have to be optimized in order to maximize the payload of the liposome formulation.

Liposomes can encapsulate materials both in their hydrophobic lipid bilayer and the aqueous compartment. Different compounds, from large proteins and enzymes to small molecules, including those of pharmaceutical interest and others have been incorporated inside liposomes' aqueous interior [4;5]. Similarly, successful entrapment of sparingly soluble drugs and related lipophilic compounds in the hydrophobic membrane have been achieved

with phosphatidylcholine and other mixed lipid-cholesterol liposomes [6;7]. Other studies have shown simultaneous entrapment of both hydrophilic and hydrophobic drugs in the same batch of liposomes [8]. Multilamellar liposomes are usually preferred for hydrophobic encapsulation, since they have multiples of lipid bilayers, while large unilamellar liposomes are desired for encapsulation of hydrophilic compounds. In a study by Stuhne-Sekalec and co-workers, the co-encapsulation of a hydrophilic compound like insulin and the hydrophobic cyclosporin was possible with liposomes prepared from egg yolk lecithin (PC), cholesterol, and stearylamine at a molar ratio of 7:2:2.25 [9]. The use of cationic liposomes for encapsulation and delivery of genes in recombinant DNA studies has become a common practice [10;11]. The incorporation of the anionic DNA molecules into the cationic liposome's lipid bilayer is driven by both electrostatic and hydrophobic interactions [12]. The future of antisense gene therapy for the treatment of various genetic disorders partly depends on a successful encapsulation of the nucleotide fragments in a non-toxic and efficient delivery vectors, like liposomes [13]. McKeon et al evaluated the efficacy of liposomal delivery of antisense oligonucleotide into cultured HeLa cell lines and have shown that there was an enhanced accumulation of the oligonucleotide in the cellular cytoplasm when liposomes were used for delivery, compared to passive permeation and electroporation methods [10]. The liposome's lipid composition has been one the major factors that influence drug encapsulation and the efficacy of delivery in to the cells during in-vitro studies [14;15].

Generally, hydrophilic compounds have to be incorporated during liposome formation process, whereas hydrophobic compounds can be incorporated into the liposome membrane both during the liposome formation process and also afterwards into the preformed liposomes. Encapsulation of biological molecules into the membrane of a preformed liposome can be facilitated by incubation with a low concentration of a detergent compound or an organic solvent like ethanol [16]. Most liposome formation methods start by dissolving the lipids in an appropriate organic solvent, like chloroform and methanol. The hydrophobic drugs, to be encapsulated, are mixed and co-dissolved in the organic solvent with the lipids and later dried to form a homogenous drug/lipid film. When the lipid film is hydrated with a buffer, the hydrophobic drugs stay solubilized in the lipid bilayer, whereas the hydrophilic compounds that are dissolved in the buffer are entrapped in the liposome aqueous cavity which is surrounded by the lipid bilayer.

Liposome's efficiency as an encapsulating agent depends on

- The nature and concentration of the material to be encapsulated
- The liposome's lipid composition
- The method used to form liposomes, and
- The size of the liposome.

In this study we examine the effect of the freeze-thaw extrusion method, and also the effect of varying the lipid and cholesterol composition on the liposome's encapsulation ability. Generally, highly charged hydrophilic compounds have better aqueous encapsulation in liposomes than neutral compounds. This is because charged solutes have low solubility in the

hydrophobic bilayer, and therefore they have a small chance of permeating (leaking) thru the membrane to the outer liposomal aqueous solution. Also, bulky and charged molecules have better encapsulation than small charged molecules since permeability is inversely related to molecular size [13]. The dependence of encapsulation on liposome size is expected to be linear, since liposomes with large diameter would typically have larger aqueous captured volumes, as long as lipid composition and the method used to make them are same. The liposome captured volume (CV), which is related to EE as noted earlier, has been shown to increase with the radius cubed, to be exact with $(r - \delta)^3$; where r is the radius and δ is the thickness of the membrane [13;49]. Accordingly, encapsulation increases in the following manner: small unilamellar vesicles, 20-100 nm (SUV) < large unilamellar vesicles (LUV), 100-200 nm < giant unilamellar vesicles, 0.5-5μm (GUV). Under certain circumstances, the liposome encapsulated volume may not increase proportionally, might even actually decrease, with an increase in liposome diameter. This might happen if the rate of increase in membrane-thickness, δ, is greater than the corresponding increase in radius as stated above and showed by equation 3-1 below,

$$EE \propto (r - \delta)^3 \qquad \textit{Equation (1)}$$

The lipid composition of liposomes is another factor that influences liposome encapsulation. Despite the extensive literature on mixed phosphatidylcholine (PC) and cholesterol liposomes, surprisingly there is limited information on the effect of lipid and cholesterol composition on the liposome encapsulation characteristics. The presence of cholesterol has been found to influence both hydrophobic (bilayer) and hydrophilic (aqueous)

encapsulation ability of liposomes [17-19]. Extended (time) encapsulation with PC liposomes has also been attained by incorporating cholesterol into the PC lipid bilayer [20;21]. Similarly, Xiang and coworkers showed the presence of a 0.25% (v/v) cholesterol in PC liposomes decreases membrane permeability by nearly ten-fold thereby enhancing retention of a hydrophilic marker which is entrapped inside the liposome aqueous interior [22]. As stated above, the primary reason for longer retention and decrease in leakage of the encapsulated aqueous compounds could be because of the enhanced hydrophobicity of the lipid bilayer in the presence of cholesterol. In a tumor targeted liposome-drug delivery design, a study by Nallamothu showed that, at 30 mol% cholesterol, soybean PC liposomes leaked the least, but at 45% cholesterol, not only did the drug loading capacity (encapsulation) decrease but the nonspecific leakage also increased [23].

Mixing charged surfactants and lipids with egg PC and cholesterol, when forming small unilamellar vesicles (SUV), have been found to enhance the encapsulation efficiency of unilamellar liposomes [24]. In the above mentioned study by Benita and co-workers using aqueous marker sodium ioxitalamate, the liposome's captured volume were higher for the charged SUVs than for the zwitterionic PC SUVs, with equal total lipid concentration. The electrostatic repulsion between the charged liposomes contributed to the enhancement of their encapsulation by curbing the nonspecific leakage caused by fusion and aggregation to which neutral SUVs are susceptible.

The other important factor that determines liposome aqueous encapsulation, beside the lipid composition, is the method (or technique) used to form the

liposomes. As mentioned before, when a dry lipid film is hydrated, it spontaneously forms large multilamellar vesicles (MLV) upon shaking or agitation. Then, to form small and large unilamellar liposomes, additional energy is applied to the MLV suspension through extrusion or sonication. MLVs have a very poor aqueous encapsulation due to their multilayer onion like membrane structure, which occupies a large part of the liposome's interior. But, the trapped aqueous volume of MLVs can be increased by breaking their extra internal-lamellae structures and forming large unilamellar liposomes (LUV) by sonication or extrusion [25]. Also, the repeated actions of freezing and thawing (FAT) of MLVs, prior to sonication or extraction, causes a physical disruption of the multilayer membranes, thereby facilitating the formation of unilamellar liposomes [26;27]. The freeze and thaw cycle serves to break apart the closely spaced lamellae of the MLV thereby enhancing the aqueous trapping volume per mole of lipid used [28;29]. The experimental results from Macdoland's study indicate that there was a 1.1L net increase in the captured volume of the LUVs per mole of lipid used, when the MLVs are freeze-and-thawed before extrusion [25]. This means, LUVs made by a combination of repeated FAT and extrusion cycles, had been found to have a captured volume that was better by a 1.1(L/mole) than just extruded LUVs [25;29]. The freeze-thaw cycle, together with extrusion, technique has commonly been used in pharmaceutical applications to improve liposome's size homogeneity and increase the encapsulation ability [30].

There are different assays to measure the aqueous captured volume and the encapsulation efficiency of liposomes that have different sizes or various

lipid compositions. The captured volume, usually defined in liters per mole lipid used, has been measured by variety of instrumental techniques. Some of the techniques used include: fluorescence spectroscopy [31;32], conductivity [33], proton NMR spectroscopy [34] and others [2]. The most common method of studying liposome encapsulation involves incorporating an impermeable fluorescent dye inside of the liposome aqueous interior, filter out the untrapped dye in the bulk solvent, lyse the encapsulated-liposome with a detergent, and measure the fluorescence signal of the released dye. The two commonly used fluorescent dyes around the neutral pH are, calcein and carboxyfluorescein. When these dyes are encapsulated in a liposome at concentrations larger than 100mM, their fluorescence is quenched by more than 90 % [35]. The mechanism of fluorescence quenching of a dye is not clearly understood when it is in aqueous solutions at concentrations >10mM and encapsulated in a liposome. However, leakage from the liposome into the bulk aqueous media and subsequent dilution of the dye would result in an increase its fluorescence signal. As can be seen in Figure 2-2 (chapter 2) these fluorescent markers have bulky molecular structures and carry multiple charges, which reduces their membrane permeation ability, making them suitable candidates for encapsulation studies. The most commonly used method to measure liposome captured volume has been the quenched fluorescent dye method. The measurement of the captured aqueous marker is done after removing the un-trapped marker by centrifugation, gel filtration or dialysis. However, most of the assays used for encapsulation studies are inefficient, time consuming, costly and mostly suffer from irreproducibility. Therefore, simple, efficient and robust

analytical techniques are still required in order to accurately characterize encapsulation of liposomal formulations. The liposome self quenched fluorescence (SQF) technique has been widely used in membrane mimicking studies. But, unfortunately the SQF technique has some disadvantages including:

- The preparation of the dye solution is tedious and complicated at neutral pH since these dyes are not readily soluble in aqueous buffers at concentrations higher than 0.5mM. The dye is initially dissolved in concentrated NaOH solution and then it is adjusted to neutral pH. Also, the solid dye from chemical suppliers usually has impurities that necessitate purification of the prepared solution by dialysis or gel filtration [36;37]. After purification, the pH and concentration are adjusted to the required concentration, and then the dye is ready for encapsulation. Therefore, the sample preparation process prior to encapsulation is tedious, time consuming and generally inefficient.
- The encapsulation of a dye with a concentration in excess of 100mM will certainly create an osmotic pressure that will destabilize liposomes and make them prone to nonspecific leakage unless the external bulk aqueous solution is osmotically balanced with addition of NaCl in excess of 100mM in order to maintain iso-molarity on both sides of the membranes of the liposomes [35]. Presence of the salt at high concentrations will most likely modify the membranes' microenvironment and compromise the reliability and accuracy of the SQF experiments.

In our study we have developed a novel and efficient method for

determination of liposome encapsulation volume using capillary electrophoresis with laser induced fluorescence (CE-LIF). The high sensitivity of the CE-LIF method allows the use of fluorescent dyes (CF or calcein) at much lower concentrations (<20μM) than that in SQF experiments. In addition, CE-LIF allows the elution and detection of peaks from: the intact (dye encapsulated) liposome, the internal standard, the leaked dye (if any) and other peaks of interest there might be in the sample within a single injection/run. This new method was used to study liposomes' encapsulation and permeability behaviors. It combines the resolving power of CE and the sensitivity of laser induced fluorescence spectroscopy.

In a related study, liposomes encapsulated with these dyes were also used to mimic drug-membrane interactions, such as the effect of drugs on the permeability of real membranes. The results indicate that the liposome permeability mainly depends on the lipid composition, beside other factors. The permeability behavior of liposome membranes show a great deal of similarity to that of natural membranes [38]. As explained earlier, liposome permeability studies using fluorescent dyes are useful in helping to determine the optimum lipid formulation for liposomal encapsulation of drugs, nucleotides, markers and other polar molecules. Permeability of liposomes changes when their membranes are exposed to chemical or physical stresses. Physical stress includes changes in temperature and pressure, while chemical stress may include changes in pH and chemical interactions with external compounds (drugs, antimicrobial peptides, etc…) that might modify the lipid packing structure. Generally, there are two possible ways of monitoring changes in liposome permeability during an

interaction with an extra-vesicular solute. One way of monitoring the change in membrane permeability, due to a solute's interaction, is to encapsulate the solute in the liposome interior and directly monitor its leakage to the extra vesicular solution. But, monitoring the solute's concentration, which might be present both inside and outside of the liposome, could be quite challenging unless the solute has fluorescence or other detection qualities to enhance its sensitivity. A simple and more rugged method to study the change in liposome permeability, due an interaction with a solute, is done by incubating the solute with a dye encapsulated liposome and measuring fluorescence of the leaked dye [39]. This perturbation by the solute may create a structural (lipid packing) defects that would cause the leakage of the encapsulated dye from the liposome aqueous interior through the lipid bilayer to the outer aqueous medium. Furthermore, the extent and rate of the dye's leakage depends on the size of the defect created (pore size), and how large the dye molecules are as compared to the pore created. The deeper a solute (from the outer aqueous medium) partition into the hydrophobic bilayer, the stronger is the perturbation on the lipid bilayer, thereby enhancing the membrane's permeability to the encapsulated dye [40;41]. Experimentally, the perturbation effect by different solutes can be compared by measuring the relative fluorescence of the leaked dye before and after the incubation of the liposome with each of the solutes. The extent of the dye's leakage from liposome due to contact with a solute is determined from the relative fluorescence (F) of the leaked dye and is calculated by

$$F = \left[\frac{F_t - F_0}{F_\infty - F_0} \right] X 100\% \qquad \textit{Equation (2)}$$

F_t – Fluorescence after incubation of liposome with a solute

F_0 – Initial fluorescence after dilution of liposome in iso-molar buffer

F_∞ – Maximal fluorescence after total lysis of liposome by a detergent

A strong solute interaction with the liposomal membrane would result an increase in the fluorescence (*F*) signal of the leaked dye, which is expected to be dependent on the nature of the solute and its concentration in the bulk aqueous solution [42;43]. A high *F* value indicates a strong solute-membrane interaction. In the absence of any perturbing solute, the latency of the encapsulated dye can be a measure for the stability of a liposome preparation. The latency of an encapsulated dye, like carboxyfluorescein (CF), is determined using a simplified version of *Eq(2)*. A large latency, *Eq(3)* below, of the dye indicates a high degree of membrane integrity with most or the entire encapsulated marker still trapped inside the liposome [43].

$$\%CF(latency) = 1 - \left[\frac{F_0}{F_\infty}\right] X 100\% \qquad \textit{Equation (3)}$$

A CE-LIF method was used to monitor the effect of propranolol on the permeability of dye encapsulated PC and PC/CH liposomes. Propranolol is a non-selective beta blocker drug that is mainly used in the treatment of hypertension. It exhibits a specific and non-specific membrane interaction effects across a wide range of concentrations. In concentrations < 10^{-7}M, it acts specifically as an antagonist of the catecholamine receptor but at higher concentrations it also displays a non-specific local anesthetic activity. In its simplest presentation, the lipid theory of anesthesia postulates that anesthetics dissolve in lipid bilayers of biological membranes and induce

loss of sensation when they reach a critical concentration in the membrane [44]. Above this critical concentration, anesthetics like propranolol affect the membrane's physical characteristics, which may indirectly influence the structural conformations of the membrane-proteins that are part of the membrane. Furthermore, the polar functional groups of anesthetic drugs could interact with the membrane-embedded proteins in selective manners [44;45]. Therefore depending on its concentration, propranolol can have local anesthetic, as well as a beta adrenergic blocking activities. As can be inferred from its molecular structure (Figure 3-1), lipophilic moieties of propranolol can interact with lipid bilayer segment of membranes that would modify the lipid packing structure thereby changing the liposomes' permeability properties. Generally, different published studies on membrane interaction with propranolol, and other beta-blockers, have showed that the naphthalene moiety of the molecule partitions in the hydrocarbon region of the bilayer modifying the lipid packing while the amine moiety of propranolol interacts with the polar lipid head groups which are located near the aqueous interfacial region [40-43;51]. In this study we developed a simple capillary electrophoresis laser induced fluorescence (CE-LIF) method, and used it to study the permeability of different liposomes, when they interact with a therapeutic dose of propranolol (~1mg/ml, @ (1:1) lipid/drug molar ratio).

Experimental

Materials & methods

Chemicals

1,2-Dipalmitoyl-*sn*-Glycero-3-Phosphocholine (DPPC), DPPG, and cholesterol are from Avanti Polar Lipids. 1M HEPES (pH 7.3 ± 0.1), propranolol and Tris-HCl buffers, Mesityl oxide were purchased from Fisher. Deionized 18MΩ water was obtained in-house from a reverse osmosis Millipore system. The hydrophilic marker dyes Calcein, Carboxyfluorescein and Alexa fluor are obtained from Probes-Invitrogen. Size exclusion gel Sephadex G-50 and MicroSpin filter columns (part # 27-5330-01) were obtained from Amersham Biosciences. The molecular structures of the lipids and fluorescent dyes used in this study are shown in chapter 2 (Figure 2-1).

Capillary Electrophoresis

The CE-UV experiments were carried out on a laboratory-built instrument. A Spellman SL30 high-voltage power supply was used to apply a positive voltage over the length of the fused silica capillary (Polymicro Technologies, Phoenix, AZ, USA), with an inner diameter of 50 μm and an outer diameter of 362 μm.

The CE–LIF system consisted of an argon ion laser (Omni Chrome, CA, USA) modulated by a chopper controlled by a lock-in amplifier (EG&G, Trenton, NJ, USA). The 488 nm modulated laser line was focused onto the 50 μm I.D.×362 μm O.D. bare fused-silica capillary (Polymicro Technologies, Phoenix, AZ, USA) through an upright microscope with a

40X fluorite objective which both sent the excited fluorescent beam and collected the emitted beam. The laser excitation beam would pass through a dichroic filter (495nm) and the subsequent emission beam would pass through a long pass (500nm) and short pass (515nm) filters and transmitted to the photomultiplier tube (Hamamatsu, Bridgewater, NJ, USA). The signal was then sent to the A/D converter and the lock-in amplifier. All data acquisition and analysis for the CE-LIF experiments was performed using PC/Chrom^{+} and LabView softwares.

Liposome size and size-distribution

The hydrodynamic diameter and the poly-dispersity (size-distribution index) of all liposome preparations were determined by Dynamic Light Scattering (DLS) technique using the Malvern Zeta Sizer model 1000HSa. The instrument calculates the average size and polydispersity (PI) of the liposomes based on the measured time-dependent fluctuations of the light scattered by liposomes [46].

Preparation of dye encapsulating liposomes

All liposome suspensions were prepared by the extrusion method developed by Hope, M.J, and coworkers, with a slight modification, using the Lipex® 10ml thermo barrel extruder (Northern Lipids Inc., Vancouver, BC Canada) [47](46). Lipids at a total concentration of 10mg/ml are first dissolved in a 3-5ml of chloroform in a 50ml round bottom flask, and a 10% methanol is also added when anionic lipids like DPPG are present. A dried thin lipid film is formed around the flask inside walls after a 30-45 minutes of rotary evaporation on the Bushi Roto-Vap, under low pressure and at 50°C. The

dried lipid film is hydrated with 3-5 mL of pure buffer or a buffered-dye solution with continuous shaking at a temperature above the lipid phase transition temperature T_m (for DPPC ≥ 41°C) to form a stable multi lamellar vesicle (MLV) suspension. After vortexing and homogenizing the MLV suspension, it was first extruded about 7 times on a *single* 200nm Nucleopore Polycarbonate membrane (Whatman Inc. USA) in the 10ml Lipex extruder at 60°C and a low N_2 pressure (<100psi). Finally, the liposome suspension was extruded at least ten times through a *double* 100nm Polycarbonate membrane at a pressure of 200-400psi. During all the extrusions the temperature was maintained at least 10°C above the lipid transition temperature (T_m), so as to maintain a reasonable flow at moderate extrusion pressures. All the final liposome preparations were stored at 4°C until further analysis.

Separation of un-trapped marker and liposome

The 6-carboxyfluorescein (6-CF) dye was encapsulated at 5μM concentration during liposome formation. For the CE-LIF experiments the encapsulated liposomes have to be separated from the free un-trapped hydrophilic dye on Sephadex G-50 gel filtration micro-columns (750μL), since the fluorescence signal due to the free (untrapped) dye interferes with detection of the liposome peak Sephadex G-50 gels have an average fractionation range of 500-10,000Daltons. The gel column is prepared first by boiling about 1g of Sephadex G-50 fine powder in 15-20ml of DI-water for an hour in a covered beaker. One gram of G-50 powder is converted to 7-9ml thick slurry or gel. The gel is cooled to room temperature before it is

filled into 1ml micro-columns filling 70% of the volume. The column is equilibrated with (100μL) blank liposomes before loading the liposome/dye mixture to separate the liposome from the unencapsulated dye. The liposome/dye mixture (50-75μL) is gently injected on to the gel micro-columns and the encapsulated-liposomes are separated from the free (unencapsulated) dye after centrifugation for 2 minutes @1000rpm. The low molecular weight dye (<5000) is trapped in the gel while the liposomes are excluded and elute first with the void-volume at almost zero dilution. The concentration of the trapped dye and the liposomes' captured volume (CV) are determined after liposome lysis and releasing of the trapped dye with a detergent solution. The liposome captured volume (CV) for different lipid compositions is determined based on dilution calculations as suggested by Perkins et al [2]. The lysing agent was either a 0.2% (v/v) Triton-X100 or a 15mM deoxycholic acid (or sodium deoxycholate) solutions. Each of the liposome samples prepared for CE-LIF run are spiked with 10nM Oregon-green dye, which serves as an internal standard for CE analysis.

Results & discussion

The objective in this part of our project was to devise CE-LIF methods to study the following liposome characteristics:

- The effect of lipid composition on the encapsulation ability of large unilamellar vesicles (LUV) made by extrusion. The encapsulation of different liposomes composed of various lipids (zwitterionic and anionic) and cholesterol are compared by measuring the fluorescence

intensity of the carboxyfluorescein dye trapped inside the liposome's aqueous compartment (after liposome lysis & leaking out the dye).

- The effect of freeze and thawing (FAT), before extrusion, on the liposome capture volume (CV).
- The effect propranolol, a beta-blocker drug, has on the permeability of dye encapsulated liposomes with different lipid compositions.

As discussed in chapter 2, the effect of size on encapsulation is linear (Figure 2-7). The CE-UV electropherogram on Figure 2-7 qualitatively shows that the fluorescence peak intensity is the largest for the 150nm liposome and was the lowest for the 76nm liposome. In general, for liposomes with the same lipid composition, the captured volume (CV) is expected to increase with size.

The captured volume of a population of liposomes can be estimated from measurements of the total quantity of the solute entrapped inside liposomes. Here an assumption is made, similar to that made by Perkins [2;48], in order to determine the (aqueous) captured volume by a mole of lipid. The assumption is that, the concentration of the dye captured inside the liposome is the same as the concentration of the loading solution (5μM). It is further assumed that dilution of the trapped 5μM dye due to osmotic imbalance is minimal, after the extra-liposomal dye is removed by gel filtration [2;48]. Then, the capture volume (CV) can be determined with a simple dilution equation given below:

$$V_{vc} = \frac{V_{lys} C_{lys}}{C_{in}} \qquad \textit{Equation (4)}$$

V_{vc}— Aqueous captured volume (μL) by liposome in the suspension.

V_{lys}— Total volume of suspension after lysing agent added (μL).

C_{lys}— Diluted concentration of dye after liposome lysis (μM), determined from calibration curve (Figure 3-3)

C_{in}— Concentration of dye entrapped by suspended liposomes, before lysis, same as loading solution concentration (5μM)

The liposome captured volume per mole of lipid (L/mole) is determined from V_{vc} and the amount of lipid (mole) in each CE-LIF injected liposome sample. Using this method, the captured volume calculated for large extruded DPPC/CH (95:5) liposomes encapsulating 5um carboxyfluorecein was 0.14L/mole (liter per mole of lipid used), while freeze-thawed (FAT) then extruded liposomes had a 0.3L/mole captured volume. The liposome captured volumes (CV) given above were calculated from the concentration of the encapsulated fluorescent dye (C_{lys}), which was determined from the calibration curve (Figure 3-2), after detergent lysis of the liposome.

The freeze-thaw process of the lipid suspension enhanced the encapsulated volume of the extruded liposomes by more than 100%. The DLS data on table 3-2 shows the effect of liposome freezing and thawing (FAT) on the encapsulation. Each of the FAT PC/CH liposome on Table 3-2B has double the fluorescence, hence double the encapsulation, than a NON-FAT PC/CH liposome with the same lipid composition seen on Table 3-2A. The freeze-thawing of the lipid suspension before extrusion doubled the CV of DPPC/CH (95:5) liposomes (0.14 to 0.30L/mole), since it breaks apart the extra multi-layers of membranes, thereby improving the encapsulation

capacity of water soluble compounds, as also cited by others [29;50]. The freeze-thaw preparation method generates a size and encapsulation variability in both pure PC and PC/Cholesterol liposomes, as seen from the fluorescence and size measurements (Table 3-2) by CE-LIF and DLS techniques. The relative fluorescence, or encapsulation, of the freeze-thawed liposomes (FAT-LUV100) in Table 3-2B is almost twice that of the non-FAT liposomes on Table 3-2A. The total lipid concentration of both liposome batches, on tables A & B, are the same but the cholesterol content increases down the table from the 95/5 to 65/35 PC/CH composition. The effect of freeze and thawing of the multiple lamellar vesicle (MLV) suspension, before extrusion, on the trapping efficiency has also been studied by others [25-30]. According to Hope et al and others [27-29], the rupturing of the inner onion like membrane layers of the MLV's during the repeated freezing process is due to the formation of ice crystals (expansion) found in-between the lipid membrane. Subsequently, fewer large diameter layers of the MLV re-seal back during thawing step, thereby increasing the trapped aqueous volume of the PC-rich (low cholesterol) liposomes. But, when the cholesterol content is increased, so does the rigidity of the (multi-layered) PC-membranes, which becomes resistant to rapture, eventually decreasing the capture volume of the unilamellar liposomes [27].

The effect of cholesterol on encapsulation property of DPPC liposomes is shown on table 3-1. When the amount of cholesterol in the DPPC liposome is increased, from 5 to 45% by mole, the relative fluorescence of the encapsulated dye decreased. In other words, as more cholesterol is incorporated in the DPPC liposome, its encapsulation decreased. The 45%

cholesterol-DPPC liposome was the largest in size, but has the lowest encapsulation for the carboxyfluorecein dye. In order to quantify the dye, it was first released from the liposome with sodium deoxycholate lysing agent and then its fluorescence intensity measured with a CE-LIF system. Similar trend on the effect of cholesterol composition and encapsulation (capacity) is seen in Table 3-2 which shows a decrease in fluorescence as the liposomes' cholesterol amount increases, using two different extrusion methods of preparation, one including freeze-and-thaw (FAT) and the other without the FAT step (non-FAT liposomes). For both FAT and non-FAT liposomes, the PC rich liposomes (95% PC) had the highest fluorescence from the encapsulated dye, while the fluorescence was low for the cholesterol rich liposomes (45% cholesterol). But this decrease in fluorescence, after increasing the cholesterol composition, was accompanied by an enlargement of the liposome's size. Predictably, one would expect the encapsulation to increase proportionally with the increase in liposome size. But, as shown on tables 3-1 and 3-2, the liposome encapsulation (relative fluorescence) decreased, despite an increase in liposome size with cholesterol composition. The possible reasons for the low aqueous encapsulation by the cholesterol-rich liposome could be that the presence of more cholesterol is excluding some dye molecules from the liposome entrapment during the extrusion and the FAT process. Since cholesterol imparts rigidity to the multi onion like membranes of the MLV, the cholesterol-rich membrane could be more resistive to extrusion process which produces the LUVs from the MLVs. As noted earlier, LUVs have a better aqueous encapsulation capacity than MLVs. From studies by others,

there has been some evidence that liposome membrane thickens with high cholesterol composition [17]. So, as mentioned earlier in the introduction (equation 3-1), an increase in membrane thickness (δ) may also in part contribute towards a decrease in encapsulation; in addition to other factors [1;17].

The effect of anionic lipid (DPPG) on liposome size and aqueous encapsulation is seen from the DLS and fluorescence results on Figure 3-2. It shows that relative fluorescence and liposome size decrease with an increase in the mole fraction of the negatively charged lipid, DPPG. The relationship between the relative fluorescence and liposome size in this case is opposite to that observed for liposomes containing cholesterol. It is evident that the liposome composition has more influence on encapsulation than the size. The liposome with the most DPPG, which is the 80/20 PC/PG liposome, had the lowest fluorescence, hence lowest CF encapsulation. The electrostatic repulsion between the anionic lipid PG and the anionic dye CF might contribute toward a decrease in encapsulation of CF by the PC/PG liposomes. The size of PC liposomes decreased, when PG is added up to10% by mole of the total lipid as seen on Figure 3-2. Generally, we have observed that pure PC liposomes were always larger in size than mixed PC/PG liposomes, for the same amount of total lipid and method of preparation. The electrostatic repulsion between individual PC/PG liposomes, which hinders aggregation, could be one of the reasons why a population of charged liposomes has an average size that is smaller than a population of pure PC and PC/cholesterol liposomes [1]. As stated in the experimental section, all the liposomes with different lipid compositions were prepared under the

same experimental conditions and finally extruded through 100nm membrane filter. But, their variability in size and encapsulation comes from their composition, mainly due to the presence of cholesterol and anionic lipid, DPPG. The presence of more cholesterol and PG in DPPC liposomes led to lower entrapment of the CF dye, as determined from the fluorescence results. There is also a clear and direct relationship between the size and cholesterol content of PC/CH liposomes.

The effect of the beta-blocker drug propranolol, on the permeability of PC-liposomes with and without cholesterol was found to be quite different. The fluorescence of the leaked dye is used for a qualitative comparison and it is based on the CE-LIF peak intensities seen on Figure 3-4 and 3-5. In addition, DLS results (table 3-3), also indicate that propranolol interacts differently with liposomes based on their cholesterol content. The peak height (Figure 3-4) of the dye that leaked from the cholesterol-rich liposome (9mM cholesterol) was the largest and the smallest was from the cholesterol-poor liposomes (1mM). This implies that the permeability/leakage of the 9mM cholesterol liposomes was more enhanced from the interaction with propranolol than the 1mM cholesterol liposomes. Correspondingly, the control experiment on the same dye encapsulated liposomes, without propranolol, did not show any fluorescence due to a leaked dye (Figure 3-4). In both Figure 3-4 and 3-5 the first eluting peak is from the intact dye-encapsulated liposomes, while peak 3 on Figure 3-5 is from the leaked dye by PC/CH liposomes incubated with propranolol. The liposomes were incubated for 24 hrs with an equimolar amount of propranolol (1mg/ml), a therapeutic dose, and the liposomes had different cholesterol composition.

The liposomes with the highest cholesterol destabilized and leaked the most from interaction with propranolol. Figure 3-4 shows that in the absence of propranolol, there was not leakage for any of the liposome formulations.

Apparently, the presence of higher level cholesterol in the membrane could enhance the interaction with propranolol, thereby creating membrane packing irregularities that facilitate permeability and leakage of the trapped dye. The perturbation of phospholipid membranes by beta blocker drugs and other membrane-active solutes has been reported by few studies [40;51-54]. The findings from differential scanning calorimetry (DSC), X-ray and neutron diffraction studies show that amphiphilic drugs, like propranolol, insert deep into the hydrophobic region of phosphatidylcholine membranes [51;55-57]. But, since all of these studies used lipid membranes without cholesterol, it was vital for us to include cholesterol in our liposomes so as to study the effect it has on the liposome's permeability and morphology during membrane-drug interaction. Generally, adding cholesterol to PC-liposomes has been found to make the middle region of the membrane more hydrophobic [58]. So, since propranolol has a very lipophilic naphthalene moiety, it is expected to partition deeper into the hydrophobic acyl region of PC/CH liposomes than in plain PC-liposomes [59-61]. The drug's penetration perturbs the lipid packing structure causing an enhanced permeability/leakage of the encapsulated dye as seen from leakage-fluorescence by the 4 and 9mM cholesterol liposomes in Figure (3-4a) and (3-4b). The control liposomes, which have the same lipid/cholesterol composition, but did not include propranolol in the buffer solution, exhibited no leakage during the overnight incubation (Figure 3-4).

The change in the average size and polydispersity index (PI) of cholesterol/PC-liposomes, after propranolol interaction, was measured by DLS. The result (Table 3-4) indicates that the liposomes with more cholesterol composition (4 and 9mM) showed larger increase in size and PI than the PC-liposomes with only 1mM cholesterol. A few studies have indicated that propranolol causes lipid rearrangement, followed by an increase in the average size and polydispersity of PC-liposomes [52;53]. A light scattering and FTIR spectroscopy study into this interaction, by Cao et al, indicated that the size of DMPC liposomes increased, by up to 10%, after interaction with D-propranolol [53]. They propose that the penetration of propranolol between the lipid molecules makes the membrane interfacial region more hydrophilic which then thickens the water-interface sub layer (of the membrane) due to the increased number of water molecules binding to the membrane interfacial region that has become more hydrophilic [51;53]. Therefore, a deeper insertion of amphiphilic molecules, like propranolol, could decrease lipid chain order and make the membrane less compact thereby increasing its permeability [59-61]. This effect may be enhanced in the presence of large cholesterol content in the membrane.

Conclusion

In this project we developed a simple and sensitive CE-LIF method to characterize the encapsulation and permeability properties of liposomes. The encapsulation volume of large extruded DPPC liposomes was determined to be 0.14 (L/mole of lipid), while the FAT liposomes roughly had twice the encapsulation (0.3 L/mole) than the non-FAT DPPC liposomes. Also, as a result of the high sensitivity of the CE-LIF method, a consistent and reproducible data was obtained that shows an inverse relationship between the cholesterol content and encapsulation capacity of DPPC/cholesterol liposomes. Furthermore, the membrane perturbing effect of propranolol was monitored using the CE-LIF and DLS techniques; which indicates that cholesterol rich membranes are more destabilized from propranolol interaction than non-cholesterol (or low cholesterol) membranes. This CE-LIF method is more efficient and simpler than the quenched fluorescence method. In addition, CE can be automated to analyze multiple samples and routinely used to characterize liposome and colloidal formulations in pharmaceutical and industrial applications. Generally, capillary electrophoresis (CE) can be used to complement size exclusion chromatography (SEC) and light scattering techniques, since electrophoretic mobility is affected by both the size and charge of the colloid particles.

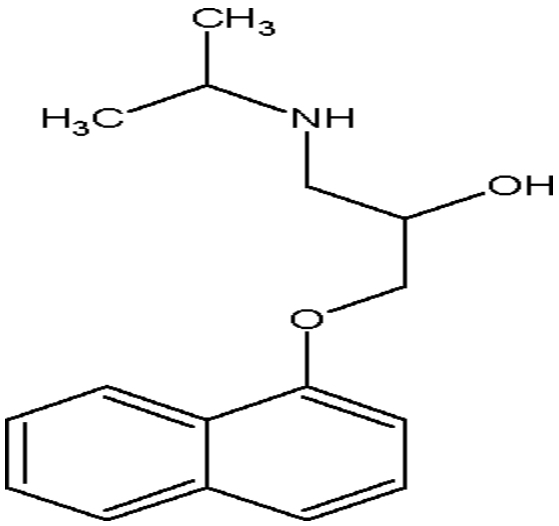

Figure 3-1. Molecular structure of Propranolol

Table 3-1. Fluorescence of encapsulated dye in a mixed DPPC (PC) and cholesterol (CH) liposomes. Relative fluorescence of encapsulated dye is measured by CE-LIF after liposome lysis with 10mM cholate solution.

Relative fluorescence of encapsulated dye in PC/CH liposomes		
PC/CH (%)mole ratio	**Relative Fluorescence (RFU)**	**Liposome size(nm) DLS data**
95/5	174	105
75/25	158	113
55/45	105	116

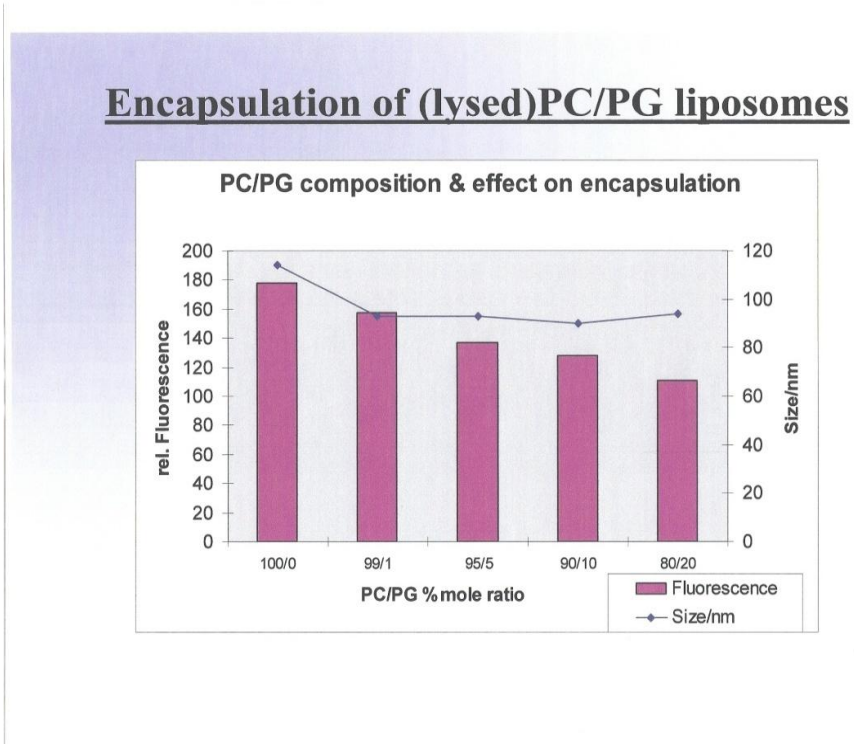

Figure 3-2. The effect of DPPG composition on the encapsulation behavior of DPPC liposomes. The relative fluorescence of liposome encapsulated dye after detergent lysis.

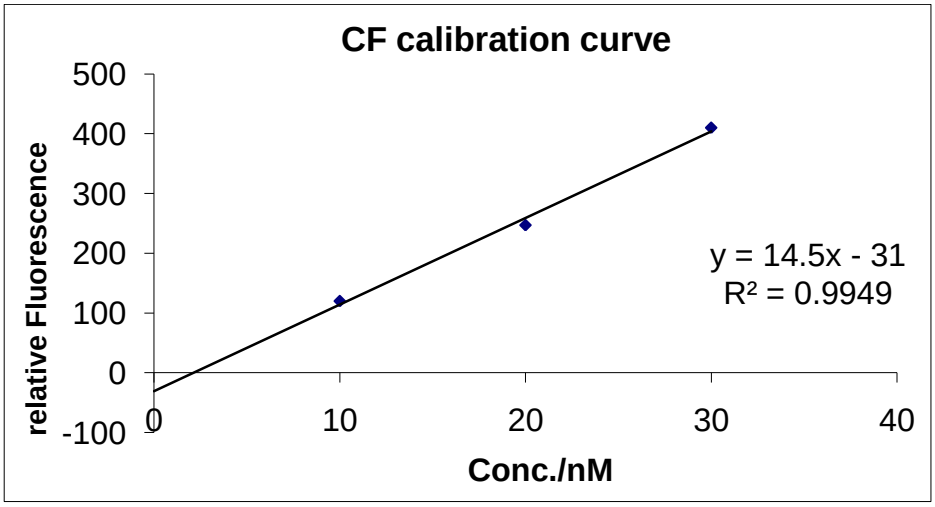

Figure 3-3 Calibration curve for the relative fluorescence of 6-carboxyfluorescein (CF) dye at 488/520nm emission/excitation.

Table 3-2 Fluorescence of the encapsulated dye by a non-FAT (A) and FAT liposomes

Table A

LUV100 (NON-FAT)

PC/CH	*Rel.Fluo.*	*Size/nm*
95/5	132	106
80/20	123	110
65/35	83	118

Table B

FATLUV100

PC/CH	*Rel.Fluo.*	*Size/nm*
95/5	250	113
80/20	240	117
65/35	179	119

Table 3-3. DLS measurements of PC/CH liposome size and polydispersity index (PI). Effect of cholesterol composition on liposome size during liposome-Propranolol interaction.

Lipid conc (PC+CH) mM	without propranolol		after propranolol interaction	
	PI	Size/nm	PI	Size/nm
(20+1) mM	0.064	101	0.07	106
(20+4) mM	0.086	112	0.131	124
(20+9) mM	0.075	118	0.118	123

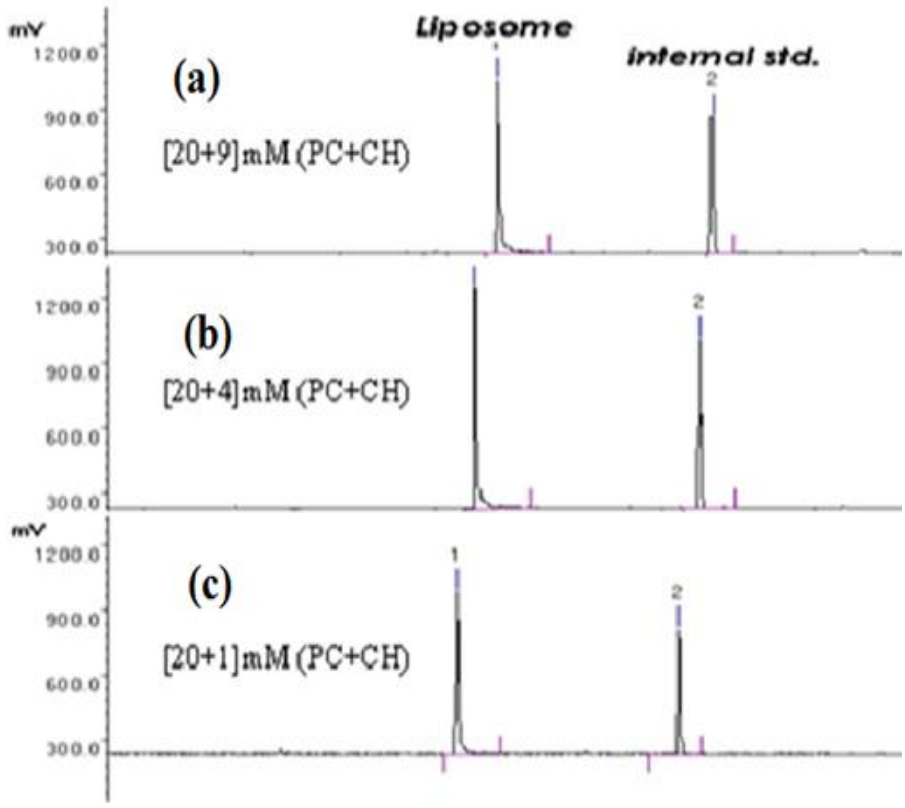

Figure 3-4. Electropherogram of dyed DPPC/CH liposomes in Hepes buffer; different cholesterol composition. Control samples (without propranolol). Normal mode CZE with LIF detector.

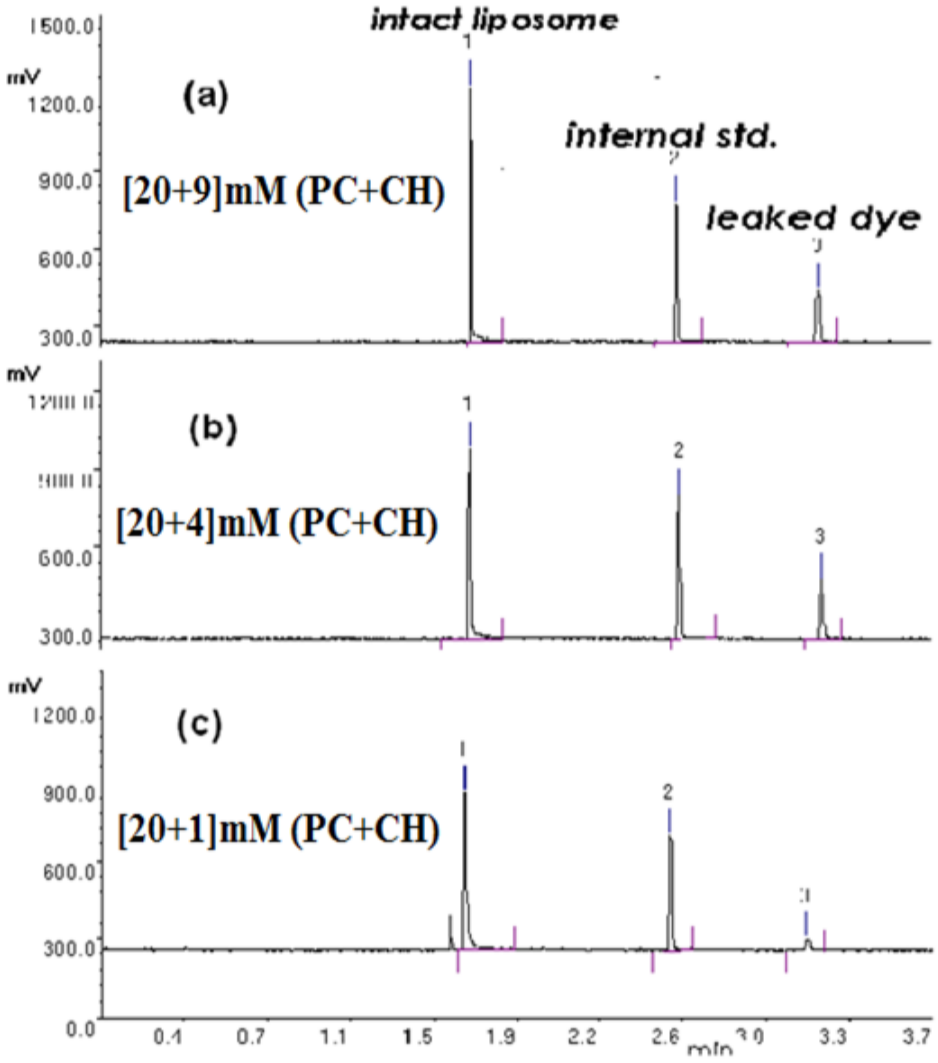

Figure 3-5. Electropherogram of dyed DPPC/CH liposomes incubated with propranol solution. CE-LIF conditions the same as in Figure 3-4.

Reference List

[1] M.Brandl, Liposomes as drug carriers: a technological approach, Biotechnol.Annu.Rev. 7 (2001) 59-85.

[2] W.R.Perkins, S.R.Minchey, P.L.Ahl, and A.S.Janoff, The determination of liposome captured volume, Chem.Phys.Lipids 64 (1993) 197-217.

[3] D.Lichtenberg and Y.Barenholz, Liposomes: preparation, characterization, and preservation, Methods Biochem.Anal. 33 (1988) 337-462.

[4] R.Banerjee, Liposomes: applications in medicine, J.Biomater.Appl. 16 (2001) 3-21.

[5] D.D.Lasic, D.Papahadjopoulos, liposomes in medicine, In: Lasic, D. D. and Papahadjopoulos, D. (Eds.), Medical Applications of Liposomes, Elsevier, New York, 2009,

[6] L.Montenegro and F.Anna Maria Panico and Bonina, Quantitative determination of hydrophobic compound entrapment in dipalmitoylphosphatidylcholine liposomes by differential scanning calorimetry, Int.J.Pharm. 138 (1996) 191-197.

[7] A.R.Mohammed, N.Weston, A.G.Coombes, M.Fitzgerald, and Y.Perrie, Liposome formulation of poorly water soluble drugs: optimisation of drug loading and ESEM analysis of stability, Int.J.Pharm. 285 (2004) 23-34.

[8] T.Nii and F.Ishii, Encapsulation efficiency of water-soluble and insoluble drugs in liposomes prepared by the microencapsulation vesicle method, Int.J.Pharm. 298 (2005) 198-205.

[9] L.Stuhne-Sekalec, J.Chudzik, and N.Z.Stanacev, Co-encapsulation of cyclosporin and insulin by liposomes, J.Biochem.Biophys.Methods 13 (1986) 23-27.

[10] J.McKeon and M.G.Khaledi, Evaluation of liposomal delivery of antisense oligonucleotide by capillary electrophoresis with laser-induced fluorescence detection, J.Chromatogr.A 1004 (2003) 39-46.

[11] D.B.Fenske and P.R.Cullis, Entrapment of small molecules and nucleic acid-based drugs in liposomes, Methods Enzymol. 391 (2005) 7-40.

[12] S.C.Semple, S.K.Klimuk, T.O.Harasym, and M.J.Hope, Lipid-based formulations of antisense oligonucleotides for systemic delivery applications, Methods Enzymol. 313 (2000) 322-341.

[13] S.Akhtar, S.Basu, E.Wickstrom, and R.L.Juliano, Interactions of antisense DNA oligonucleotide analogs with phospholipid membranes (liposomes), Nucleic Acids Res. 19 (1991) 5551-5559.

[14] J.M.Fernández-Romero and A.Gómez-Hens, Analytical methods for the control of liposomal delivery systems, TrAC Trends in Analytical Chemistry 25 (2006) 167-178.

[15] J.McKeon, M.J.Cho, and M.G.Khaledi, Quantitation of intracellular concentration of a delivered morpholino oligomer by capillary electrophoresis-laser- induced fluorescence: correlation with upregulation of luciferase gene expression, Anal.Biochem. 293 (2001) 1-7.

[16] C.H.Wang and Y.Y.Huang, Encapsulating protein into preformed liposomes by ethanol-destabilized method, Artif.Cells Blood Substit.Immobil.Biotechnol. 31 (2003) 303-312.

[17] K.Moribe, K.Maruyama, and M.Iwatsuru, Encapsulation characteristics of nystatin in liposomes: effects of cholesterol and polyethylene glycol derivatives, Int.J.Pharm. 188 (1999) 193-202.

[18] R.Ganapathi and A.Krishan, Effect of cholesterol content of liposomes on the encapsulation, efflux and toxicity of adriamycin 1, Biochem.Pharmacol. 33 (1984) 698-700.

[19] X.Armengol and J.Estelrich, Physical stability of different liposome compositions obtained by extrusion method, J.Microencapsul. 12 (1995) 525-535.

[20] A.Ishida, C.Otsuka, H.Tani, and T.Kamidate, Fluorescein chemiluminescence method for estimation of membrane permeability of liposomes, Anal.Biochem. 342 (2005) 338-340.

[21] M.pel-Paz, G.F.Doncel, and T.K.Vanderlick, Impact of membrane cholesterol content on the resistance of vesicles to surfactant attack 1, Langmuir 21 (2005) 9843-9849.

[22] T.X.Xiang, J.Chen, and B.D.Anderson, A quantitative model for the dependence of solute permeability on peptide and cholesterol content in biomembranes, J.Membr.Biol. 177 (2000) 137-148.

[23] R.Nallamothu, G.C.Wood, C.B.Pattillo, R.C.Scott, M.F.Kiani, B.M.Moore, and L.A.Thoma, A tumor vasculature targeted liposome delivery system for combretastatin A4: design, characterization, and in vitro evaluation, AAPS.PharmSciTech. 7 (2006) E32.

[24] S.Benita, P.A.Poly, F.Puisieux, and J.Delattre, Radiopaque liposomes: effect of formulation conditions on encapsulation efficiency, J.Pharm.Sci. 73 (1984) 1751-1755.

[25] R.C.MacDonald, R.I.MacDonald, B.P.Menco, K.Takeshita, N.K.Subbarao, and L.R.Hu, Small-volume extrusion apparatus for preparation of large, unilamellar vesicles, Biochim.Biophys.Acta 1061 (1991) 297-303.

[26] S.Sriwongsitanont and M.Ueno, Effect of freeze-thawing and polyethylene glycol (PEG) lipid on fusion and fission of phospholipid vesicles, Chem.Pharm.Bull.(Tokyo) 52 (2004) 641-642.

[27] C.J.Chapman, W.L.Erdahl, R.W.Taylor, and D.R.Pfeiffer, Factors affecting solute entrapment in phospholipid vesicles prepared by the freeze-thaw extrusion method: a possible general method for improving the efficiency of entrapment, Chem.Phys.Lipids 55 (1990) 73-83.

[28] M.J.Hope, M.B.Bally, P.R.Cullis, and G.Webb, Production of large unilamellar vesicles by a rapid extrusion procedure. Characterization of size distribution, trapped volume and ability to maintain a membrane potential., Biochimica et Biophysica Acta 812 (1985) 55-65.

[29] L.D.Mayer, M.J.Hope, P.R.Cullis, and A.S.Janoff, Solute distributions and trapping efficiencies observed in freeze-thawed multilamellar vesicles, Biochim.Biophys.Acta 817 (1985) 193-196.

[30] J.D.Castile and K.M.Taylor, Factors affecting the size distribution of liposomes produced by freeze-thaw extrusion, Int.J.Pharm. 188 (1999) 87-95.

[31] F.Ishii and Y.Nagasaka, Simple and Convenient Method for Estimation of Marker Entrapped in Liposomes, J.Dispersion Sci.Technol. 22 (2001) 97-101.

[32] N.Oku and R.C.MacDonald, A simple procedure for the determination of the trapped volume of liposomes, Biochimica et Biophysica Acta 691 (1982) 332-340.

[33] D.Lidgate and R.Maskiewicz, Conductivity measurement as a convenient technique for determination of liposome capture volume, Int J Pharm 96 (1993) 51-58.

[34] X.M.Zhang, A.B.Patel, R.A.de Graaf, and K.L.Behar, Determination of liposomal encapsulation efficiency using proton NMR spectroscopy, Chem.Phys.Lipids 127 (2004) 113-120.

[35] N.J.Zuidam, R.D.Vrueh, D.J.A.Crommelin, Characterization of Liposomes, In: Torchilin, V. and Weissig, V. (Eds.), Liposomes: A Practical Approach, Oxford University Pres, London, 2003, pp. 75-76.

[36] T.M.Allen, Calcein as a tool in liposome methodology, Liposome Technology, CRC Press, Boca Raton, FL, 1984, pp. 177-182.

[37] E.Ralston, L.M.Hjelmeland, R.D.Klausner, J.N.Weinstein, and R.Blumenthal, Carboxyfluorescein as a probe for liposome-cell interactions effect of impurities, and purification of the dye, Biochim Biophys Acta 649 (1981) 133-137.

[38] G.Sessa and G.Weissmann, Phospholipid spherules (liposomes) as a model for biological membranes, J Lipid Res. 9 (1968) 310-318.

[39] J.Barbet, P.Machy, A.Truneh, and L.D.Leserman, Weak acid-induced release of liposome-encapsulated carboxyfluorescein, Biochim.Biophys.Acta 772 (1984) 347-356.

[40] S.Butler, R.Wang, S.L.Wunder, H.Y.Cheng, and C.S.Randall, Perturbing effects of carvedilol on a model membrane system: role of lipophilicity and chemical structure, Biophys.Chem. 119 (2006) 307-315.

[41] G.Zardeneta and P.M.Horowitz, Analysis of the perturbation of phospholipid model membranes by rhodanese and its presequence 6, J Biol.Chem 267 (1992) 24193-24198.

[42] X.Liu, Q.Yang, C.Nakamura, and J.Miyake, Avidin-biotin-immobilized liposome column for chromatographic fluorescence on-line analysis of solute-membrane interactions, J Chromatogr.B Biomed.Sci Appl. 750 (2001) 51-60.

[43] J.N.Weinstein, E.Ralston, L.D.Leserman, R.D.Klausner, P.Dragsten, R.Blumenthal, Selfquenching of carboxyfluorescein fluorescence: uses in studying liposome stability and liposome-cell interaction, In: Gregoriadis, G. (Ed.), Liposome Technology, CRC Press, Boca Raton, 1984, pp. 183-204.

[44] A.S.Evers, Cellular and molecular mechanisms of Anesthesia, In: Cullen, B. F., Barash, P. G., and Stoelting, R. K. (Eds.), Clinical Anesthesia, Lippincott Williams & Wilkins, Philadelphia, 1997, pp. 40-48.

[45] K.Tu, M.Tarek, M.L.Klein, and D.Scharf, Effects of anesthetics on the structure of a phospholipid bilayer: molecular dynamics investigation of halothane in the hydrated liquid crystal phase of dipalmitoylphosphatidylcholine, Biophys.J 75 (1998) 2123-2134.

[46] Malvern instruments. Dynamic Light Scattering: An Introduction in 30 Minutes. http://www.malvern.com/common/downloads/campaign/MRK656-01.pdf , 2009.

[47] M.J.Hope, R.Nayer, L.D.Mayer, P.R.Cullis, Reduction of liposome size and preparation of unilamellar vesicles by extrusion techniques, In: Gregoriadis, G. (Ed.), Liposome Technology: liposome preparation and related techniques, CRC Press Inc., Boca Raton, FL, 1993, pp. 123-139.

[48] R.R.C.New, Characterization of liposomes, In: New, R. R. C. (Ed.), Liposomes: a practical approach, Oxford University Press, New York, 1990, pp. 125-137.

[49] J.Hernandez, J.Estelrich, and R.Pouplana, Determination of the encapsulation efficiency in liposomes obtained by the extruder method, J.Microencapsul. 4 (1987) 315-320.

[50] T.Ohsawa, H.Miura, and K.Harada, Improvement of encapsulation efficiency of water-soluble drugs in liposomes formed by the freeze-thawing method, Chem Pharm Bull.(Tokyo) 33 (1985) 3945-3952.

[51] L.Herbette, A.M.Katz, and J.M.Sturtevant, Comparisons of the interaction of propranolol and timolol with model and biological membrane systems, Mol.Pharmacol. 24 (1983) 259-269.

[52] G.Albertini, C.Donati, R.S.Phadke, M.G.Ponzi Bossi, and F.Rustichelli, Thermodynamic and structural effects of propranolol on DPPC liposomes, Chem.Phys.Lipids 55 (1990) 331-337.

[53] A.Cao, E.Hantz-Brachet, B.Azize, and G.Perret, The interaction D-propranolol and dimyristoyl phosphatidylcholine large unilamellar vesicles investigated by quasielastic light scattering and Fourier-transform infrared spectroscopy, Chem.Phys.Lipids 58 (1991) 225-232.

[54] W.K.Surewicz and W.Leyko, Interaction of propranolol with model phospholipid membranes. Monolayer, spin label and fluorescent spectroscopy studies, Biochim.Biophys.Acta 643 (1981) 387-397.

[55] L.G.Herbette, D.W.Chester, and D.G.Rhodes, Structural Analysis of Drug Molecules in Biological Membranes, Biophys J 49 (1986) 91-94.

[56] L.Herbette, C.A.Napolitano, F.C.Messineo, and A.M.Katz, Interaction of amphiphilic molecules with biological membranes. A model for nonspecific and specific drug effects with membranes, Adv.Myocardiol. 5 (1985) 333-346.

[57] S.L.Krill, K.Y.Lau, W.Z.Plachy, and S.J.Rehfeld, Penetration of dimyristoylphosphatidylcholine monolayers and bilayers by model beta-blocker agents of varying lipophilicity, J Pharm Sci 87 (1998) 751-756.

[58] W.K.Subczynski, A.Wisniewska, J.J.Yin, J.S.Hyde, and A.Kusumi, Hydrophobic barriers of lipid bilayer membranes formed by reduction of water penetration by alkyl chain unsaturation and cholesterol, Biochemistry 33 (1994) 7670-7681.

[59] D.B.Goldstein, The effects of drugs on membrane fluidity 1, Annu.Rev.Pharmacol.Toxicol. 24 (1984) 43-64.

[60] K.Ondrias, A.Stasko, V.Jancinova, and P.Balgavy, Comparison of the effect of eleven beta-adrenoceptor blocking drugs in perturbing lipid membrane: an ESR spectroscopy study, Mol.Pharmacol. 31 (1987) 97-102.

[61] K.Y.Pang, L.M.Braswell, L.Chang, T.J.Sommer, and K.W.Miller, The perturbation of lipid bilayers by general anesthetics: a quantitative test of the disordered lipid hypothesis, Mol.Pharmacol. 18 (1980) 84-90.

Chapter 4

Liposome lysis immunoassay using spectrofluorometric and capillary electrophoresis methods

Abstract

The behavior and immunoassay application of contact sensitive (self lysing) liposomes was studied using spectrofluorometric, DLS (dynamic light scattering) and CE-LIF (capillary electrophoresis with laser induced fluorescence) techniques. The non-lamellar DOPE lipid (dioleoyl phosphoethanolamine) was mixed with a 20% stabilizer DPPC (dipalmitoyl phosphatidylcholine) and 1% hapten-attached DPPE (dipalmitoyl phosphoethanolamine) lipids to form a stable contact-sensitive dye encapsulating liposomes. The biotin-attached liposomes aggregate and then leak their marker content in a standard avidin solution. Similarly, anti-DNP (dinitrophenol) antibodies have the same effect on DNP-attached liposomes. The extent of aggregation and dye leakage is dependent on the concentration of avidin (or anti-DNP). The DLS data shows the average size (Z_{av}) and polydispersity index (PI) of (biotin/DNP attached) liposomes increased after incubation with avidin and anti-DNP solutions. The relative fluorescence of the leaked dye also increased with each increase in avidin and anti-DNP concentrations. The fluorescence working range was expanded at higher incubation temperatures (70-80°C) in both avidin and anti-DNP binding curves. In addition, a 4-carbon linker moiety (-Cap-) enhanced the sensitivity, and widens the response range of the anti-DNP fluorescence detection, as opposed to when the DNP is directly attached to the liposome

surface. The smallest concentration of avidin standard detected using the fluorometric method was 50ng/ml.

Introduction

Liposomes are spherical vesicles which consist of a phospholipid bilayer surrounding an inner aqueous reservoir. Liposomes have found a number of applications in different biotechnical and biomedical areas including drug delivery, gene therapy and immunodiagnostics. Liposomes can be armed with target-specific ligands, receptors, and antigens (or antibodies) that act as homing or anchoring probes. Specifically, antibody (AB) directed liposomes are called immunoliposomes. Furthermore, during or after the preparation of the immunoliposomes it is possible to entrap almost any water-soluble molecule (drugs, DNA, enzymes, dyes, etc…) within the liposome interior.

Liposomes have been applied to numerous fields of research owning to their unique structure. Their similarity to biological membranes makes them ideal for studying cell membrane properties and their capacity to encapsulate a large number of molecules in the core or in the bilayer makes them ideal vehicles for drug delivery. These features, combined with the availability of a large number of functional groups on the surface to which various receptor molecules can be attached, makes them suitable for drug and genetic material delivery as well as immunodiagnostic applications. Liposomes can be made from charged or neutral lipids, and may also have a reactive surface depending on the functionality of the lipid head group. These reactive surface moieties have functional groups like amines, carboxyls, sugars or thiols on to which homing or ligand molecules can be coupled [1].

Immunoassays are methods used to detect analytes like antibodies, antigens, hormones or drugs in biological samples. They are routinely used in bio-analytical studies, food analysis, and in the detection of environmental pollutants and toxins. These assays rely on specific binding of an analyte to its conjugate molecule, followed by detection of the resulting complex. Such an assay is the detection, and quantitation, of an antigen in a sample using a specific antibody (or vice versa). The antibody is labeled with a reporter or a marker molecule to produce a desired signal and enhance the detection of the antigen. Various signal generating agents such as enzymes, dyes, isotopes, and spin labels are commonly used.

Immunoassays can be either homogeneous or heterogeneous depending on whether or not a separation step is required during the process. In a homogeneous immunoassay all the components are mixed in the same vessel and it does not require a (physical/manual) separation step prior to the detection process. A heterogeneous immunoassay will require an extra step to remove unbound antibody or antigen from the site, usually using a solid phase reagent, before the detection step. Because homogeneous assays do not require this step, they are typically faster and easier to perform. Also, these assays can be either competitive or non-competitive based on presentation of the analyte. In competitive formats, unlabelled analyte (usually antigen) in the test sample is measured by its ability to compete with a labeled antigen in the immunoassay. The unlabeled antigen (analyte) blocks the ability of the labeled antigen to bind because the binding site on the antibody is already occupied. In the one step competitive format, both the labeled antigen reagent (Ag*) and the unlabeled analyte compete for a

limited amount of antibody. There is an inverse relationship between the observed signal and analyte. In a non competitive assay, the signal measured is directly proportional to the amount of analyte bound to its conjugate.

Liposomes, when used as marker labels, are found to have a signal enhancement effect leading to higher sensitivities in various immunoassay applications since they provide an aqueous core, which encapsulates large number of marker/reporter molecules. Also, a functionalized liposome surface can provide sites for the attachment of ligands (antibodies or antigens) as well as reporter molecules. Consequently, for every ligand molecule on the liposome surface, there could be thousands of related marker molecules, as opposed to conventional immunoassays that carry one or a few marker molecules per analyte molecule. In principle, this liposome signal enhancement effect provides a low detection limit and requires a very small sample size. Liposome immunoassays have been developed in both heterogeneous and homogeneous formats [2].

Various assay methods based on the selective interaction between antigen and antibody have been used to detect specific antigens and antibodies. Among many assay methods that depend on this immuno-interaction, ELISA (enzyme linked immunosorbent assay) is the most popular, however, it is tedious and time consuming. ELISA usually requires multiple steps of manual separation of free and antigen-bound antibodies and many repeated incubation and washing steps [3]. Liposome immunoassay is one of the more recent alternatives to ELISA and other conventional immunoassays that attempt to increase efficiency and sensitivity by amplifying the analytical signal. The sensitivity is enhanced since each liposome can carry

many ligand molecules on its surface and encapsulate a large number of marker molecules in the interior compartment.

Liposome Immune Lysis Assay (LILA) is a homogeneous assay where the liposomes carry a ligand (antibody or antigen) on the surface and marker molecules in their interior compartments. Upon interaction between analyte and the receptor (antigen or antibody), the encapsulated marker molecules are released into the bulk aqueous solution and detected [3-5]. Liposome lysis and marker release can happen after self-lysis or facilitated by an external agent. For example, an antigen in a sample is analyzed using its specific antibody-linked liposome, which after incubation forms the antigen-antibody complex on the liposome surface. Adding a lysis facilitator compound, like "complement" proteins, breaks-down the antigen-antibody complex, which then destabilizes the liposome causing lysis and leakage. Since complement specifically attacks the antigen-antibody pair, liposomes that only have the conjugated antigen-antibody pair on their surface will destabilize/lyse and release their marker contents. The fluorescence of the released marker is related to the concentration of the antigen (analyte/sample) that's bound to the antibody-liposomes. The complement system is a group of proteins that recognize and bind to antibody-antigen complexes on membrane surfaces, whose activation eventually results in the destruction of cells, invading microorganisms or in this case the complex bound liposomes. Further sensitivity enhancement, by signal amplification, can be gained by encapsulating a marker-generating enzyme like β-Galactosidase, which can catalytically form multiples of marker molecules from non-fluorophore substrates. In addition, the encapsulated enzymes

exhibit longer encapsulation than smaller marker molecules, due to their bulkier size, which may enhance sensitivity of the assay [4-6]. But, enzymes need a substrate to create a detection signal and are less rugged and create more back ground noise than fluorescent dyes.

The sensitivity, and specificity, of a liposome lysis assay (LLA) can be enhanced by separating the analytical (signal) from the rest of the sample matrix, which can potentially create interference during fluorescence detection. Accordingly, the combination of CE's resolving power, speed of separation, small sample requirement, low reagent consumption and a potential for a fully automated operation coupled with the high sensitivity detection by LIF makes CE-LIF the method of choice for liposome immune lysis assay.

Different techniques have been used to prepare liposomes for potential applications in immunoassays [7]. The liposome's encapsulation volume and its chemical/physical stability are two of the most important factors that are determined by the liposome composition and preparation method appropriate for a specific immunoassay format. Although there are different types and ways of making liposomes for analytical detection purposes, the discussion here will focus on unilamellar-vesicles made from phospholipids, cholesterol and other reactive chemical groups used to functionalize the liposome surface. As explained in the earlier chapter extrusion is the best method to make homogeneously sized large unilamellar vesicles (LUV), or liposomes, which are most suitable for immunoassay purposes. These liposomes have an average diameter of 100nm, which provides a large interior volume for marker encapsulation and an ample outer surface area to

immobilize antigen or antibody-fragments (or Fab) for an optimal immunoassay. Usually, haptens (small molecules, like antigens, that elicit immune response) are covalently coupled to the lipid head-groups, like phosphatidylethanolamine (PE), and mixed with other lipids in an organic solvent to prepare the surface-active liposomes. There are basically two ways to couple haptens and antibody-fragments (Fab) onto the liposome surface. They can be covalently bonded to the head-group of a lipid like PE via their amine, carbohydrate, or thiol moieties, and then mixed with other lipids to form the liposomes. Alternatively, an antigen or a fragment of an antibody can also be conjugated to a preformed liposome that has a reactive surface containing an amine, sulfhydryl, maleimide or a carbohydrate groups. Separation of free Fab/antigens, which are not linked to the liposome, can be done with chromatography or other physical means, like centrifugation and dialysis. Ultimately, during the immunoassay application of these antigen/Fab attached liposomes, the fluorescence of the leaked marker will correlate with the concentration of antibody binding to the antigen that is on the liposome surface. Various types of markers have been encapsulated in liposomes including organic dyes, enzymes, substrates, isotopes and other labels. The most commonly used are fluorescent and colorimetric dyes like calcein, carboxyfluorescein (CF) and sulforhodamine B which are soluble in water and can be encapsulated at high concentration (~100mM) [8]. The fluorescence of the encapsulated markers is quenched during encapsulation, but the fluorescence increases when it is leaked from the liposome and is diluted in the extra-liposomal aqueous solution.

Enzymes like horseradish peroxidase (HRP) and alkaline phosphatase (AP)

have also been trapped inside liposomes for detection purposes [9]. The entrapped enzyme, upon release, converts the substrate molecules in the bulk solution, to signal generating molecules. Although there is an advantage of signal amplification, this assay lacks ruggedness and simplicity since the enzymes require special handling and storage. In addition, the signal generated from the substrate, may not be instantaneous with leakage of the enzyme from the liposome. Radioactive labeled markers are also sensitive, but their health hazard and the expensive instrumentation make them the least preferred method. For some analytes, a comparison of the sensitivity between a liposome-based and non-liposomal assays (ELISA and fluorescein-labeling methods) has shown that there can be as much as a hundred fold enhancement in sensitivity from using marker encapsulated liposomal methods [2;10;11].

Generally, liposome assays can either be based on lysis of the liposome and measuring the signal corresponding to the released marker that is related to analyte concentration, or analysis of the analyte can be based on the measuring the fluorescence of the marker still trapped inside the intact liposome, without lysis, and relate the fluorescence to the analyte concentration. The latter case is not very common and is based on selective precipitation of the antigen/antibody cross-linked liposomes by centrifugation and collecting the aggregated liposomes from the bottom of the tube then measuring the marker associated with the aggregated liposomes. In addition to monitoring the encapsulated marker, the aggregation of receptor-anchored liposomes, by specific multidentate ligands, has been monitored using light scattering/turbidimetry techniques

and proposed as a possible method for the determination of antibodies in biological samples [12].

Lytic assays can be either homogeneous or heterogeneous. Homogeneous liposome lysis assays are done in solution phase with no washing of unbound ligand required before detection. In heterogeneous lytic assay the marker-encapsulated-ligand-coupled liposomes compete with a free ligand (analyte) in the sample for a limited antibody that is immobilized on a solid surface. After the incubation, the unreacted liposomes that didn't bind to the surface ligand will have to be rinsed away before measuring the fluorescence of the marker from the surface bound liposomes. In a competitive assay format, the signal intensity of the released marker is inversely related to the amount of free ligand (analyte) in the sample. Generally, the fluorescence of the encapsulated marker is measured following its release from the liposomes' interior by lysis or perforation of the membrane. Commonly, there are four distinctly different methods used to induce liposome lysis, namely the complement system, use of cytolytic agents, using surfactants or detergents, and through self lysis due to phase transition by the lipids [5;7]. The complement system is a group of proteins that belong to the innate immune system that can be used to selectively lyse liposomes that carry the bound antigen-antibody complex on their surface [13]. An antigen-antibody complex formation is necessary to initiate the activation of the complement protein. The complement can be used in both competitive and non-competitive assays and the signal from the liposome released marker is monitored using the appropriate detection technique. In competitive or inhibition assay format, the signal generated is inversely proportional to the

concentration of analyte in the sample [14]. Complement-based lytic liposome assays have been shown to have comparable or even higher sensitivity than conventional ELISA in a number of studies [2;15;16]. But, the analytical application of complement enzymes has been limited due to their delicate nature and non-specific lytic action . The non-specific lysis and leakage of liposomes that do not carry the antigen-antibody complex is known to occur in some assays, contributing to a high level of noise (signal) which decreases sensitivity and reproducibility of the assay [17].

Lysis of marker encapsulated liposomes can also be performed by a detergent, like Triton-X100, or a potent cytolytic agent like melittin. Melittin is a natural 26-amino acid protein from bee venom and lyses liposomes rather slower than complement [18]. Melittin lyses lipid bilayers and does not require the formation of an antigen-antibody on the liposome's surface, like complement does. In a homogeneous competitive cytolysin-mediated liposome immunoassay, the antigen (analyte), an antigen-cytolysin conjugate and the antibody are incubated altogether, and then the dye encapsulated liposomes are added. The antigen-cytolysin conjugate has the ability to lyse and leak the liposomes. During the incubation, the conjugated antigen-cytolysin is competing with the antigen (analyte/sample) for the limited antibody. When antibody binds to the antigen-cytolysin (conjugate), the cytolysin becomes impotent to lyse the liposome. The more antibodies bind to the antigen-cytolysin, and then less of it will be available to lyse the liposome, which decreases the fluorescence signal. In general, cytolysin-based assays require fewer steps, are faster and comparatively more versatile than the complement-based assays. A main disadvantage of the cytolysin

methods is reproducibility and some non-specificity by the lysing agent. In addition, lysing agents like Melittin are poisonous venoms that can cause harm unless extreme caution is taken while handling and working with them. Also, covalently linking the cytolysin agent to either an antibody or antigen, without any significant loss in immunological and cytolytic activities, is a challenge. Therefore, the most efficient lysis assay would be one that depends on self lysing liposomes, without adding external lysing agents like Melittin and detergents (Triton X-100). And that is what we propose to do in this part of the project.

There is a very limited amount of literature available on immunoassay applications that depend on self lysing liposomes. Most of these studies were published by Huang and coworkers who used a non-bilayer forming lipid, like dioleoylphosphatidylethanolamine (DOPE) with other stabilizers to form stable self lysing liposomes for immunoassay application [17;19]. These liposomes with a target specific molecule (antigen or antibody) attached to their surface are stable and only undergo bilayer destabilization when the antigen-antibody complex is formed on their surface. For example, if a sample containing a multidentate antibody to be analyzed is incubated with the antigen-attached liposomes (marker- entrapped), it cross-links and destabilizes the liposomes causing aggregation and a stoichiometric leakage of their marker content. In our study we have used these contact sensitive liposomes to detect avidin and anti-DNP antibody on a conventional fluorimeter and CE-LIF instrumental setups. An extended explanation about their characteristics, synthesis and application in fluorescence assays is given later in this chapter.

Most immunoassay techniques currently used have a multiple well format in order to increase throughput, and the different mixing, washing and detection steps require automation. These non-flow based techniques are usually sensitive, but suffer from some detection reproducibility due to sample matrix interference. These and other problems often cause significant well-to-well and plate-to-plate variations in the data collected [20;21]. Flow injection assay (FIA) techniques have been found to help alleviate these shortcomings and FIAs' can also be automated easily [21]. FIA techniques offer better analytical reproducibility through a more precise delivery, analysis, and detection of the sample in a flow based reactor column [21;22]. But still, FIA methods do require some steps of washing to separate the unbound (excess) marker molecules and to regenerate the reactor column after every sample run. Therefore there is still a need for a more efficient and reproducible method that includes a simultaneous online separation and detection of the analytical signal on a flow based chromatographic setting [23]. In the last decade or so, a limited number of chromatographic and electrophoresis based liposome immunoassays have been developed to analyze drugs, toxins, antigens and antibodies [23-25]. A liposome immune-chromatographic method to detect the pollutant chemical, Alachlor, in water and soil samples was developed by R.A. Durst [21;26]. In this assay, capillary action causes Alachlor and Alachlor-tagged-dye-containing-liposomes to migrate through an anti-Alachlor antibody zone on a plastic-backed nitrocellulose strip where competitive binding occurs. Unbound liposomes continue migration to a liposome capture zone, where they are quantified colorimetrically. The amount of liposome-entrapped dye that is

measured in this zone is directly proportional to the Alachlor concentration in the sample. The nitrocellulose (TLC) plate serves as a sieving medium, and a flow controlling media, for the migrating tagged liposomes. Similarly, an immunochromatography method for the detection of Aflatoxin-B1 (AFB1), a fungi toxin, using a dye encapsulating (AFB1)-tagged liposomes, was developed by Wauchope and Ho [27]. This technique was capable of detecting Aflatoxin B1 as low as 20ng, and was comparatively efficient and cheaper than ELISA methods. Likewise, an electrophoretic technique developed by Tsukagioshi et al. used Eosin Y-attached liposomes to determine antibodies of human serum albumin with a capillary electrophoresis technique. The intensity of the dye released from the Eosin Y-attached liposomes, due to antigen-antibody interaction on the liposome surface, was measured online with a chemiluminescence detection system [25]. Being a competitive assay, the intensity of released dye was inversely related to the concentration of analyte in the sample. Likewise, the dynamic light scattering (DLS) technique has also been used to determine the antibody-induced aggregation of receptor attached liposomes [28-30]. The average size and polydispersity index of the liposomes increases when they are incubated with specific antibodies due to their ensuing aggregation.

Our objective here is to study the binding interaction between a free multivalent antibody and a liposome-anchored antigen using DLS, spectrofluorimeter and CE-LIF instruments in a homogenous solution. In addition, we intend to utilize these surface-active liposomes to develop antigen/antibody assays using a capillary electrophoresis laser induced fluorescence (CE-LIF) instrument setup. As indicated earlier, the majority

lipid (about 70-90%) used to make these liposomes is DOPE, which does not form stable liposomes by itself, due its small hydrophilic head group. But when it is mixed with a small percentage of stabilizing lipids, like PG, PA and PC, it forms stable lipid bilayers and liposomes. These stabilizing lipids have larger head groups than DOPE, and when present at 10-30% of the total lipid content, they geometrically complement the smaller head group of DOPE, and together pack into a planar or vesicular membrane structures. Stabilizer lipids that have been used by others, and the resulting compositions, are given in Table 4-1, including their minimum respective concentration needed to form stable liposomes [17]. A crude but useful model to predict the shape of lipid structures, when they are hydrated, is the critical packing parameter (CPP), which is defined as

$$CPP = \left(\frac{V}{A \times L} \right) \qquad \textit{Equation (1)}$$

V – Volume of lipid molecule

A – Lipid's polar head group area

L – Lipid's acyl chain length

According to this simple empirical model, single chain structures (surfactants & detergents) pack into spherical (CPP < $\frac{1}{3}$) or rod like micelles ($\frac{1}{3}$ < CPP < $\frac{1}{2}$). Double chained lipids are characterized with $V \cong (AL)$, i.e. CPP ~ 1, and they can pack best into planar bilayers, and vesicles. Some lipids, like DOPE, with relatively small polar heads ($V > (AL)$, i.e. CPP>1)

tend to pack into cone shaped inverse structures (inverted micelles and Hexagonal II phases) [31;32]. In addition, a stabilizer can also be constructed by linking the immunoreactant molecule onto a lipid head-group, like DNP-DPPE, and mix it at low proportions (~12%) with DOPE to form stable marker encapsulated liposomes. Ultimately the stabilizer, the DNP moiety that is attached to the DPPE, undergo an immunoreaction with its conjugate (anti-DNP), in the sample solution, causing adjacent liposomes to crosslink and aggregate. Such an example is given by Huang and Ho, where DNP-PE stabilized (DOPE) liposomes lyse and leak their marker due to an induced non-bilayer phase transition when the DNP-liposomes are cross-bound by the multivalent anti-DNP antibodies [33]. Similarly, one of the stabilizers on Table 4-1 (15% DPPG), together with a (0.1-1 % mole) of the targeting molecule attached lipid (DNP-PE), can be mixed with DOPE to form a stable liposome that is used to detect the corresponding conjugate of the targeting molecule. A 0.1-1 mole % of the targeting molecule can also be incorporated on a preformed stable DOPE liposome which is then used to detect the corresponding conjugate of the targeting molecule. The preformed liposome will have linker moieties like MPB (maleimidophenyl butyramide) to attach the targeting molecules on their surface [34;34]. The different methods of attaching a targeting molecule to liposomes are discussed in review journal articles [1].

Generally, under conditions where DOPE based liposomes are brought in close proximity, via a multivalent cross linker, they undergo a transition from a bilayer to a reversed-hexagonal phase which results in the loss of liposome integrity and membrane lysis, accompanied by leakage of their

interior content [17]. Further, the factors stated below influence the extent of liposome self-destabilization, and the ensuing content leakage.

- The binding affinity (strength) between the liposome attached ligand and its conjugate (in solution) to be analyzed strongly influences the efficiency of the assay. For instance, a strong affinity between the free avidin and biotin-attached-liposomes, leads to an extensive liposome destabilization and leakage of the encapsulated dye. These attributes provide an assay method with a wide working range for detection [30].
- The concentration of antibody in solution affects the aggregation of antigen-attached-liposomes. The rate and extent of aggregation increases as the amount of antibody added to the antigen-liposomes increases. Carbonell and co-worker also observed the concentration effect when they measured turbidity of biotin-liposome in the presence of avidin. The turbidity of the liposomes was dependent on the avidin concentration [29;30].
- Higher temperatures also facilitate the bilayer to a hexagonal (H_{II}) non-bilayer phase transition. DOPE prefers the hexagonal (H_{II}) phase above 10ºC, so incubation temperatures of up to 70ºC have been used to induce faster lysis of the antigen-attached DOPE liposomes during incubated with the specific antibody solution [21].
- The length of the organic spacer moiety that connects the antigen to the liposome also determines the antigen-antibody binding strength and the extent of liposome aggregation and content leakage [35;36].

In the present study we investigated the interaction of biotin and DNP attached DOPE-liposomes with avidin and anti-DNP antibodies, respectively, in a homogeneous solution using DLS, fluorometry and CE-LIF techniques. Our results demonstrate that avidin and anti-DNP antibodies were able to induce dose dependent aggregation, and content leakage, from DOPE liposomes that have biotin or DNP attached on their surfaces, respectively. The aggregation of biotin-liposomes was inhibited by adding free biotin which competes with the biotin-attached liposomes, for the limited avidin present. The direct method, with biotin-liposomes, can be used for avidin/streptavidin detection, while the competitive assay requires the presence of free biotin to analyze avidin in different biological samples. In addition, the qualitative effects of the spacer arm length and the incubation temperature on the extent of liposome aggregation and the subsequent dye-leakage were also examined. The DOPE liposomes were stabilized by a 20% DPPC lipid.

Experimental

Chemicals, Materials & methods

Chemicals

1,2-Dimyristoyl-*sn*-Glycero-3-Phosphocholine (DMPC), 1,2-Dimyristoyl-*sn*-Glycero-3-Phosphocholine (DPPC), 1,2-Dioleoyl-*sn*-Glycero-3-Phosphoethanolamine (DOPE), 1,2-Dipalmitoyl-*sn*-Glycero-3-Phosphoethanolamine-N-[6-[(2,4-dinitrophenyl)amino]caproyl] (DNP-cap-PE), 1,2-Dipalmitoyl-*sn*-Glycero-3-Phosphoethanolamine-N-(2,4-dinitrophenyl) (DNP-PE), 1,2-Dipalmitoyl-*sn*-Glycero-3-

Phosphoethanolamine-N-Biotinyl (Biotin-DPPE), 1,2-Dioleoyl-*sn*-Glycero-3-Phosphoethanolamine-N-Cap-Biotinyl (Biotin-cap-DPPE) were from Avanti Lipids. Anti-DNP antibody, Avidin, Biotin, Carboxyfluorescein, Alexafluor, 10mM HEPES (4-(2-hydroxyethyl)-1-piperazineethanesulfonic acid) buffer at pH=7.5, and Whatman liposome extrusion polycarbonate filters were purchased from Fisher Scientific. The hydrophilic marker dyes Carboxyfluorescein and Alexa-flour were supplied by Molecular Probes-Invitrogen Corporation. The size exclusion gel Sephadex G-50 and MicroSpin filter columns (part # 27-5330-01) were obtained from Amersham Biosciences. Figures (2-1), (2-2), (4-4) and (4-5) show the molecular structures of the lipids and fluorescent dyes used in this study. Deionized water having a resistivity ≥ 18MΩ/cm was obtained in-house from a reverse osmosis Millipore system.

Materials & methods

Preparation of dye encapsulating liposomes

Liposomes were prepared by the extrusion method, which was developed by Hope and coworkers, with a slight modification, using the Lipex® 10mL thermo barrel extruder (Northern Lipids Inc., Vancouver, BC Canada) [37;38]. The lipid mixtures were first dissolved in 3-5mL of chloroform in 50mL round bottomed flask. A dried thin lipid film was formed around the inside walls of the flask after a 30-45 minutes of rotary evaporation on the Buchi Rotavapor R-3000, under low pressure and >50°C. The dried lipid film was hydrated with 3-5mL of pure buffer, or a buffered-dye solution, with continuous shaking at a temperature above the lipid phase transition

temperature, T_c, (for DPPC ≥ 42°C) to form a stable multi-lamellar vesicle (MLV) suspension. After vortexing and homogenizing the MLV suspension, it was first extruded at least 5 times on a *single* 200nm Nucleopore polycarbonate membrane (Whatman Inc., USA) in the 10mL Lipex extruder at 60°C and low N_2 pressure (<100psi). Finally, the liposome suspension was extruded about ten times through a *double* 100nm polycarbonate membrane at a pressure of 250-350psi. After the last extrusion, the liposomes should have an average size of 100nm and a very low (size) polydispersity index (<0.1).

Biotin and DNP attached lipids

The biotin and DNP molecules are covalently attached to DPPE lipid head group and are obtained from Avanti Polar Lipids. The attachment is either directly to the lipid head group or via a four carbon spacer moiety (CAP) as shown on Figure (4-4) and (4-5). Both varieties are obtained from Avanti with the biotin, or DNP, already bonded to the PE head group of the DPPE lipid. A 1-2% mole of the DNP or the biotin attached DPPE is mixed with DOPE and DPPC (stabilizer), which are all, dissolved in the organic solvent. After the hydration of the dried lipid with an aqueous dye solution and multiple extrusion cycles, the dye-encapsulated ligand-attached liposomes are formed.

Separation of un-trapped marker and liposome

The dye-encapsulated liposomes are separated from the free un-trapped dye on Sephadex G-50 gel filtration micro-columns (Amersham Biosciences, P/N 275330). The filtration micro-columns were prepared and packed in-

house according to the following steps: The gel column was prepared first by boiling about 1g of Sephadex G-50 fine powder in 15-20 mL of DI-water for an hour in a covered beaker. One gram of G-50 powder was swelled to 7-9mL gel volume. The gel was cooled to room temperature and packed into 70% of the micro-column's total volume. The column was equilibrated with (100μL) blank liposomes before it was used for separation of free and liposome-encapsulated dye. The liposome / free dye mixture (~50μL) was gently placed on the gel micro-column and the encapsulated liposomes were separated from the un-trapped dye after centrifugation for 2 minutes at 1000rpm. The low molecular weight dye (<5000) was trapped in the gel while the liposomes were excluded and eluted first with the void-volume without dilution [39].

Measurement of liposome size and size-distribution

The hydrodynamic diameter and the polydispersity (size-distribution index) of all liposome preparations were determined by DLS using the Malvern Zeta-Sizer model 1000HSa. The Malvern measures the time-dependent fluctuations of light scattered by the liposomes and uses it to calculate the average size and polydispersity index (PI) of the liposomes [40]. The PI indicates the width of the size distribution for a batch of liposomes. 100uL of the liposome suspension was diluted with 900uL of a buffered salt solution having a comparable osmolality of the liposome's aqueous interior, in a 1mL low volume cuvette to make the liposome size measurements. The DLS measurement of the avidin and anti-DNP incubated liposomes is done prior to the fluorometer and CE-LIF measurements.

Capillary Electrophoresis and spectrofluorometer analysis

The CZE-LIF experiments were carried out on a laboratory-built CE instrument. A Spellman SL30 high-voltage power supply was used to apply a positive voltage over the length of the fused silica capillary (Polymicro Technologies, Phoenix, AZ, USA), with an inner diameter of 75μm and an outer diameter of 362μm. The LIF system consisted of an argon ion laser (Omni Chrome, CA, USA) modulated by a chopper and controlled by a lock-in amplifier (EG&G, Trenton, NJ, USA). The 488 nm modulated laser line was focused onto the capillary through an upright microscope with a 40X fluorite objective that both beamed the excited fluorescent beam and collected the emitted beam. The laser excitation beam would pass through a dichroic filter (495nm) and the subsequent emission beam would pass through both a long pass (500nm) and a short pass (515nm) filter and be transmitted to the photomultiplier tube (Hamamatsu, Bridgewater, NJ, USA). The signal was then sent to the A/D converter and the lock-in amplifier. All data acquisition and analysis for the CE-LIF experiments was performed using PC/Chrom^{+} and LabView softwares. The assigned excitation/emission wavelengths are 495/515nm on the LIF detector for all the dyes used in this experiment. The samples for CE-LIF analysis are in 50μL aliquots and contain 25μL of the dye encapsulated liposome (20μM dye), 1μL of the Alexa-fluor internal standard, and different amounts of avidin (or anti-DNP), then diluted to volume with the buffer solution. The detailed description of the Shimadzu spectrofluorometer and the CE-LIF system are given in the experimental section of previous chapters.

Conventional fluorescence experiments were performed on a Shimadzu RF5301 spectrofluorometer instrument. Carboxyfluorecein fluorescence measurements were conducted at 490/520nm (excitation/emission). After gel filtration, the liposome which has the 50mM carboxyfluorecein has to be diluted up to 100 times with a buffer in order to bring the fluorescence signal down to the fluorometer detectable range, since that is where the fluorescence is linearly related to concentration (<30μM). The samples for a fluorometer run were prepared from a 10uL aliquot of ligand-attached liposome solution mixed with varying amounts of antibody (or avidin) and diluted to 1mL by a 10mM HEPES buffer, with a 50mM NaCl at pH 7.4. The liposomes were incubated with avidin (or anti-DNP antibody) in a water bath, upto 70°C, for 5-10 minutes, to facilitate liposome aggregation and leakage [17]. The fluorescence of the leaked dye is measured with a Shimadzu spectrofluorometer and CE-LIF instruments.

The fluorescence readings from the CE-LIF are used to calculate the relative fluorescence units (RFU), which is used in Table 4-5 and Figure 4-2. The RFU is the ratio of the peak areas of the leaked dye (Carboxyfluorescein) and the internal standard (Alexa Fluor) in the electropherogram.

$$RFU = \left(\frac{F}{F_{std}} \right) \qquad \textit{Equation (2)}$$

F – Fluorescence after avidin or antibody addition

F_{std} – Fluorescence of internal standard (Alexa) in each sample

The fluorescence readings from the Shimadzu fluorometer are used to

calculate relative fluorescence (%***F***), which is related to degree of the marker leakage and the concentration of the avidin, or antibody. The relative fluorescence (%***F***) is calculated by

$$\%F = \left[\frac{F - F_0}{F_t - F_0}\right] \times 100\% \qquad \textit{Equation (3)}$$

F – Fluorescence after avidin or antibody addition

F_0 – Initial fluorescence before avidin or antibody addition

F_t – Maximum fluorescence with Triton X-100, complete liposome lysis

The *RFU* and *%F* increase proportionally with the increase in concentration of either avidin (for biotin-attached liposomes) or anti-DNP antibodies (for DNP-attached liposomes). This is because the more analytes (anti-DNP & avidin) are added more liposomes are cross-linked and aggregated, leading to greater leakage of their dye content. The fluorescence values of this (concentration dependent) leakage can be used to construct a binding curve, relating the analyte concentration to fluorescence intensities, as shown in Figure 4-1 and Table 4-5 for avidin and anti-DNP, respectively.

Results and discussion

As described in the experimental section, two pairs of reactants (biotin/avidin and DNP/anti-DNP) were used to study the factors affecting their binding on the liposome surface and also to examine the applicability of self-lysing dye-encapsulated liposomes for antigen/antibody type binding assay applications. The stability of the antigen attached liposomes has to be

checked and confirmed before their reaction (incubation) with antibody can be studied. This is done through DLS and fluorescence (latency) measurements. A relatively high PI and fluorescence value, of a diluted liposome sample, indicates lack of liposome stability. The extrusion method yielded biotin and DNP-attached liposomes with low PI of 0.069 and 0.121, with an average size of 165 and 121nm respectively. In both these cases the DOPE lipid is stabilized by ~20% of DPPC to form stable dye-encapsulated liposomes. Other workers have typically used charged lipids, with DOPE, to form stable liposomes, and few anionic lipid examples are given in Table 4-1 [17]. Although, both the neutral DPPC and charged lipids attract interfacial water molecules and stabilize the DOPE-mixed lipids into forming a stable unilamellar liposomes, we were only able use the uncharged DPPC-DOPE liposomes for capillary electrophoresis (CE) based analysis method. Charged liposomes have broader peaks in CE that would reduce the accuracy of measuring peak migration time and area. In addition, if a charged stabilizer is used, the non-specific electrostatic interaction, between a charged liposome surface and some oppositely charged constituents of a sample, could adversely affect the (antigen-antibody) binding and the sensitivity of the liposome lysis method. This electrostatic interaction might create steric and other interferences, making the surface antigen less accessible and weaken the affinity between the liposome-attached-antigen and the antibody in solution. So instead, using the zwitterionc DPPC to stabilized DOPE-liposomes would help us fulfill the objective of developing a more reliable CE-LIF based liposome immunoassay method.

In this study, we used both conventional fluorescence and CE-LIF techniques that showed a strong correlation between the avidin concentration and the relative fluorescence of the leaked dye, after the biotin-liposomes bind with the avidin in solution. The reaction between DNP-liposomes and anti-DNP antibodies also showed similar fluorescence-concentration relationship, but with lower sensitivity. Generally, antigen/antibody type binding assays using dye-encapsulated-liposomes with fluorescence detection, has been the most preferred technique, over radioactive or enzymatic encapsulation, because of its ruggedness and simplicity [7]. Together with fluorescence, DLS measurements are performed, on the liposome samples, before and after incubation with the avidin or anti-DNP antibody solution. Following the DLS analysis, the fluorescence of each avidin spiked biotin-liposome sample was measured with a spectrofluorometer and the % F calculated using *Eq2*. The Fluorescence (%F) increases as more avidin reacts with biotin-liposomes. The DLS results also showed an increase in liposome size and PI values as the avidin (or anti-DNP) concentrations were raised.

The extent of aggregation in the biotin-attached liposomes has been found to be avidin concentration dependent and a similar trend was also observed for DNP-liposomes when they were incubated with anti-DNP antibodies. Both of the liposome size parameters, polydispersity index (PI) and the average diameter (Z_{av}), of the biotin-liposomes increased proportionally with each increase of avidin concentration, as can be seen in Table 4-2. Light scattering techniques, like DLS and turbidimetry, have been used previously to develop analytical methods that relate concentration of the

analyte/antibody with the liposome's average size and polydispersity index [12;41]. The data from other published studies, and our DLS results show that specific antibodies were the causes for the aggregation of the antigen-attached liposomes. This is further supported by the data from the competitive binding results on Table 4-4, where after each successive addition of free biotin, the Z_{av} and PI of biotin-liposomes decreased proportionally, in the presence of limited avidin. The successively added biotin binds and deactivates the avidin thereby inhibiting the biotin-liposomes from cross-linking and aggregation.

The results in Tables 4-2 and 4-3 show that with an increase in Avidin concentration, the liposome's average size (Z_{av}) and its polydispersity index (PI) as well as the percent fluorescence (%F) of the released marker all increased due to the non-competitive binding between Avidin and biotin-cap-liposomes. The DLS results (Z_{av} and PI) in Table 4-2 show that a 0.5μg avidin was smallest concentration that initiated significant (or detectable) aggregation on this set of biotin-liposomes, than the blank solution. There was an increase of 7% in liposome average size (Z_{av}), and a 61% increase in the polydispersity index (PI), from what it was in a blank (non-avidin) buffer solution. But for the same biotin-liposome batch, a 1μg avidin was lowest concentration that caused a significant %F increase (~23%), over the blank (non-avidin) solution, as seen on Table 4-3. Comparing the DLS and fluorescence results in Table (4-2), the smallest avidin concentration detected by DLS was lower by 50% than by fluorescence, using this set of biotin-liposomes at room temperature. This could be because the antibody induced aggregation is a prerequisite before the marker leakage and a

significant change in %F is detected. That means a detectable change in %F was lagging behind the changes in size and polydispersity index. A few other studies have also indicated that the antibody induced aggregation of the antigen-attached-liposomes proceeds via an inverted micelle, or a similar non-bilayer structure before a significant leakage of the encapsulated fluorescent dye, as illustrated by the cartoon on Figure 4-6 [17;19;33;42]. An expanded fluorescence binding curve, with a wider avidin concentration and response ranges, was generated at higher incubation temperatures (80°C) as shown in Figure 4-1. The avidin (detectable) concentration range covered in Figure 4-1 was twice than in Table 4-3, and the fluorescence response range (%F, y-axis) was 72% wider. In addition, the smallest avidin concentration detected with this fluorescence binding curve (Figure 4-1) was 50ng using the Shimadzu spectrofluorometer, or 50ng/ml since all the fluorometer run samples have 1ml total volume. At elevated temperatures, the low degree of hydration around the small DOPE head-group, may contribute for the facilitated aggregation and leakage of the liposomes [17;43].

The accessibility of the biotin, DNP and other hapten molecules by the specific antibody (anti-DNP and avidin) in solution depends on the length of the linker used that connects the hapten molecules to the liposome surface [44-46]. We have found that when the DNP moiety is attached to the liposome through a 4-carbon carpoyl linker (DNP-Cap-PE) instead of a direct (DNP-PE) attachment, it provided better sensitivity for anti-DNP antibodies, as shown in Table (4-5B) than (4-5A). In addition, the DNP-Cap might have a better stabilizing effect than just the DNP moiety since the DNP-Cap-PE liposomes show a lower non-specific leakage (RFU_{avg}= 484),

when diluted in a blank buffer (zero AB), than DNP-PE liposomes (RFU_{avg}= 635). According to the results on Table 4-5B, the 4-carbon linker moiety enhanced the sensitivity, and widen the response range of the anti-DNP fluorescence detection, as opposed to when the DNP is directly attached to the liposome surface(4-5A). This is consistent with other studies that focused on determining the immunogenicity of DNP and other hapten/antigen molecules that are attached to liposomes through different length carbon chain linkers [44-47]. In a study by McConnell and Balkrishnan, the binding affinity of the anti-DNP antibody, was enhanced by two orders of magnitude when the DNP (antigen) is attached to the liposome via a PEG-linker, compared to when DNP is directly attached to the liposome (without a PEG linker) [45]. Similarly, a trinitorphenyl (TNP) hapten attached to membranes with sufficiently short or long hydrophobic spacers are known to be less effective for antibody binding than those with intermediate chain lengths. Twelve (C_{12}) and zero (C_0) carbon linkers were less effective, since the hapten on the liposome surface becomes less accessible for antibody binding than when an optimal six carbon (C_6) linker is used. The reason suggested for the decrease in binding affinity, with the short (C_0) linker, has been the lack of accessibility to some of the hapten moiety that is buried in the membrane and/or is due to steric constraints [46]. While the long spacer (C-12) weakens the TNP binding affinity, toward the antibody in solution, since the long spacer is more inclined to fold back onto the liposome surface thereby creating unwanted interaction between the TNP and the liposome surface functional groups [46].

The effect of incubation temperature on the detector response range of the binding between biotin-liposomes and free avidin is shown on Figure (4-2). The CE-LIF response range is wider, with more data points, in Figure (4-2B) than in (4-2A). Similarly, the fluorometer data (Figure 4-1) also shows a wider working range for the binding between avidin (antibody) and the biotin-liposomes (immunoliposomes) at elevated temperatures, as well observed by Huang and co-workers using a fluorescence spectroscopy technique [17;19;42].

A fluorometer based competitive binding experiment between biotin and biotin-liposomes for a limited amount of avidin on Table 4-4 shows a decrease in fluorescence signal intensity due to a decrease in leakage of the liposome encapsulated dye. This is because the cross-linkage and aggregation of the biotin-liposomes decreases as more avidin binds to the free biotin, thereby decreasing avidin's availability to cross-link the biotin-liposomes. This is supported by the DLS results in Table 4-4, which show a decrease in size (Z_{av}) and polydispersity index (PI) of the biotin-liposomes, as more free biotin competes for a limited avidin sites. In the absence of avidin no significant aggregation or increased leakage (fluorescence) was observed even at higher incubation temperatures, further confirming that avidin induced cross linkage and aggregation is a prerequisite for liposome-membrane destabilization and appreciable dye leakage [17].

Conclusion

In this study our aim was to show that dye encapsulated, antigen attached liposomes can be used to study antigen-antibody binding and further show that this (antigen-attached) liposomes can also be used for the detection of the specific antibodies in solution using fluorescence, CE-LIF and DLS techniques. The lysis of the antigen-liposomes, due to a multidentate antibody (or avidin), and the ensuing fluorescence analysis of the leaked dye was successfully performed without a need for an exogenous lysing agent like complement-proteins. Also, due to the simplicity, stability and ruggedness of dye-encapsulated liposomes, they are better detection signal enhancement tools, than enzymes or isotopic markers. The DLS and fluorescence techniques showed that the liposomes' size variables (PI, Z_{av}) and the relative fluorescence (%F) of the leaked dye were all avidin (and anti-DNP) concentration dependent.

In addition, this self-lysis liposome technique offers a wide fluorescence signal range since the liposomes can encapsulate a very high concentration of dye. Because of this, low concentrations of avidin standard solutions were detected using the liposome/fluorescence technique. The fluorometer data in Figure 4-1 shows the smallest concentration of avidin detected was 50ng/ml, while the CE-LIF data on Figure 4-2 shows a higher value (~20µg/ml). This liposome-fluorescence method, although not maximally optimized, was able to provide comparable detection limits, even lower than some of the other techniques, cited in the literature seen on Figure (4-3).

Adapting a self-lysis liposome assay to CE-LIF was also successful in both avidin and anti-DNP analysis. The CE-LIF technique can provide qualities that are mainly needed in high throughput screening of a huge library of candidate compounds and bioanalytical assay labs, since:

- The assay takes comparatively a short time and it can easily be automated on a CE-LIF setup.
- The resolving power of CE and the detection range of LIF together have the potential to provide assays with low sensitivities and good reproducibility using an internal standard (a second fluorescent dye). The CE can resolve the analyte from the interferents in sample matrix and usage of an internal standard is possible with CE-LIF (not fluorometer).
- The sample and reagent sizes requirement in CE is significantly smaller than conventional fluorescence or similar colorimetric assays. (lipids, dyes, antibody…)

Generally, the fluorescent-liposome techniques, together with DLS, can have wide analytical applications since different hydrophilic or hydrophobic molecules (also fragments of macro-molecules) can be linked or encapsulated with liposomes as mentioned earlier. A shortcoming of the method is that the sensitivity of the assay is dependent on binding strength between the analyte and its conjugate antibody (or antigen) molecule that is attached to the liposome. There could be orientational (or spatial) restrictions involved during the liposome immunoassay, than in free solution immunoassays, which could also affect the binding affinity. The smallest concentration detected and the fluorescence working range was better for

avidin analysis than anti-DNP, since an avidin/biotin binding is 6-7 orders of magnitude stronger than the DNP/anti-DNP binding. Also, the accessibility of the liposome-attached target molecule and the incubation temperature seem to have an effect on the sensitivity and the working range of the fluorescence method.

A broader application of this technique in the field of immunoassays will depend on the success and ease of attaching different ligands to the liposome surface, as noted in introduction of this chapter. A more detailed future study using ligand/receptors, or antigen/antibodies pairs, with real world samples, can further show some of the potentials and advantages of using marker encapsulated liposomes over other labeling techniques, like enzymes, isotopes and single-molecule markers. In recent years quantum dots and nano-particles have been successfully encapsulated in liposomes as new classes of fluorescent probes to enhance detection sensitivity and overcome the limitations (quantum-yield and chemical interference) encountered from using organic fluorescent molecules in biological assay and imaging applications [48].

Table 4-1. Charged lipid stabilizers and their minimum concentration required to form stable DOPE liposomes. (Reference # 16)

Stabilizer	minimum mole % required to form stable liposomes	Charge
DOPS	15	anionic
DPPG	15	anionic
DMPG	15	anionic
DOPA	20	anionic
DOPG	20	anionic

DOPS – dioleoyl glycero-phosphatidylserine

DPPG – dipalmitoyl glycero-phosphatidylglycerol

DMPG – dimyristoyl glycero-phosphatidylglycerol

DOPA – dioleoyl glycero-phosphate

DOPG – dioleoyl glycero-phosphatidylglycerol

Table 4-2. Size, polydispersity and fluorescence measurement of biotin-attached-liposomes*, using DLS and spectrofluorometric techniques after reaction with different amounts of avidin.

Avidin(μg)	Z_{av}(nm)	PI	%F**
0	165	0.069	44
0.5	176	0.111	38
1	181	0.137	54
2	219	0.231	59
4	252	0.244	65
8	450	0.741	73

Z_{av} – Liposome average size in nanometers

PI – Liposome polydispersity index

* – Liposome composition: Biotin-Cap-DPPE:DPPC:DOPE (1:20:79 mole %), 10mM total lipid, 10mM Hepes buffer with 50mM Carboxyfluorescein @ pH of 7.5, assay run at room temp (~ 25°C). standard samples have 1ml total volume

** – %F determination and calculations given in Table 4-3

Table 4-3. Spectrofluorometer* measurement of dye released from biotin-liposomes** after a stoichiometric reaction with avidin.

Avidin (µg)	F_o	F	F_t	$\%F$
0	*14*	*30*	*55*	*44*
1	*14*	*35*	*57*	*54*
2	*14*	*36*	*53*	*59*
4	*14*	*38*	*54*	*65*
8	*14*	*42*	*55*	*73*

$$\%F = \left[\frac{F - F_0}{F_t - F_0} \right] \times 100\%$$

* Fluorescence measurement – spectrofluorometer set @ 480/520nm, assay incubation temp ~ 25°C

** Liposome composition: same as in Table 4-2

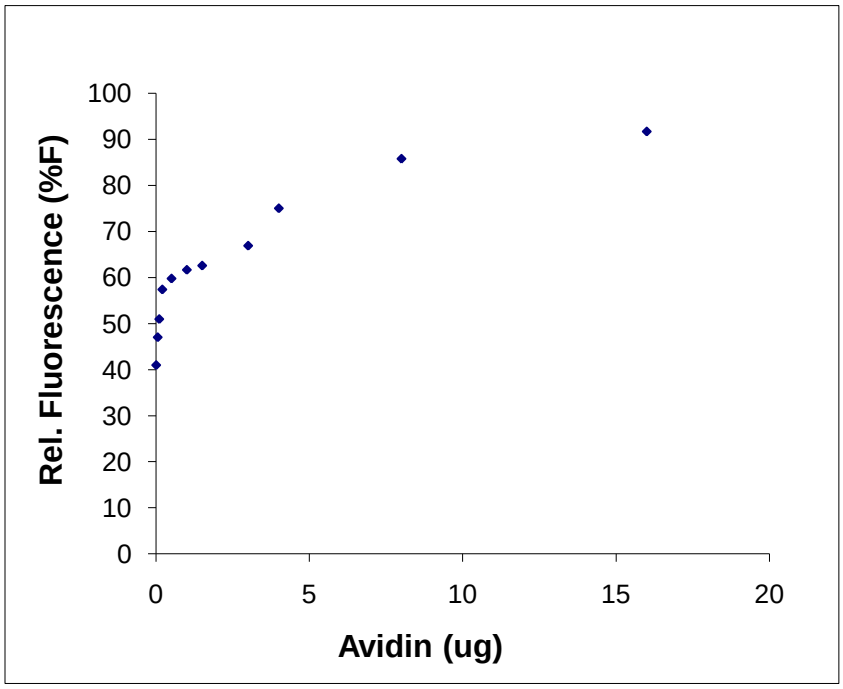

Figure 4-1. An expanded binding curve; a wide fluorescence response range for biotin-Liposomes and standard avidin solutions incubated at 80°C. (spectrofluorometric conditions and sample sizes same as Table 4-2).

(A)

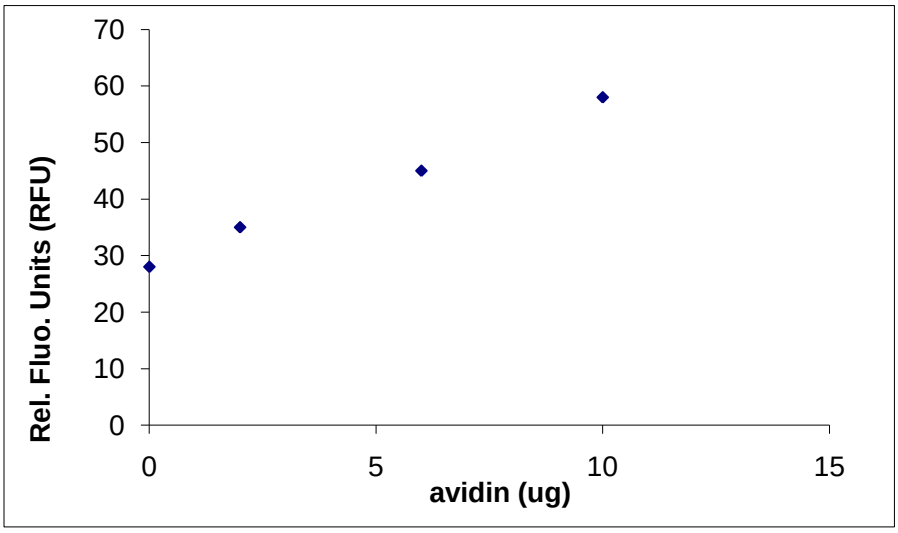

(B)

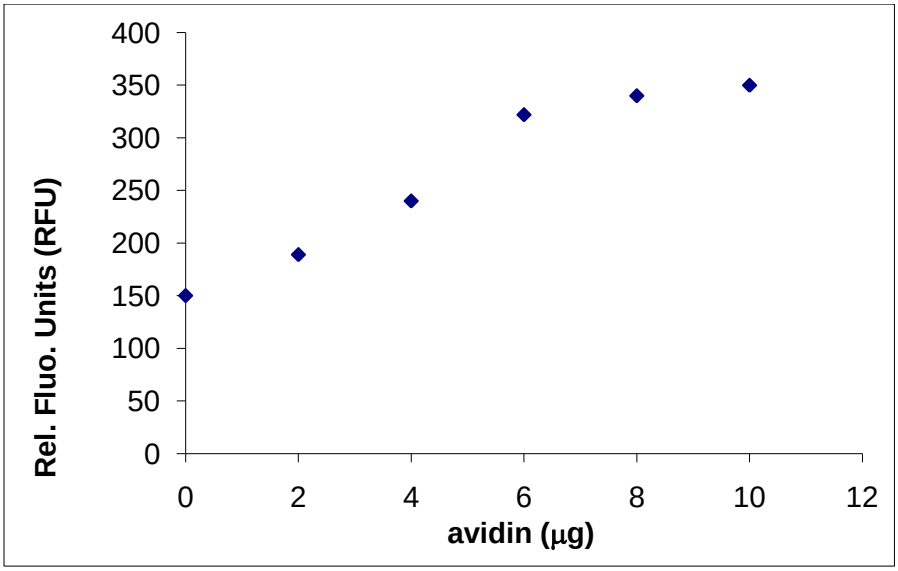

Figure 4-2. Effect of increased incubation temperature on the working range of the avidin CE-LIF assay using biotin-attached liposomes. The temperature is raised from 25°C, as shown below in (A), to 70°C in (B).

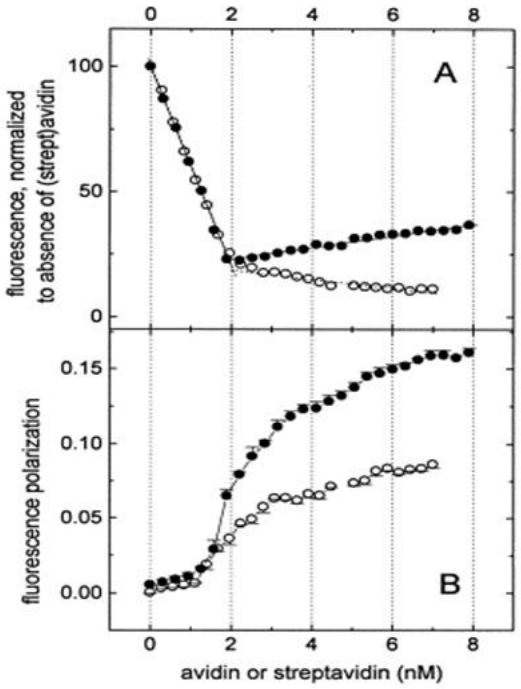

Table I. Detection Limits of Available Avidin–Biotin Assays

method	detection limits [avidin], ng/mL	detection limits [biotin], ng/mL	Assay time
fluorometric	170 000	250	minutes
colorimetric	50 000	100	minutes
colorimetric	3	100	minutes
radioisotopic	5 000	50	minutes
radioisotopic	100		hours
potentiometric	5 000	20	minutes
fluorometric		20	minutes
spectrophotometric	3 000	5	minutes
radioisotopic	10 000	0.6	hours
fluorometric	40	0.5	minutes
radioisotopic	100	0.2	hours
chemiluminescent		0.2	minutes
fluorometric	5	0.1	minutes
bacterial		0.025	days
radioisotopic		0.01	day
immunoassay	100	0.2–0.002	1–20 h
bacterial		0.001	day

Figure 4-3. Detection limits of Avidin/Streptavidin for different analytical techniques, from the literature*.

(*) Graph – Kada, G., Gruber, H.J, Kraiser, K., & Falk, H. *Bochimica et Biophysica Acta* 1427 (1999) 44-48
Table – Schray, K.J. & Artz, P.G. *Anal. Chem*. 1988, 60, 853-855 and references, therein.

Table 4-4. (A) & (B) DLS and fluorometer results for the competitive binding of free biotin, and biotin-attached-liposomes, with limited avidin present in solution

(A)

avidin (μg)	biotin (μg)	Z_{av} (nm)	PI	%F
4	*0*	*1530*	*1*	*53*
4	*2*	*312*	*0.561*	*39*
4	*4*	*215*	*0.249*	*26*
4	*6*	*196*	*0.195*	*23*
4	*8*	*191*	*0.241*	*24*

(B)

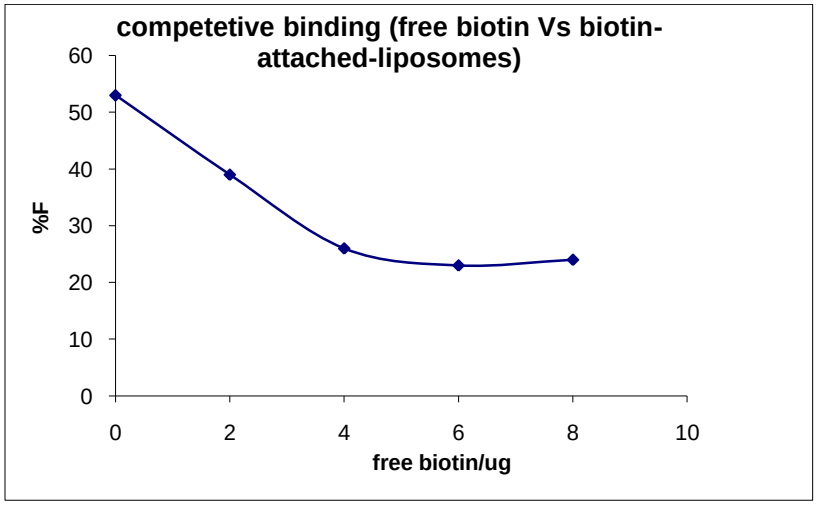

Table 4-5. CE-LIF assay to determine the effect of (ligand) spacer on the binding between DNP-liposomes and anti-DNP antibodies. (A) DNP directly attached to the lipid DPPE (DNP-PE), (B) DNP attached via a four-carbon spacer arm to DPPE (DNP-cap-PE)

(A)

Anti-DNP (ug)	Rel. Fluo. Units (RFU)1	Rel. Fluo. Units (RFU)2 duplicate	Average (RFU_{avg})
0	*644*	*625*	*635*
1	*657*	*627*	*642*
2	*692*	*669*	*681*
3	*815*	*835*	*825*
4	*778*	*789*	*784*

(B)

Anti-DNP (ug)	Rel. Fluo. Units (RFU)1	Rel. Fluo. Units (RFU)2 duplicate	Average (RFU_{avg})
0	*500*	*468*	*484*
1	*547*	*562*	*555*
2	*725*	*700*	*713*
3	*926*	*872*	*899*
4	*1011*	*922*	*967*

Table 4-6. Binding interaction results between DNP-attached-liposomes and anti-DNP antibodies. DLS and fluorometer results as the anti-DNP concentration is increased

Anti-DNP IgE(ug)	Zav (nm)	PI	%F (60ºC)
0	*121*	*0.121*	*63.63*
0.05			*62.22*
0.1			*62.91*
0.5			*62.95*
1	*137*	*0.203*	*63.43*
2			*64.28*
5	*148*	*0.307*	*64.98*
10			*66.21*
20	*867*	*1.000*	*67.70*

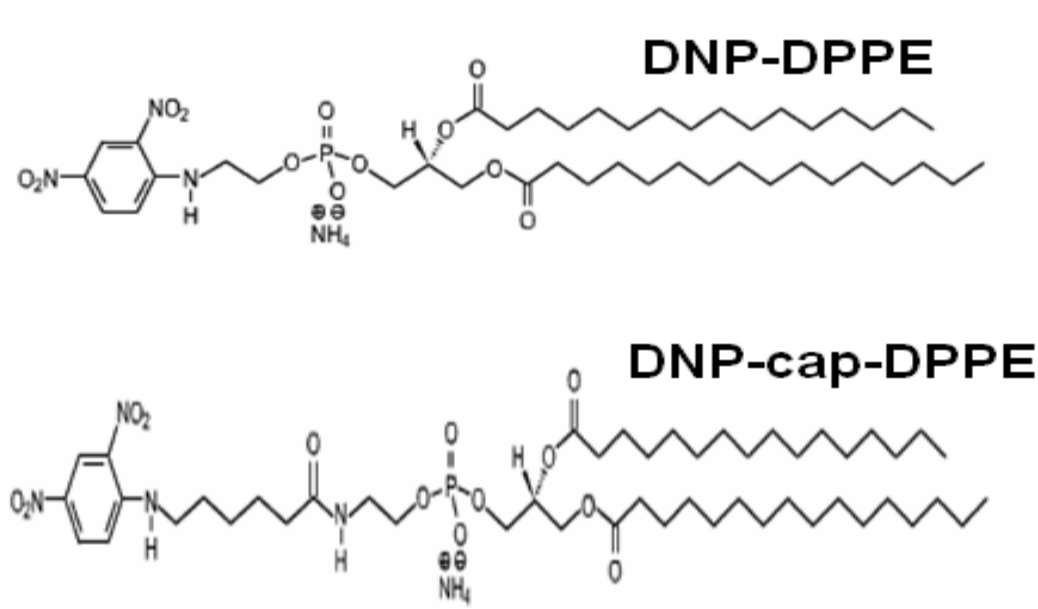

Figure 4-4. Molecular structures of DNP-DPPE and DNP-cap-DPPE lipids

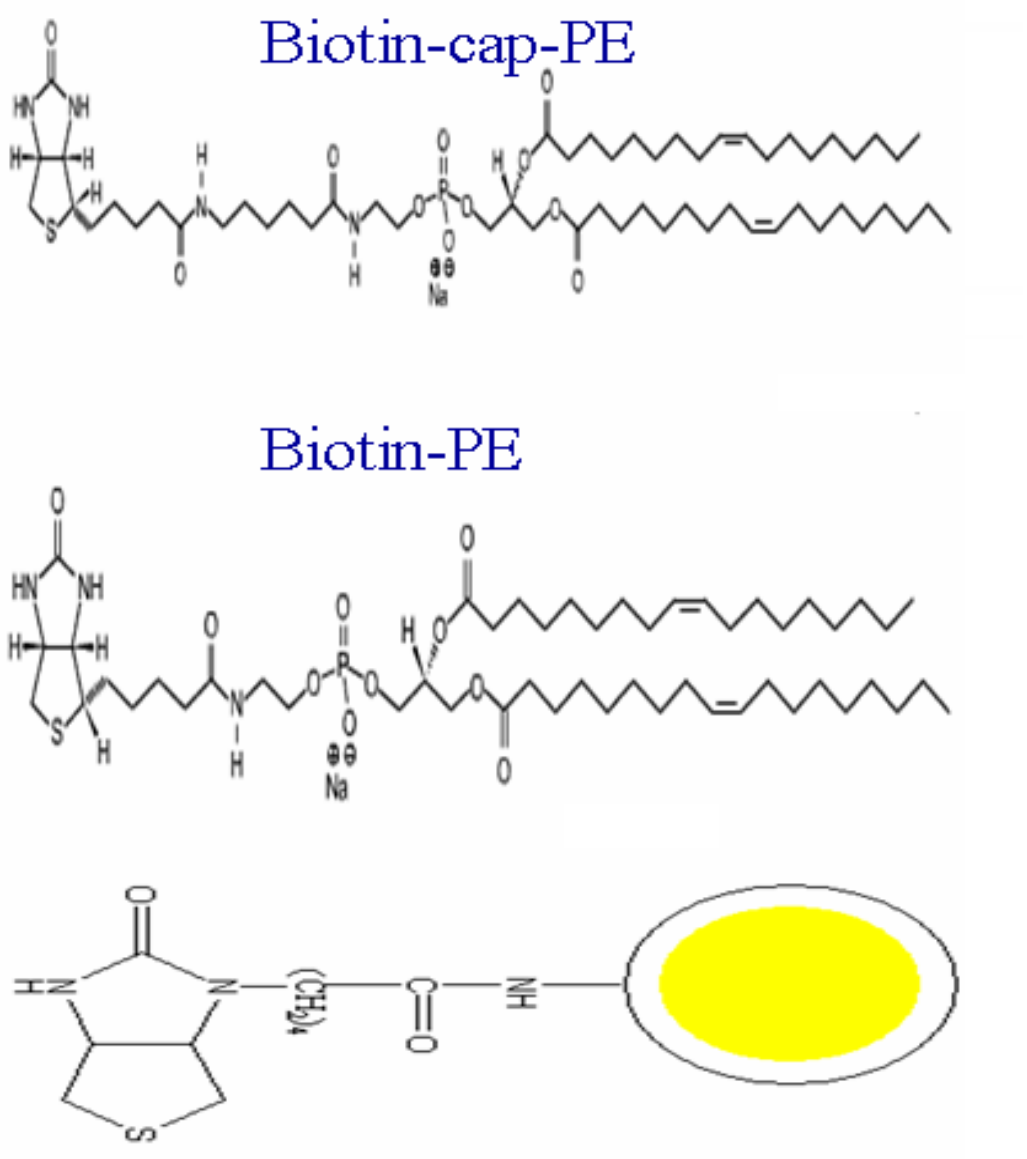

Figure 4-5. Molecular structures of Biotin-DPPE, biotin-cap-DPPE and a diagram of a dye encapsulated liposome composed of Biotin-cap-DPPE (and other) lipids.

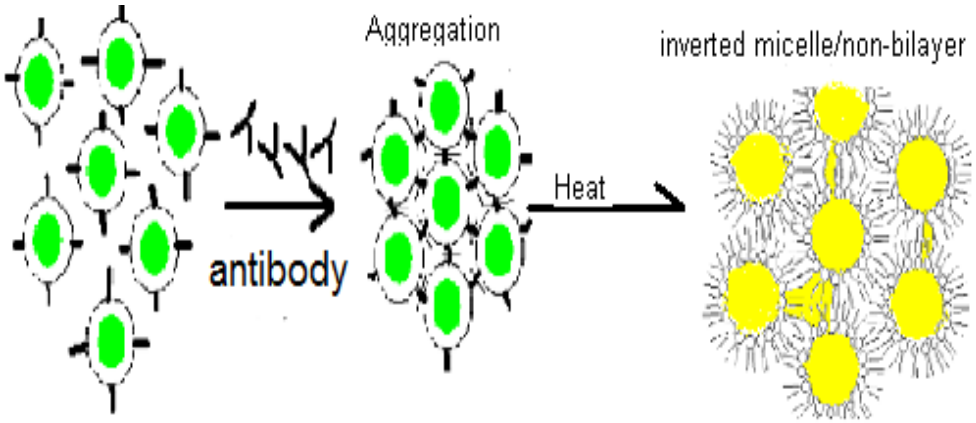

Figure 4-6. A hypothetical mechanism (*) of avidin (antibody) induced aggregation and leakage of dye-encapsulated, biotin-attached liposomes (via a non-bilayer formation step)

* G.K.Humphries and H.M.McConnell, Immune lysis of liposomes and erythrocyte ghosts loaded with spin label, Proc.Natl.Acad.Sci.U.S.A 71 (1974) 1691-1694.

Reference List

[1] L.Nobs, F.Buchegger, R.Gurny, and E.Allemann, Current methods for attaching targeting ligands to liposomes and nanoparticles, J.Pharm.Sci. 93 (2004) 1980-1992.

[2] K.A.Edwards and A.J.Baeumner, Liposomes in analyses, Talanta 68 (2006) 1421-1431.

[3] S.Katoh, M.Kishimura, and K.Tomika, Immune lysis assay of antibodies by use of antigen-coupled liposomes, Colloids Surf., A 109 (1996) 195-200.

[4] B.S.Yu, Y.K.Choi, and H.H.Chung, Development of immunoassay methods by use of liposomes, Biotechnol.Appl.Biochem. 9 (1987) 209-216.

[5] A.J.Singh, R.G.Carbonell, Liposomes in Immunodiagnostics, In: Lasic, D. D. and Barenholz, Y. (Eds.), Handbook of Nonmedical Applications of Liposomes: From Gene Delivery and Diagnosis to Ecology, CRC Press, Boca Raton, FL, 1995, pp. 209-216.

[6] A.K.Singh, S.Schoeniger, R.G.Carbonell, Liposomes as Signal-Enhancement Agents in Immunodiagnostic Applications, In: Yang, V. C., That, T. N., and Ngo, T. T. (Eds.), Biosensors and their applications, Plenum Publishers, New York, 2009, pp. 131-145.

[7] H.A.Rongen, A.Bult, and W.P.van Bennekom, Liposomes and immunoassays, J.Immunol.Methods 204 (1997) 105-133.

[8] Haugland, R. P. The Handbook: A Guide to Fluorescent Probes and Labeling Technologies, Invitrogen/Molecular Probes, Carlsbad, CA, 2005.

[9] P.Pinnaduwage and L.Huang, A homogeneous, liposome-based signal amplification for assays involving enzymes, Clin.Chem. 34 (1988) 268-272.

[10] M.A.Jones, P.K.Kilpatrick, and R.G.Carbonell, Preparation and characterization of bifunctional unilamellar vesicles for enhanced immunosorbent assays, Biotechnol.Prog. 9 (1993) 242-258.

[11] O.D.Hendrickson, S.N.Skopinskaya, S.P.Yarkov, A.V.Zherdev, and B.B.Dzantiev, Development of liposome immune lysis assay for the herbicide atrazine, J.Immunoassay Immunochem. 25 (2004) 279-294.

[12] K.D.Lee, A.B.Kantor, S.Nir, and J.C.Owicki, Aggregation of hapten-bearing liposomes mediated by specific antibodies, Biophys.J. 64 (1993) 905-918.

[13] J.A.Haxby, O.Gotze, H.J.Muller-Eberhard, and S.C.Kinsky, Release of trapped marker from liposomes by the action of purified complement components, Proc.Natl.Acad.Sci.U.S.A 64 (1969) 290-295.

[14] E.Canova-Davis, C.T.Redemann, Y.P.Vollmer, and V.T.Kung, Use of a reversed-phase evaporation vesicle formulation for a homogeneous liposome immunoassay, Clin.Chem. 32 (1986) 1687-1691.

[15] Y.Tatsu, S.Yamamura, and S.Yoshikawa, Fluorescent fibre-optic immunosensing system based on complement lysis of liposome containing carboxyfluorescein, Biosens.Bioelectron. 7 (1992) 741-745.

[16] G.K.Humphries and H.M.McConnell, Immune lysis of liposomes and erythrocyte ghosts loaded with spin label, Proc.Natl.Acad.Sci.U.S.A 71 (1974) 1691-1694.

[17] B.Babbitt, L.Burtis, P.Dentinger, P.Constantinides, L.Hillis, B.McGirl, and L.Huang, Contact-dependent, immunecomplex-mediated lysis of hapten-sensitized liposomes, Bioconjug.Chem. 4 (1993) 199-205.

[18] W.J.Litchfield, J.W.Freytag, and M.Adamich, Highly sensitive immunoassays based on use of liposomes without complement, Clin.Chem. 30 (1984) 1441-1445.

[19] P.Pinnaduwage and L.Huang, Stable target-sensitive immunoliposomes, Biochemistry 31 (1992) 2850-2855.

[20] C.Selby, Interference in immunoassay, Ann.Clin.Biochem. 36 (Pt 6) (1999) 704-721.

[21] S.G.Reeves, S.T.A.Siebert, R.A.Durst, Liposome-Amplified Immunodetermination of Environmental Contaminants, In: Lasic, D. D. and Barenholz, Y. (Eds.), Handbook of Nonmedical Applications of Liposomes, from Gene Delivery and Diagnosis to Ecology, CRC press, Boca Raton, FL, 1996, pp. 245-254.

[22] Y.Fintschenko and G.S.Wilson, Flow injection immunoassays: a review, Mikrochimica Acta 129 (1998) 7-18.

[23] K.Shahdeo and H.T.Karnes, Combining immunoassays with chromatographic and electrophoretic separation techniques - a review, Mikrochimica Acta 129 (1998) 19-27.

[24] M.A.Bacigalupo, A.Ius, R.Longhi, and G.Meroni, Homogeneous immunoassay of atrazine in water by terbium-entrapping liposomes as fluorescent markers, Talanta 61 (2003) 539-545.

[25] K.Tsukagoshi, H.Akasaka, Y.Okumura, R.Fukaya, M.Otsuka, K.Fujiwara, H.Umehara, R.Maeda, and R.Nakajima, Immunoassay using chemiluminescence detection of dyestuff-containing liposomes as a labeling reagent, Analytical Sciences 16 (2000) 121-124.

[26] S.T.A.Siebert, S.G.Reeves, M.A.Roberts, and R.A.Durst, Improved Liposome Immunomigration Strip Assay for Alachlor Determination, Analytica Chimica Acta 311 (1995) 309-318.

[27] J.A.Ho and R.D.Wauchope, A strip liposome immunoassay for aflatoxin B1, Anal.Chem. 74 (2002) 1493-1496.

[28] F.J.Martin and V.T.Kung, Use of Liposomes As Agglutination-Enhancement Agents in Diagnostic-Tests, Methods in Enzymology 149 (1987) 200-213.

[29] N.J.Lynch, P.K.Kilpatrick, and R.G.Carbonell, Aggregation of ligand-modified liposomes by specific interactions with proteins .1. Biotinylated liposomes and avidin, Biotechnology and Bioengineering 50 (1996) 151-168.

[30] N.J.Lynch, P.K.Kilpatrick, and R.G.Carbonell, Aggregation of ligand-modified liposomes by specific interactions with proteins .2. Biotinylated liposomes and antibiotin antibody, Biotechnology and Bioengineering 50 (1996) 169-183.

[31] P.R.Cullis, M.J.Hope, and C.P.S.Tilcock, Lipid Polymorphism and the Roles of Lipids in Membranes, Chemistry and Physics of Lipids 40 (1986) 127-144.

[32] V.V.Kumar, Complementary molecular shapes and additivity of the packing parameter of lipids, Proc.Natl.Acad.Sci.U.S.A 88 (1991) 444-448.

[33] R.J.Ho and L.Huang, Interactions of antigen-sensitized liposomes with immobilized antibody: a homogeneous solid-phase immunoliposome assay, J.Immunol. 134 (1985) 4035-4040.

[34] F.J.Martin and D.Papahadjopoulos, Irreversible coupling of immunoglobulin fragments to preformed vesicles. An improved method for liposome targeting, J.Biol.Chem. 257 (1982) 286-288.

[35] R.J.Lee and P.S.Low, Delivery of Liposomes Into Cultured Kb Cells Via Folate Receptor-Mediated Endocytosis, Journal of Biological Chemistry 269 (1994) 3198-3204.

[36] S.C.Kinsky and R.A.Nicolotti, Immunological properties of model membranes, Annu.Rev.Biochem. 46 (1977) 49-67.

[37] M.J.Hope, M.B.Bally, G.Webb, and P.R.Cullis, Production of Large Unilamellar Vesicles by A Rapid Extrusion Procedure - Characterization of Size Distribution, Trapped Volume and Ability to Maintain A Membrane-Potential, Biochimica et Biophysica Acta 812 (1985) 55-65.

[38] M.J.Hope, R.Nayer, L.D.Mayer, P.R.Cullis, Reduction of liposome size and preparation of unilamellar vesicles by extrusion techniques, In: Gregoriadis, G. (Ed.), Liposome Technology: liposome preparation and related techniques, CRC Press Inc., Boca Raton, FL, 1993, pp. 123-139.

[39] D.W.Fry, J.C.White, and I.D.Goldman, Rapid separation of low molecular weight solutes from liposomes without dilution, Anal.Biochem. 90 (1978) 809-815.

[40] Malvern instruments. Dynamic Light Scattering: An Introduction in 30 Minutes. http://www.malvern.com/common/downloads/campaign/MRK656-01.pdf . 2009.

[41] A.Agirre, S.Nir, J.L.Nieva, and J.Dijkstra, Induction of aggregation and fusion of cholesterol-containing membrane vesicles by an anti-cholesterol monoclonal antibody, J.Lipid Res. 41 (2000) 621-628.

[42] R.J.Ho, B.T.Rouse, and L.Huang, Target-sensitive immunoliposomes: preparation and characterization, Biochemistry 25 (1986) 5500-5506.

[43] X.Li and M.Schick, Theory of lipid polymorphism: application to phosphatidylethanolamine and phosphatidylserine, Biophys.J. 78 (2000) 34-46.

[44] G.F.Dancey, P.C.Isakson, and S.C.Kinsky, Immunogenicity of liposomal model membranes sensitized with dinitrophenylated phosphatidylethanolamine derivatives containing different length spacers, J.Immunol. 122 (1979) 638-642.

[45] K.Balakrishnan, S.Q.Mehdi, and H.M.McConnell, Availability of dinitrophenylated lipid haptens for specific antibody binding depends on the physical properties of host bilayer membranes, J.Biol.Chem. 257 (1982) 6434-6439.

[46] K.Kimura, Y.Arata, T.Yasuda, K.Kinosita, and M.Nakanishi, Location of membrane-bound hapten with different length spacers, Immunology 69 (1990) 323-328.

[47] H.Jung, T.Yang, M.Lasagna, J.Shi, G.Reinhart, and P.S.Cremer, Impact of Hapten Presentation on Antibody Binding at Lipid Membrane Interfaces, Biophys.J. (2008).

[48] C.-S.Chen, J.Yao, and R.Durst, Liposome encapsulation of fluorescent nanoparticles: Quantum dots and silica nanopa, Journal of Nanoparticle Research 8 (2006) 1033-1038.

Chapter 5

Analyzing the interaction of liposomes with Indolicidin using electrophoretic, fluorescence and light scattering techniques

Abstract

The interaction of indolicidin, a 13-mer cationic antimicrobial peptide, and liposomes with various lipid and cholesterol composition was investigated using light scattering, fluorescence and capillary electrophoresis methods. Dynamic light scattering (DLS) results show a change in liposome size/size-distribution after indolicidin interaction. The extent of this liposome morphological change, in part depends on the liposome's lipid composition. Indolicidin caused lipid mixing and aggregation mostly in zwitterionic DMPC and DMPC/CH (1,2-Dimyristoyl-*sn*-Glycero-3-Phosphocholine/Cholesterol) liposomes, but anionic DMPC/DMPG (dimyristoyl glycerophosphocholine + dimyristoyl phosphotidylglycerol) liposomes did not show any significant DLS detectable aggregation after interaction with an equal amount of indolicidin. Indolicidin's innate tryptophan fluorescence showed that the emission λ_{max} was blue shifted to a lower wavelength in the presence of liposomes, and the $\Delta\lambda_{max}$ was larger in the presence of DMPC/PG anionic liposomes. In addition, the emission intensity of the peptide at λ_{max} was larger when incubated with anionic liposomes. Fluorescence dequenching (leakage) experiments showed that calcien encapsulated anionic liposomes leaked the most after indolicidin interaction, and cholesterol mixed DMPC liposomes leaked the least. It is assumed that the deeper membrane insertion of the hydrophobic residues

caused the calcein leakage, and this effect is reinforced by the electrostatic attraction between the cationic residues of the peptide and the anionic lipid head groups. Indolicidin's affinity for zwitterionic and anionic lipid bilayers was compared using a capillary electrophoresis method. The CZE (Capillary zone electrophoresis) separation of the lipid unbound peptide showed only 37% and 50% of the peptide stayed bound to DMPC/CH and DMPC liposomes respectively, while 100% of the peptide was irreversibly bound to the anionic DMPC/PG and DMPC/CH/PG liposomes, due to the additional electrostatic attraction. A low pH LEKC (liposome electrokinetic chromatography) injection of indolicidin, with DMPC/CH liposomes used as pseudostationary phase, showed the peptide eluting in only 5.6 minutes, indicating that cholesterol attenuates the peptide's hydrophobic interaction with zwitterionic liposomes. But, the LEKC with pure PC liposomes did not elute the peptide peak within the specified run time, suggesting a stronger binding than with DMPC/CH liposomes.

Introduction

All living matters use a complex array of biological and chemical mechanisms to defend themselves from invading pathogens. In mammals, as in many other organisms, the major components of innate immune defense mechanism against harmful pathogens are the cationic antimicrobial peptides (AMP), which are produced in response to infection by pathogens [1]. AMPs are produced predominantly in animals' most exposed tissues (skin, eyes, tongue, etc…), which are most likely to come in contact with microorganisms. In higher organisms they are produced mainly on epithelial surfaces and phagocytic cells. The typical character of AMPs is their cationicity and amphipathicity by which they protect the host against microbial infection [2-4].

The reason for the high interest in AMPs is because many of them appear to act via a selective, but non-receptor mediated, permeabilization of microbial membranes, and this confers a considerable potential for their development as novel therapeutic agents that could overcome the (antibiotic) resistance problem. AMPs might provide a new generation of antibiotics that will address this drug resistance problem. Investigation of their structure-activity behavior with artificial bilayers is helpful in deciphering the orientation of proteins in membranes and in better understanding membrane interfacial activity, which affects cell-signaling and membrane transport activities, among others [2;5].

The modes of action of antimicrobial peptides elucidated to date include inhibition of (bacterial) cell wall formation, membrane perturbation or

deformation, formation of pores in the membrane resulting in the disruption of membrane potential with eventual lysis of the cell and, finally, inhibition of nuclease activity involving RNase and/or DNase activity[6-8]. In all cases, an initial interaction with the outer membranes of bacteria is necessary. This first point of interaction between the peptides and their targets is often also the site of antimicrobial action as they interfere with the membrane function to cause bacterial cell death. This interaction mainly involves two binding properties:

1. The electrostatic interaction at the membrane interface among the lipid head-groups, the polar residues of the peptide, and the solvent molecules.
2. Once the peptide contacts the membrane, the hydrophobic interaction between the non-polar peptide residues and the membranes hydrophobic parts can take effect. Recent studies show that insertion of the peptide's hydrophobic moieties into the bilayer, which could be followed by excessive permeabilization or destabilization of the membrane is largely caused by this hydrophobic interaction. Generally, the effect of these peptide interactions can be: perturbation/deformation of the membrane, aggregation of apposing bilayers, or the complete lysis and breakdown of the lipid bilayer [8;9].

Formation of lipid domains in the membrane due to differences in affinity toward the peptide by the different lipid components can also cause membrane deformation or an aggregation between apposing membranes

[10]. Cholesterol can create domains, or rafts as they are also called, in the membrane due to solubility differences of the AMP.

Fundamental differences exist between microbial and mammalian cell membranes that may represent a target for antimicrobial peptide action. Two of the main differences between bacterial and mammalian cell membrane types include lipid composition and packing structure. The plasma bilayer membrane of many mammalian cells like erythrocytes is asymmetric with neutral (zwitterionic) phospholipids and cholesterol comprising their outer membrane leaflet. Bacterial membranes, in contrast, have predominantly negatively charged lipids on their outer membrane surface. The structure of AMPs is composed of both hydrophobic and hydrophilic moieties, also termed as "amphipathic" property n, which is believed to play a key role in antimicrobial mechanism of action. The hydrophilic and the cationic features of AMPs are proposed to initiate interaction with the negatively charged bacterial surface and other anionic phospholipid bilayer membranes. Then, the hydrophobic moiety of the AMP will facilitate the insertion of the peptide into the membrane's interior [1;7].

Liposomes are convenient model systems to study the interaction between AMPS and real membrane systems. Their composition can be varied to resemble those of specific real membrane systems, both prokaryotic and eukaryotic. Usually, a combination of zwitterionic lipids like phosphatidylcholine (PC), sphingomyelin, phosphatidylserine, phosphatidylethanolamine (PE) and cholesterol are used to mimic mammalian or eukaryotic membranes. While PE and PC mixed with anionic lipids like phosphatidylglycerol (PG), or PG derivatives such as

diphosphatidylglycerol (DPPG) and cardiolipin are used to make membranes resembling those of bacterial and prokaryotic cells [11]. Characterization of liposomes charge and size prior to peptide interaction is important as they can influence their interaction with AMPs. The lipid composition and its concentration are also important parameters since the extent of liposome-AMP interaction is primarily affected by the type of lipids and the (lipid-to-peptide) concentration ratio. Compared to zwitterionic membranes, anionic membranes have been found to be more susceptible to AMP action, mainly due to the enhanced binding caused by the electrostatic attraction [12;13].

AMPs can be classified based on their structure, sequence homologies and functional similarities [8;14]. Based on their structure they can be divided into four broad families: 1) linear α-helical peptides include: cecropins, magainins and mellittins, which adopt a random structure in dilute aqueous solution and form α-helices or a helix-bend-helix motif in organic solvents and upon contact with cell membrane phospholipids; 2) extended linear structure peptides that are rich in proline, arginine, or aromatic amino acids, like indolicidin from the cytoplasmic granules of bovine neutrophils; 3) β-sheet structure peptides, like gramicidin-S; 4) loop peptides cyclized with a single cystine disulphide bond, like bacteriocins. Since many of these AMPs, which are similar in structure, can have differences in spectrum of activity; they can also be classified based on their activity against membranes:

1. AMPs that are highly potent against bacteria but not against mammalian cells and fungi (e.g. insect cecropins, magainins, and dermaseptins). These are active against both gram positive and negative bacteria.

2. Those toxic to both bacteria and mammalian cells including pig cecropins, cattle indolicidin and insect defensins. However there are also several AMPs that are active against fungi but not against mammalian nor bacterial membranes [2;8;13].

AMPs range in size from 12 to 50 amino acid residues and there are now more than 800 known in number that are derived from different animal and plant species. The Cathelicidin group of AMPs were discovered over a decade ago and possess a broad spectrum of antimicrobial activity. Cathelicidins, which Indolicidin is one of, are gene-encoded "natural antibiotics" that are produced by several mammalian species on epithelial surfaces and within the granules of phagocytic cells. They have also been found to be cytotoxic and homolytic toward both bacterial and mammalian cells. Since their discovery over a decade ago, cathelicidins have been speculated to function within the innate immune system, contributing to a first line of host defense against an array of microorganisms. Consequently, cathelicidins have captured the interest of basic investigators in the diverse fields of cell biology, immunology, protein chemistry and microbiology [15]. Their broad antimicrobial activity makes cathelicidins ideal templates in combinatorial chemistry to design de-novo antimicrobial peptides for therapeutic applications.

Indolicidin is a Cathelicidin, and also one of the smallest natural peptides known to date. Its unique composition distinguishes it from the other mostly α-helical or β-structure cationic peptides. It has a linear structure with 13 amino acids including, five tryptophans (39%), three prolines (23%), and an

amidated carboxy terminus [16].Indolicidin has the highest Trp composition of any natural peptide or protein known:

H-Ile-Leu-Pro-Trp-Lys-Trp-Pro-Trp-Trp-Pro- Trp-Arg-Arg-NH2

The linear/extended conformation of indolicidin might be due to the bulky tryptophan and proline residues. Structural analysis by H-NMR has revealed that the substitution of proline with alanine enables the modified (Indolicidin) peptide (CP10A) to adopt a helical conformation, rather than the extended linear structure of the native Indolicidin [17]. Even though indolicidin does not adopt a β-turn nor α-helix structures in membrane mimicking environments, it has a tendency to readily partition into liposomes with different lipid composition. Indolicidin's strong interaction with anionic membranes is driven by the electrostatic interaction while its partitioning capability into neutral lipid bilayers is mostly driven by the energetically favorable hydrophobic effect due to the five tryptophan residues [18;19]. Indolicidin is toxic to both prokaryotic and eukaryotic cells. It has been shown to effectively kill gram-positive and gram-negative bacteria, different fungi, mammalian lymphocytes and erythrocytes, including that of humans'. Similarly, in studies with model lipid-bilayer membranes, indolicidin has effectively leaked the encapsulated aqueous-dye from both zwitterionic and anionic liposomes. But changing the Trp amino acid residues to Phe has been shown to eliminate indolicidin's hemolytic activity [20]. Also, the amidation of indolicidin at the carboxy terminus enhances its activity against anionic model membranes and bacteria due to added cationicity [21].

Indolicidin's exact mode of action against membranes is not clearly known, although different mechanisms have been proposed based on observations from experiments with real and artificial membranes. Some of the mechanisms include: I) membrane permeablization by channel formation [21]; II) membrane insertion and formation of torroidal pore [22]; III) creating a trans-membrane defect by forming a head-to-tail peptide dimer across the bilayer [23]; IV) forming a transient trans-membrane aqueous pore[24] and V) inhibition of DNA synthesis after self-permeation into the cytoplasm [25]. The true mechanism can be one or a combination of the above, depending on the lipid composition and nature of the membrane. Although the exact mechanism of action is still under debate, it is clear that indolicidin must first interact with the microbe's external membrane thereby enhancing its permeability and leak out its contents, or enter the cytoplasm and disrupt cellular function. In light of this, it is apparent to see the importance of characterizing the interaction between indolicidin and lipid bilayers since knowing the nature of such interactions: 1) helps in understanding the mechanisms employed by AMPs that will significantly improve our understanding of how AMPs act to defend against infection; 2) helps in designing peptide drugs that effectively kill pathogens, but are safe for the host animal; and 3) helps to get a better insight into how membrane proteins effectively anchor themselves within the lipid bilayers through their membrane-active segments/moieties.

Different analytical techniques have been used to characterize the interaction between indolicidin and different membrane mimetic entities. Some of the techniques include: NMR spectroscopy [26], circular dichroism [27],

fluorescence spectroscopy [22;23;28;29], Fourier transform infrared-attenuated total reflection spectroscopy (FTIR-ATR) [30], quartz crystal microbalance [24], electron microscopy [31], and turbidimetry [32]. But mostly, the different forms of fluorescence technique have been the preferred methods due to their simplicity and the extensive information that can be gained from them.

The application of fluorescence spectroscopy to the study of membrane-active peptides usually takes advantage of the presence of naturally occurring, or engineered, tryptophan (Trp) residues in their primary structure, and uses them as a probe. Several properties of this intrinsic-fluorescent probe (Trp), including fluorescence lifetime and quantum yield, are solvent environment dependent and can be used to determine the peptide's membrane partitioning and depth of penetration [33]. In addition, spectral shifts undergone by the emission spectra of Trp residues, as well as changes in accessibility to aqueous quenchers can be exploited to characterize peptide membrane binding. Further information regarding the transverse location (degree of penetration) of the membrane-bound peptide molecules can be gained through depth-dependent fluorescence quenching experiments by attaching (hydrophobic) quenchers along the acyl chain of membrane-building lipids [33].

The fluorescence intensity from Trp residues generally exhibits a significant increase upon interaction with lipid bilayers. This enhancement reflects an increase in the quantum yield, Φ, of the Trp residues upon inclusion in a less polar environment. This is usually accompanied by a corresponding variation in its mean fluorescence excited state lifetime. In addition to the

fluorescence quantum yield, the position of the maximum emission spectrum, λ_{max}, is also sensitive to its solvent environment. The transfer of the peptide from the aqueous (polar) environment to the lipid bilayer (less polar) characteristically causes a blue-shift in the emission from around 350 nm to as low as 325 nm. This property can therefore be used to obtain an approximate description of the location/environment of peptide's Trp residues in the membrane [33].

Fluorescence quenching using acrylamide and iodide quenchers has been used extensively to investigate the microenvironments of tryptophan residues in liposome suspensions [33]. As noted earlier, a peptide's Trp residues buried in the liposome's hydrophobic core are somewhat shielded from the aqueous solution. That means if the peptide inserts deep into the liposome membrane, and the membrane's integrity is not compromised, an aqueous quencher present in the extra-liposomal solution should have a minimal quenching effect on the peptide's innate fluorescence. In quenching studies, the neutral acrylamide is usually preferred in order to avoid non-specific electrostatic side-interactions between the quencher and other charged species in solution. The Stern-Volmer relationship (Eq. 5-1) can be used for a more quantitative relationship between the extent of fluorescence quenching and the quencher's concentration [33].

$$\frac{F_0}{F} = 1 + K_{sv}[Q] \qquad \textit{Equation(1)}$$

Where K_{sv} is the collisional Stern-Volmer constant, F_0 and F are the fluorescence intensities of the peptide in the absence and presence of the

quencher respectively, and [Q] is the quencher concentration. The K_{sv} constant is dependent on the chemical composition of the quencher, which inhibits the excitation (of peptide) by depopulating the excited state and decreasing the excited state lifetime and intensity. A plot of (F_0/F) as a function of [Q] yields a linear plot with a slope equal to K_{sv}. A peptide that is better protected from the aqueous quencher, i.e. one that is buried deeper into membrane, will have a lower slope than one binding to the outer membrane surface, which is accessible to aqueous quencher. For semi-quantitative studies the (F_0/F) ratio can be used to compare the extent of Trp quenching in different lipidic solutions at a constant quencher concentration. In our study liposomes of different lipid composition were incubated with constant concentration of indolicidin and acrylamide, in order to monitor the extent of tryptophan fluorescence quenching due to collisional contact, between quencher and indolicidin. The quenching of a peptide's fluorescence by an aqueous-quencher can mean one of two things:

1. The peptide stays at the liposome interface, so the aqueous quencher had easy access to it (weak interaction between liposome and peptide), or
2. The peptide destabilized the membrane to the extent where water was also able to penetrate deeper and cause a contact between peptide and the quencher.

Another fluorescence experiment generally done in lipid interaction studies, involves the usage of an aqueous dye encapsulated in liposome at high (quenched) concentrations [34;35]. When these liposomes are incubated

with membrane-active-peptides their lipid-bilayer undergoes a structural change that causes the encapsulated dye to leak out to the extra-liposomal buffer solution. Upon leakage, the quenched dye is diluted by the buffer outside of the liposome, and starts to fluoresce according to its concentration. The amount of leakage is usually proportional to the extent of structural damage, or morphological change, caused on the lipid packing by the peptide [12;22;36;37].

Dynamic light scattering (DLS) techniques have been used to monitor morphological changes of liposome membranes after contact with cationic antimicrobial peptides[32]. Because these peptides have both hydrophilic and hydrophobic parts, like detergents, they readily partition into lipid bilayers causing morphological and size changes to the liposome membrane [10;32;38]. These changes in liposome size and size distribution can be monitored with the DLS technique by measuring the liposome's average diameter (Z_{av}) and polydispersity index (PI) before and after peptide addition [32;39]. Due to the strong hydrophobic peptide-membrane interaction, several investigators have observed an overall increase in the Z_{av}, PI and turbidity of their liposome and bicelle suspensions [39;40].

Peptides carry a net charge at any pH different from their inherent p*I*-value, which easily facilitates their characterization and separation using electrokinetic methods like Capillary Electrophoresis (CE). The simplicity of Capillary Zone Electrophoresis (CZE), with its high separation efficiency, short analysis time and its ability to be coupled with multiple detection techniques, including mass spectrometry, makes it an ideal technique for the analysis of AMPs. However, there could be a problem of a non-specific

electrostatic binding between cationic peptides and the capillary surface silanol groups, which are ionized above a pH of 3. This wall interaction effect at the surface of the bare fused silica capillary may degrade the separation performance, and can lead to loss of sample, peak tailing, unstable electro-osmotic flow and generally poor separation reproducibility [41]. One way of circumventing this effect is to suppress the dissociation of the silanol groups by running the separation at a very low pH, e.g. 2.5 [42]. But, using low pH running buffers (e.g. phosphate, pKa1=2.15) will keep the capillary silanols protonated, which eradicates the EOF and excessively extends the run time. During low pH electrophoresis, the peptide's own electrophoretic mobility will be its only migration mechanism though the capillary.

Micellar Elektrokinetic Chromatography (MEKC) and Liposome Electrokinetic Chromatography (LEKC) have been used in the past, to some degree, for the separation and characterization of peptides [43-45]. The use of micellar or lipid bilayer structures as a pseudo-stationary phase in the mobile phase during peptide electrophoresis can give significant information about the nature of the interaction between real membranes and peptides [46-49]. A few LEKC studies have shed some light on how membrane-peptide interactions are affected by liposome composition and the nature of the peptide [45;47;50;51]. But surprisingly, the amount of published work related to the study of cationic antimicrobial peptides using CE methods has been very limited. Mills and Holland studied the interaction of six cationic peptides, including indolicidin, with bicelles by varying the short-to-long lipid ratio (q-value) of the bicelles at different temperatures [47]. The

peptide's capacity factor seems to increase with higher q-values of the bicelle. The capacity factor (k') indicates the affinity of the peptide toward the lipid bilayer, and its value decreases, for a fixed q-value of the membrane, as the temperature is increased during the assay. In a different study, Hertog et al monitored the binding and permeablization effects of Histatin-5 and Histatin-5 derived peptides on liposome membranes with CE and zeta potential techniques [52]. In Hertog's study, trypsin encapsulated liposomes were incubated with the Hestatin-5 family of peptides to investigate the membrane translocation/perturbation ability of each peptide. The strongest membrane perturbing peptide resulted in the leakage of the trypsin from the liposome aqueous interior that leads to subsequent degradation of the peptide outside of the liposome by trypsin. The extent of peptide degradation by trypsin is monitored by comparing the peptide's peak height before and after incubation with the (trypsin) encapsulated liposome. In this case, CE is used to separate and accurately quantify the free peptide from its other lipid-bound forms and the rest of the sample matrix. One the most popular methods used to separate and quantify the liposome-unbound free peptide from the bound (or vice versa) has long been the centrifugation technique, where the separation is based on differences in density between the heavier lipid aggregates and the rest of the supernatant solution [52;53]. But, since large unilamellar vesicles (LUVs), or liposomes, do not sediment well under centrifugation, heavier multilamellar vesicles (MLVs), or sucrose loaded LUVs are used which have a higher density than the extra-liposomal solution. The heavier (up to 170mM sucrose-loaded) liposomes, together with their bound peptide, pellet during centrifugation, leaving the (liposome)

unbound peptide in the supernate. The concentration of the unbound peptide in the supernate solution is determined after filtration [53]. Another potential problem with this method is that the peptide can aggregate and co-sediment without a significant binding with the liposome. Also, some peptide can be lost due to the strong interaction between the peptide's hydrophobic moieties and the centrifuge tubes' inside surface during the high-speed centrifugation. On the other hand, CE is free of all the problems centrifugation has, and in addition, it can offer better efficiency and sensitivity than the centrifugation method for peptide-lipid interaction studies.

In this study, the interaction between indolicidin, a 13 residue cationic antimicrobial peptide, and liposomes of different composition is monitored using light scattering, fluorescence and CE methods. The lipid composition of the liposomes is varied between zwitterionic to anionic. Cholesterol is also incorporated in the DMPC liposomes to examine its effect on peptide action (on the membrane). The average size (Z_{av}) of the liposome and its polydispersity index (PI) are measured by DLS before and after peptide incubation. The change in both Z_{av} and PI values can give insight into the nature of perturbation caused by the peptide on the liposome membrane and any fusion that has occurred thereafter. Indolicidin's innate fluorescence, from its tryptophan residues, is monitored during interaction with the anionic and zwitterionic liposomes. The peptide's fluorescence intensity increases when it inserts into the hydrophobic membrane while its emission λ_{max} will be blue shifted. After the peptide-liposome incubation, the extent of (peptide's) fluorescence quenching by aqueous acrylamide solution is monitored to check the hydrophobicity and/or the structural integrity of the

membrane microenvironment where the peptide is located. . The indolicidin-induced leakage of calcein from zwitterionic and anionic liposomes is compared using fluorescence measurements. The encapsulated dye is quenched inside an intact liposome, but it dequenches and the fluorescence increases after leakage and dilution in the extra liposomal-solution due to peptide and surfactant action. CZE and LEKC methods are used to compare the peptide's affinity for zwitterionic and anionic liposomes. The interpretation of the free (liposome-unbound) peptide's peak area and retention times data are used to support the observations with DLS and fluorescence experiments.

Materials and methods

Chemicals

1,2-Dimyristoyl-*sn*-Glycero-3-Phosphocholine (DMPC), 1,2-Dimyristoyl-*sn*-Glycero-3-Phosphocholine (DMPG), and cholesterol were from Avanti Polar Lipids. 1M HEPES (pH 7.3 ± 0.1), sodium phosphate monobasic, phosphoric acid (99.99+%), 4-amino benzylamine, and acrylamide crystals (electrophoresis grade) were purchased from Fisher. Deionized water ($18M\Omega cm^{-1}$) was obtained in-house from a reverse osmosis Millipore system. Indolicidin (99.6% purity), and $(Trp)_3$-OH peptides were purchased from American Peptide Co. The hydrophilic marker dye Calcein was obtained from Probes-Invitrogen. Size exclusion gel Sephadex G-50 and MicroSpin filter columns (part # 27-5330-01) were obtained from Amersham Biosciences. The molecular structures of the lipids and

fluorescent dyes used in this study are given in chapter 2, figures 2-1 and 2-2 respectively.

Preparation of dye encapsulating liposomes

All the liposome suspensions were prepared by the extrusion method developed by Hope and coworkers, with a slight modification, using the Lipex® 10mL thermo barrel extruder (Northern Lipids Inc., Vancouver, BC Canada) [54]. The lipids were first dissolved in a 3-5mL of chloroform in 50mL round bottomed flask. A dried thin lipid film was formed around the inside walls of the flask after a 30-45 minutes of rotary evaporation on the Bushi Roto-Vap, under low pressure and >50°C. The dried lipid film was hydrated with 3-5mL of pure buffer, or a buffered-dye solution, with continuous shaking at a temperature above the lipid phase transition temperature, T_c, (for DMPC ≥ 22°C) to form a stable multi lamellar vesicle (MLV) suspension. After vortexing and homogenizing the MLV suspension, it was first extruded about 7 times on a *single* 200nm Nucleopore polycarbonate membrane (Whatman Inc. USA) in the 10mL Lipex extruder at 60°C and a low N_2 pressure (<100psi). Finally, the liposome suspension is extruded at least ten times through a *double* 100nm polycarbonate membrane at a pressure of 250-3500psi. During all the extrusions the temperature has to be maintained at least 10°C above the lipid transition temperature (T_c) of the liposome, so as to maintain a reasonable flow at moderate extrusion pressures. All the final liposome preparations were stored in a refrigerator (4°C) until further analysis.

Separation of un-trapped marker and liposome

For fluorescence experiments, quenched-calcein dye (50mM) encapsulated liposomes were separated from the free un-trapped dye on Sephadex G-50 gel filtration micro-columns (Amersham Biosciences, P/N 275330). The filtration microcolumns can also be prepared and packed in-house according to the following steps: The gel column is prepared first by boiling about 1g of Sephadex G-50 fine powder in 15-20 mL of DI-water for an hour in a covered beaker. One gram of G-50 powder swells to 7-9mL gel volume. The gel was cooled to room temperature and filled into 70% of the micro-columns' total volume. The column is equilibrated with (100μL) blank liposomes before it's used for free-dye/liposome separation. The liposome/dye mixture is gently placed on the gel micro-columns and the encapsulated-liposomes are separated from the un-trapped dye after centrifugation for 2 minutes at 1000rpm. The low molecular weight dye (<5000) is trapped in the gel while the liposomes are excluded and elute first with the void-volume at almost zero dilution. All four liposome compositions had 10 mM DMPC, and additionally: the DMPC/PG liposomes contain 5% DMPG, the DMPC/CH contain 5% cholesterol, and the DMPC/CH/PG contain 5% DMPG and Cholesterol.

Capillary Electrophoresis

The CZE-UV and LEKC-UV experiments were carried out on a laboratory-built CE instrument. A Spellman SL30 high-voltage power supply was used to apply a positive voltage over the length of the fused silica capillary (Polymicro Technologies, Phoenix, AZ, USA), with an inner diameter of

75 μm and an outer diameter of 362 μm. The temperature of the system was maintained at 25 °C using a circulating oil bath. The absorbance was measured at 214 nm using a SSI 500 variable-wavelength UV detector. All data acquisition and data analysis for CE-UV experiments was performed using PC/Chrom^{+} software (H & A Scientific, Greenville, NC). A 20mM Hepes buffer was used as CE background electrolyte at pH 7.3 and an equimolar phosphate buffer used at pH 2.5. Samples were injected hydrodynamically by manually elevating the sample vial ~3cm above the level for 4-6sec. All CE runs are performed under normal voltage polarity, with a positive voltage applied at the injection port while detection was done at the cathode end. The relative peak area is the ratio of the indolicidin and the internal standard peak areas; the internal standard is (0.01%v/v) aminobenzylamine solution. The indolicidin calibration solutions are prepared in 10M Hepes buffer and have 10, 26, 52 and 104μM concentrations.

Liposome size and size-distribution

The hydrodynamic diameter and the poly-dispersity index (PI, size-distribution index) of all liposome preparations were determined by Dynamic Light Scattering (DLS) technique using the Malvern Zeta Sizer model 1000HSa. The Malvern measures the time-dependent fluctuations of light scattered by the liposomes and uses it to calculate the average size and poly-dispersity of the liposomes [55].

Spectrofluorometric analysis

All fluorescence measurements were done on a Shimadzu RF5301 instrument (Kyoto, Japan). Indolicidin's innate tryptophan fluorescence was measured before and after liposome incubation between the range of 340-355nm (emission), after it was excited in the 290-295nm range. The extent of fluorescence quenching of liposome-interacting peptide was done by 0.2mM of acrylamide. Calcein dequenching measurements are done at 490/520nm (excitation/emission). After gel filtration, the calcein encapsulated liposome suspension had to be diluted up to six times by the buffer in order to bring the fluorescence down to a detectable range, where the fluorescence is linearly related to concentration (<30μM).

Results and Discussion

Effect of indolicidin on liposome morphology (a DLS perspective)

Different studies have shown that the action of AMPs cause membrane perturbations and defects such as phase separation or membrane thinning, pore formation, promotion of non-bilayer lipid structure or membrane disruption, aggregation or fusion, depending on the physical and molecular properties of both the lipid and the peptide [9;10;23]. We performed DLS measurements on the liposomes before and after peptide incubation to examine the effect of indolicidin on the size and size distribution of liposomes with various lipid composition liposomes. The three different lipid compositions include: 10mM DMPC, 10mM DMPC with 5%DMPG and 10mM DMPC with 5% cholesterol. The liposomes were incubated for a short duration (<30min), or overnight, at ~20-500 lipid-to-peptide (L/P)

molar ratios after which light scattering measurements were done. Also, a tri-tryptophan hydroxide (TRP_3-OH) neutral peptide was also used to compare its effect on liposome morphology to that of indolicidin's. A higher TRP_3 concentration (L/P=50) was required than that of indolicidin, to cause just a small increase in the average size (Z_{av}) and polydispersity index (PI) on the DMPC and DMPC/CH liposomes, as seen on Table 5-1c. A more pronounced effect on liposome structure is expected, from indolicidin, due to its greater interaction with membranes and the subsequent disruption/deformation of the liposome. As shown in Tables 5-1a & b, indolicidin caused greater changes to the liposome Z_{AV} and PI values at a much smaller peptide concentration than TRP_3, at L/P of 571 and 100. The averaged DLS results on Tables 5-1a and 5-1b indicate that indolicidin seems to change the morphology, size and size distribution of zwitterionic liposomes more than anionic liposomes. Mainly, the mixed DMPC-cholesterol liposomes are showing the largest increase in average size and widening of their size distribution after interaction with the peptide.

The difference between Tables 5-1a and 5-1b is the concentration of indolicidin and its duration of incubation with the liposomes. The average increase in Z_{AV} and PI values is larger in table (a), than (b), since a higher concentration of indolicidin is used. For pure DMPC liposomes, table (a) shows a further increase of Z_{AV} and PI after 24 hours incubation. The detailed results from the individual DLS experiment seen on Tables 5-2, 5-3 and 5-4 show how the liposome sizes, and the size-distribution, change after adding 20μg/ml peptide (L/P=100). The intensity, from the different sizes, in these detail tables is further broken-down based on the relative area

distribution of different liposome populations. Hence, the DMPC-cholesterol (DMPC-5%CH) liposomes (Table 5-3) show major differences both in size and PI values after indolicidin interaction. As seen on the Table 5-3a, most of the signal intensity by the indolicidin-free DMPC/CH liposomes, comes from the 75-129nm size range, and it is decreased substantially when bigger sizes (169-381nm) appear in large proportions after indolicidin incubation as seen on Table 5-3b. That is, larger liposomes were formed (169-381nm) after indolicidin interaction, which account for 25% of total liposome size. This size range (169-381nm) was not registered (or did not exist) by the DMPC-5%CH liposomes, prior to indolicidin addition. The change in size distribution intensity (Table 5-2b) by DMPC liposomes, after an equimolar indolicidin addition, was much lower than the DMPC-5%CH liposomes. That is, only 3.3% of the total DMPC liposomes formed aggregates with sizes in the 381nm range. While the PG mixed DMPC liposomes showed extremely low size variability and no larger aggregates were created after incubation with indolicidin, as seen on Table 5-1a. Also, the detailed DLS run, Table 5-3, shows that >25% the DMPC/CH liposomes aggregated due to the peptide, forming new sizes ranging from 222 to 382nm. Before peptide addition, only 1.5% of the original liposomes had the largest 169.7nm size. These larger size vesicles (222-382nm) are aggregates formed by the action of indolicidin. In comparison, only 3.3% of the DMPC liposomes aggregated to a 381.6nm size after reacting with the same concentration of indolicidin. The anionic DMPC/PG liposomes did not show any significant aggregation or change in size distribution at the same peptide concentration (L/P=100). The peak width, which is the width of the size

distribution (related to PI), showed the smallest change by the DMPC/PG liposomes, after indolicidin addition. Also, a higher indolicidin concentration used in table 5-1b caused a more drastic change on the liposome morphology than when lower concentration was used as seen on table 5-1a. In a similar DLS experiment we did to test the effect of multiple tryptophan residues on liposome size and size distribution, we used a neutrally charged tri-tryptophan hydroxide peptide (TRP_3-OH). At twice the indolicidin concentration (L/P=50), TRP_3 induced a much smaller change on the liposome morphology compared to what indolicidin did, as seen on table 5-1c. For the DMPC/CH liposomes the change in the average size due to TRP_3 was about 6% (87nm to 93nm) and the PI increased by 25% (0.069 to 0.092). In comparison, at half the concentration used for TRP_3 (L/P=100), indolicidin caused a 26% change in liposome average size (88.5nm to 120nm) and a 67% increase in the PI (0.076 to 0.233) on the same DMPC/CH liposomes. The higher membrane perturbation effect of indolicidin, than TRP_3, even at half the concentration, is to be expected since it has six more hydrophobic and three more cationic residues, plus an amide termination.

The zwitterionic membrane perturbation abilities of this comparatively short cationic AMP, indolicidin, can be attributed to the hydrophobic effect operating mainly on the 5 tryptophan and 3 proline residues, as noted by Wimley and White [18]. A similar light scattering study done by others on the aggregation of phosphatidylcholine (PC) vesicles by a similar peptide fragment from the hemagglutinin HA2 protein showed a two to three fold increase in the average diameter of the vesicles after peptide interaction, as

measured by DLS [39]. The fusion and aggregation of zwitterionic liposomes by proline rich [56] and some cationic α-helical peptides has been reported in other studies [38;39]. The honey bee venom, melittin, a cationic 26 amino acid peptide that is highly hemolytic, has also been found to be fusogenic and inducing phosphatidylcholine bicelles into forming very large lipid aggregates at low (P/L) concentrations [40].

The higher degree of aggregation, induced by the (cationic) peptide, that was observed in the zwitterionic liposomes (Table 5-1) than the anionic liposomes might at first look like an experimental anomaly. But actually, the low peptide concentration used may not be enough to overcome the electrostatic repulsion between apposing anionic membranes and cause significant aggregation, or fusion, between adjacent liposomes. As for the interaction of indolicidin with zwitterionic bilayers, the hydrophobic residues that are spread out along the peptide chain at different orientations can simultaneously interact with adjacent liposomes and induce membrane mixing and fusion. So in the presence of indolicidin, cholesterol could play a role in the lipid mixing process which destabilizes (or aggregates) cholesterol containing DMPC liposomes, more than pure DMPC liposomes.

In a recent study on indolicidin, including three other related AMPs, and their interaction with model membranes, it was learned that indolicidin had a significant effect on the morphology of giant PC/cholesterol liposomes [8]. Peptide induced polymorphism has also been observed in a regular DPPC liposomes with NMR and electron microscopy methods [57;58]. In another study, an AFM (Atomic Force Microscopy) scanning experiment showed the coalescence of sphingomeylin/cholesterol suspended liposomes into larger

aggregates after reacting with a 0.5μg/ml indolicidin [59]. Gramicidin-A, another tryptophan rich non-cationic AMP, has also been reported to cause aggregation of phosphatidylcholine (PC) liposomes via a (proposed) transient non-bilayer structure forming mechanism [58;60]. Similarly, the bacterial toxin peptide pneumolysin was found to cause lipid mixing and fusion between cholesterol rich membranes [61]. This is because cholesterol has a small hydroxyl head group and wide cross-sectional area around its fused-ring structure that can be induced to pack into a transient non-bilayer (H_{II}) structure [62;63]. This structure of cholesterol enhances the membrane fusion process once the peptide induced lipid mixing commences between adjacent membranes [64;65]. In another study, the size distribution of a 100nm extruded POPC (1-Palmitoyl-2-Oleoyl-*sn*-Glycero-3-Phosphocholine) liposomes became broader after incubation with a very high concentration (L/P=3.3) of TRP_3 peptide [32]. But, when the POPC liposomes are incubated with a very low concentration of indolicidin (L/P>100), the turbidity measurements showed an immediate and sharp increase. The increase in turbidity implies the formation of larger liposome aggregates [32].

In all the studies mentioned above, including ours, the major driving force behind membrane perturbation is suggested to be the strong hydrophobic effect from the multiple tryptophan groups present in the peptides. The presence of five tryptophan residues enables indolicidin to strongly interact with zwitterionic membranes that may cause a packing disruption near the interface and down the lipid acyl chain [8;32;66]. In some studies, changing the Trp residue into a different amino acid has drastically decreased the

hemolytic activity of indolicidin toward zwitterionic membranes [20;67;68]. Besides strong membrane partitioning, due to its hydrophobicity, the size of the aromatic side chains in tryptophan also plays an important role in disrupting membrane integrity both in anionic and zwitterionic membranes [69]. This is why, as mentioned above, replacing the Trp residues of a hemolytic-peptide by Tyr or another aromatic amino acid reduces the activity of the mutated peptide toward zwitterionic bilayers [66;70]. Therefore, in the absence of a significant electrostatic interaction between indolicidin and the zwitterionic liposomes (DMPC and DMPC/CH), the only cause for liposomes morphological change can be attributed to the Trp hydrophobic effect that creates the membrane fusion and aggregation, via lipid mixing, as observed in our DLS results [30].

Tryptophan insertion and membrane permeability (a fluorescence perspective)

Two distinctly different fluorescence methods were used to monitor the degree of interaction between the peptides, indolicidin and TRP_3, and the liposome membrane. In one, the intensity and the Stokes shift by the emission band of the innate tryptophan fluorescence, around 295/350nm ex/em, was measured in the presence of liposomes with different lipid compositions. While in the other method, the percent fluorescence change of the leaked aqueous dye (calcein), due to membrane perturbation by indolicidin, was measured and compared for the different composition liposomes at 488/520nm (excitation/emission).

Figure 5-1 shows indolicidin's innate fluorescence emission after incubation in a 1mM liposome solution and a 10mM Hepes buffer. The liposomes are incubated with 10μM indolicidin, which gives a lipid-to-peptide (L/P) ratio of 100. As seen in Figure 5-1, the maximum tryptophan fluorescence emission is observed for the peptide in DMPC/PG/CH liposome ([1] I-p-g-h). The next highest emission is also by the peptide in the anionic liposome DMPC/PG solution ([2] I-p-g). The lowest emission is observed when peptide is in the 10mM Hepes buffer. Indolicidin registered lower emission intensity in both zwitterionic liposomes than when it was in the anionic liposomes. Also, the tryptophan emission maximum (λ_{max}) was blue shifted to a lower wavelength (343nm) in the anionic liposomes than from its emission in Hepes buffer (356nm), a 13nm difference. But, when the same liposomes are incubated with uncharged tri-tryptophan (TRP_3) peptide, the order of emission intensity was reversed, with the peptide having the maximum emission in the zwitterionic DMPC and DMPC/CH liposomes. The (L/P) ratio used with the tri-tryptophan peptide was lower than with indolicidin, i.e. a larger TRP_3 concentration was used. The blue shift in emission ($\Delta\lambda_{max}$~6nm) observed for TRP_3in the DMPC was small; 350nm in DMPC to 357nm in Hepes, compared to that of indolicidin's ($\Delta\lambda_{max}$=13nm) in the anionic liposomes. In other words, the $\boldsymbol{\lambda}$-shift in Figure 5-1(indolicidin) is larger (~13nm) than in Figure 5-2 (TRP_3), which is ~7nm. Generally, the cationic indolicidin shows wider blue shift and higher intensity in anionic liposomes while the neutral tri-tryptophan peptide has higher emission intensity and a small blue shift in zwitterionic liposomes.

The fluorescence spectrum of peptides, like indolicidin, is dominated by its Trp fluorescence, which is sensitive to the hydrophobicity of the solvent [33;36;71;72]. Generally, the maximum fluorescence wavelength (λ_{max}) of a tryptophan moiety that is exposed to an aqueous/hydrophilic environment (e.g., lying on the surface of a lipid bilayer) is around 354nm. But the λ_{max} will be blue shifted (Stokes shift), to a shorter wavelength, for tryptophan residues that are buried deeper into the more hydrophobic environments, like the acyl chain region of a membrane. Also, tryptophan's fluorescence quantum yield (emission intensity) increases upon binding with lipid bilayers, compared to when it is in an aqueous solvent [71;72]. The fluorescence spectra on Figure 5-1 show that indolicidin's maximum fluorescence (λ_{max}) was blue shifted more, from the Hepes buffer, when it was incubated with anionic than zwitterionic liposomes. The Trp λ_{max} was 343nm in DMPC/PG/CH liposomes and 347nm in DMPC/CH liposomes. But still, Trp has the longest emission wavelength (356nm) when in the lipid-free Hepes buffer. Similar results are obtained in other published studies with indolicidin having the shortest emission λ_{max} when interacting with anionic micelles and lipid bilayers [22;26]. This means, the Trp resides are buried deeper into the more hydrophobic acyl chain when indolicidin interacts with anionic artificial lipid bilayers and anionic bacterial membranes, than zwitterionic membranes [16]. The main reasons suggested for the enhanced membrane perturbation ability of indolicidin, and other AMPs, against anionic membranes is the initial association and further sequestration of the cationic peptide by the anionic lipid head groups via electrostatic attraction. Once the peptide is sequestered onto the liposome

surface, via electrostatic interaction, it is followed by the rapid insertion of the bulky tryptophan residues, and the other hydrophobic residues between the lipid head groups that eventually cause perturbation on the lipid packing structure of the bilayer [22;35;68;73].

The importance of the peptide's charge for membrane action is covered well in the literature. One such study by Dathe et al. on the AMP magainin discovered that increasing the peptide's net charge from +3 to +5 enhances its antimicrobial activity against bacteria [74]. In our study, the uncharged tri-tryptophan peptide (TRP_3) showed an opposite Trp-fluorescence profile than indolicidin when interacting with anionic and zwitterionic liposomes. As seen on Figure 5-2, the fluorescence intensity for TRP_3 was larger when interacting with zwitterionic liposomes than with anionic liposomes. Also, the maximum fluorescence blue shift for TRP_3 in liposome solutions was shorter (~7nm) than that of indolicidin's (13nm). Although TRP_3 has a high content of tryptophan residues as indolicidin, it was not able to insert deeper even at twice the concentration of indolicidin, and cause a significant blue shift as the Trp residues in indolicidin. This could be due to lack of charged residues that could have electrostatically anchored the tri-peptide to the bilayer surface thereby facilitating the insertion of TRP residues into the bilayer.

Indolicidin's innate fluorescence quenching by a 0.2mM aqueous acrylamide solution was performed to monitor accessibility of tryptophan residues, to the polar quencher. The acrylamide quencher was reacted with the same compositions used above in the emission experiment (L/P=100, 10μM indolicidin & 1mM lipid) and the extent of quenching is compared when the

peptide is in zwitterionic and anionic liposomes (Vis-à-vis in plain buffer). As seen in Figure 5-3, after reacting with 0.2mM acrylamide, indolicidin's fluorescence emission dropped by 33% in plain buffer, by 31% in DMPC/CH, by 15% in DMPC and by 12% in DMPC/PG liposomes. The lowest fluorescence drop for tryptophan was in DMPC/PG anionic liposome solution. The quenching experiment indicates that the anionic liposomes offers better shielding than DMPC or DMPC/CH, for the peptide's tryptophan residues from the polar acrylamide quencher. All tryptophan fluorescence measurements for the peptide-liposome samples have been background subtracted with the blank liposomes. The tryptophan residues (of indolicidin) that are incubated with PG containing liposomes had the lowest acrylamide quenching (12%) than both DMPC (15%) and DMPC/CH (31%), since they were located in the hydrophobic membrane region and were shielded better from the polar acrylamide than the ones incubated with the zwitterionic DMPC and DMPC/CH liposomes. The tryptophans of indolicidin were protected the least from the aqueous quencher when incubated with the cholesterol/DMPC liposomes. The tryptophan fluorescence quenching results in Figure 5-3, by aqueous acrylamide, also support the proposed mechanism where the indolicidin's membrane insertion is strengthened due to the electrostatic sequestration of the peptide by the anionic lipid head groups. Generally, indolicidin in the presence of liposomes, whether zwitterionic or anionic, showed less fluorescence decrement than when in a buffer, since its Trp residues were less accessible to the polar quencher, as is also observed in other published reports [8;22;75].

The next fluorescence experiment involved the use of a dye-encapsulated liposome to monitor the interaction of indolicidin with the lipid membrane. The liposomes had different anionic and zwitterionic lipid compositions, including cholesterol, and a 50mM quenched calcein dye inside. Fluorescence measurement of the leaked calcein dye from the encapsulated liposomes, due to membrane perturbation, was done at a lipid-to-peptide (L/P) concentration of 48. Lower peptide concentration (L/P) ratios did not induce detectable leakage change or reproducible results. Also, we avoided using very high peptide concentrations, (L/P) of below 10, since indolicidin has been found to permeablize both anionic and zwitterionic membranes similarly at elevated peptide concentrations [28]. The maximum fluorescence intensity corresponding to 100% leakage was determined after complete membrane disruption with 0.1% (v/v) Triton X-100. The percent leakage (%F), after each peptide interaction, was calculated as follows:

$$\%\mathrm{F} = \frac{(F - F_0)}{(F_t - F_0)} X100 \qquad \textit{Equation (2)}$$

Where, F_0 and F denote the fluorescence intensity before and after peptide addition, and F_t represents the fluorescence intensity after addition of Triton X-100. The fluorescence results on Figure 5-4 show that the anionic DMPC/PG liposomes leaked the most with %F of 83 , while the zwitterionc liposomes, DMPC and DMPC/CH, had a 63 and 45 (%F) respectively. Note that, the DLS result in Table 5-2b, where DMPC/CH liposomes destabilized

or aggregated the most after indolicidin interaction, seems contradictory to the calcein leakage results on Figure 5-4. However, the reason calcein leakage was minimal for DMPC/CH liposomes, in spite of aggregation/fusion, might be because their fusion/aggregation mechanism involves minimal or no leakage of the liposomes' aqueous content. In addition, cholesterol is also known to make the membrane less permeable to ions and polar substances. So, this attenuation in (peptide) action could also be due to inhibition of peptide's deeper insertion by the cholesterol in the bilayer. Cholesterol is shown to curb the (peptide-induced) lysis in a study by Raghuraman, where a >50% decrease in calcein leakage observed when the 40% cholesterol is incorporated into DOPC liposomes [76]. As also indicated by others [8;22], the high %F of the leaked calcein from the anionic DMPC/PG liposomes is either induced by indolicidin's membrane perturbation effect, or formation of organized indolicidin pores (or both) despite having the lowest change in PI and size variability after indolicidin interaction. Similar leakage-fluorescence results have been observed by others, after anionic liposome interaction with indolicidin at a comparable (L/P) concentrations [14;77].

Affinity of Indolicidin for lipid bilayers (a capillary electrophoresis study)

One way to study indolicidin's affinity toward lipid membranes is via a separation technique that helps determine the amount of free (membrane-unbound) peptide. Separation and detection of free indolicidin from the bound (liposome+indolicdin) was done on a Capillary Zone Electrophoresis instrument, with UV detection (CZE-UV), for each of the four different liposome compositions, at a low pH. At low pH values, the silanol groups of

the capillary wall are protonated (uncharged) and the EOF is extremely low. Similarly, the peptide becomes cationic and migrates toward the cathode (detector). But zwitterionic, and also anionic, liposomes will not elute due to lack of EOF, during low pH CZE. The electropherogram peak area of free (unbound) indolicidin is compared when it is incubated with different liposomes, against a standard calibration where indolicidin is in Hepes buffer. The lowest relative peak area by the free peptide, or absence of a peak, indicates a strong binding with the liposome (whose peak didn't elute at low pH CZE). The relative peak area is the ratio of the indolicidin to the internal standard peak area, and the internal standard (aminobenzylamine) has equal concentration in all liposome and calibration samples. A 10μM indolicidin is incubated with each of the different liposome solutions, zwitterionic and anionic. In addition, the degree of indolicidin's affinity toward lipid membranes was also monitored with both zwitterionic and anionic liposomes used as a pseudostationary phase in a Liposome Electrokinetic Chromatography system (LEKC). A strong binding between the peptide and liposomes will lead to the peptide co-eluting with the liposome peak at the longest retention time of the run (T_{lipo}-liposome retention time). But, for weaker binding between the peptide and liposome, most or all of the peptide will elute in a reasonable time somewhere between the internal standard peak and T_{lipo}. The LEKC run seen in Figure 5-5 is an injection of a 16 μM standard indolicidin solution, into 10mM DMPC/CH LEKC at pH 2.5, which shows the internal standard peak at 2.179 and indolicidin peak at 5.640 minutes. But, there was no indolicidin peak eluting when pure PC liposomes were used as an LEKC pseudo stationary phase. As

expected, there were no indolicidin peaks observed during the LEKC with anionic DMPC/PG liposomes (data not shown here).

From the tables in Figure 5-6 and 5-7, the relative peak area of the free (unbound) indolicidin in the liposome solution is compared with that of the indolicidin calibration solution (Figure 5-8). The relative peak area of the 10μM indolicidin in the calibration buffer solution (from Figure 5-8) is larger than the area of the unbound indolicidin in the liposome solutions (Figure 5-6 & 5-7), since some of the indolicidin is bound in the liposome samples. The relative peak area of the 10 μM standard solution was 1.945 as determined from the calibration curve (Figure 5-8). The relative peak area of the unbound indolicidin peak in the DMPC/CH liposome solution was ~47% of that of the standard calibration solution with the same concentration. While the unbound indolicidin in DMPC liposome solution had ~37% of the area compared to same 10 μM calibration standard solution. This peak area comparison indicates that more indolicidin stays bound to DMPC liposomes than to the mixed DMPC-cholesterol liposomes. So, it can be said that cholesterol could be weakening indolicidin's binding to PC (phosphatidylcholine) membranes. This observation is also supported by the acrylamide quenching results (Figure 5-3), since after liposome-indolicidin interaction, the accessibility of the aqueous acrylamide quencher to the tryptophan residues, was the highest for the cholesterol rich liposomes [78;79]. So most of the indolicidin molecules are not strongly bound to liposome, hence migrate as a free cationic peptide during the CE run. But for the peptide in the DMPC/PG, and DMPC/CH/PG anionic liposomes, a peak from a free indolicidin is absent from the electropherogram (Figure 5-7)

since the entire peptide is bound to the liposomes. Obviously, under the acidic CZE conditions, neither the liposome-peptide conjugate nor the free liposomes (anionic or zwitterionic) are expected to elute due to EOF absence at low pH. As expected, the DMPC/PG electropherogram (Figure 5-7) shows no peak from a free (liposome-unbound) indolicidin, since almost 100% of the peptide stays bound to the anionic DMPC/PG liposome. It is also expected that a multi-cationic peptide like indolicidin will have a strong binding to the anionic liposomes due to strong electrostatic interaction. In addition, the insertion of tryptophan residues into the bilayer interior that observed from Trp fluorescence experiments (Figure 5-1) indicates a significant hydrophobic interaction, which can also complement the electrostatic binding that exists between indolicidin and anionic liposomes.

The interaction of a 16μM indolicidin with a DMPC/CH zwitterionic liposome is shown on the LEKC run in Figure 5-5, which shows the internal standard (amino benzylamine) and the indolicidin peaks at 2.179 and 5.6min, respectively. The background electrolyte is a 20mM phosphate buffer at pH 2.5 and contains 10mM DMPC/CH liposomes as a pseudo-stationary phase. Normally, a solute with a very strong hydrophobic interaction with the liposome pseudo-stationary phase would be expected to have the same elution time as the liposome peak (T_{lipo}). Also, under acidic and normal electrode polarity LEKC conditions the DMPC/CH liposomes, together with a strongly partitioning solute, are not expected to elute due to lack of bulk electro osmotic flow (EOF). However, the indolicidin peak eluting at 5.6min (Figure 5-5) indicates that some of the peptide molecules are not strongly bound to the DMPC/CH liposome, and migrate as free

peptide. This could be because cholesterol prohibits the peptide from a strong hydrophobic interaction and deep insertion into the zwitterionic lipid bilayer, as observed for a similar AMP, melittin [80]. After comparing the CZE-electropherograms of indolicidin when it is with zwitterionic and anionic liposomes, it can be said that the major driving force behind its partitioning ability onto membranes is electrostatic interaction. Together with the DLS and fluorescence findings, both CZE and LEKC results seem to support the argument that the majority of the indolicidin molecules stay in the (zwitterionic) liposome interfacial aqueous region, especially when cholesterol is present, and induce morphological changes to apposing liposome membranes. In addition to separation and analysis of indolicidin in a liposome solution, CZE has been used to monitor the stability of the liposomes after peptide addition. At neutral pH, CZE runs of liposome samples with up to 79μM indolicidin yields a liposome peak, confirming that liposomes stay intact even at such a high peptide concentration (Data not shown here).

Conclusion

Indolicidin is amphiphilic and has been found to perturb both zwitterionic and anionic liposome membranes. It induces a lipid mixing and fusion even in otherwise stable phosphatidylcholine (DMPC) and mixed DMPC-cholesterol liposomes. Detailed examination of the DLS results show variability in size and size distribution (PI) of zwitterionic liposomes after indolicidin interaction. The concentration of indolicidin was ~10μM at lipid-to-peptide ratio of 100 in both zwitterionic and anionic liposomes, but the anionic liposomes did not show any significant change in size or PI after the interaction. Cholesterol seems to enhance the lipid rearrangement and fusion of the DMPC-cholesetrol liposomes in the presence of indolicidin.

Indolicidin's innate Trp fluorescence maximum (λ_{max}) was blue shifted and its emission intensity increased in the presence of liposomes, than when it was in Hepes buffer. The blue shift by the uncharged tri tryptophan peptide (TRP_3) in liposome solutions was smaller than indolicidin's, i.e., 3nm for $TRP_3$and 13nm for indolicidin. Indolicidin's fluorescence intensity increases in the following order when incubated with the liposomes; Hepes buffer < DMPC/CH < DMPC < DMPC/PG < DMPC/PG/CH. Also, indolicidin's Trp fluorescence was better protected from aqueous acrylamide quenching when incubated with anionic than zwitterionic liposomes. The extent of quenching by acryamide increases in the order: DMPC/PG < DMPC < DMPC/CH < buffer.

When calcein encapsulated liposomes were incubated with indolicidin they showed variability in degree of leakage based on their lipid composition.

Anionic liposomes leaked more than zwitterionic liposomes, although the zwitterionic DMPC/CH liposomes underwent significant lipid mixing and fusion after indolicidin interaction, as seen from the DLS results. The dye leakage, and the Trp fluorescence result, seems to indicate that indolicidin inserts deeper into anionic membranes causing more permeablization than in zwitterionic membranes.

It was possible to separate and quantify the free indolicidin (liposome-unbound) from the zwitterionic liposome-indolicidin mixture with a CZE-UV method under low pH. About 47% of the peptide was in free lipid-unbound form when incubated with DMPC-cholesterol liposomes, compared to 37% when incubated with just DMPC liposomes. But, all of the indolicidin was in a liposome-bound form when incubated with anionic liposomes, since there was no peak detected of the free liposome-unbound indolicidin.

For the most part, CE and fluorescence results have demonstrated that the electrostatics is the more dominant factor, than the hydrophobic, during indolicidin interaction with anionic membranes. Indolicidin interacts hydrophobically at the zwitterionic membrane interface inducing lipid mixing and liposome fusion. The fluorescent dye leakage results mainly, together with that of CZE and LEKC, clearly show that cholesterol decreases the effect of indolicidin on the phospholipid bilayers, at least by reducing the penetration of the peptide deep into the membrane.

Table 5-1. DLS results (size & PI) of peptide-liposome samples. Liposome diffracted light was measured at a 90º angle from the incident.

Table 5-1. (a) & (b). Liposome size & PI was measured after 30 min and 24hrs incubation with indolicidin @ (L/P) molar ratio of 571 (a) and 100 (b).

Table 5-1(c). Liposome size & PI after incubation with tri-tryptophan peptide (3-TRP) at peptide (L/P) concentration of 50.

Table 5-1a

	without indolicidin		***with indolicidin (40ug/ml), (L/P~571)***			
			30min incubation		24-hrs incubation	
lipid comp	Zav/nm	PI	Zav/nm	PI	Zav	PI
10mM DMPC	*87.7±0.2*	*0.066*	*102.6±0.0*	*0.177*	*110.6±2.0*	*0.253*
10mM PC+ 5% CH	*86.6±0.7*	*0.069*	*106.5±0.0*	*0.219*	*102.3±2.1*	*0.21*
10mM PC+ 5%PG	*86.8±0.3*	*0.041*	*87.2±0.0*	*0.0415*	*87.5±0.6*	*0.04*
10mM PC+ 5% PG+ 5%CH	*85.6±0.3*	*0.047*	*88.2±0.0*	*0.0616*	*86.9±0.3*	*0.056*

Table 5-1b *(30min incubation)*

	without indolicidin		with indolicidin (L/P=100)	
lipid comp	Zav/nm	PI	Zav/nm	PI
10mM DMPC	*87.7±0.2*	*0.066*	*114.3±1.0*	*0.195*
10mM PC+ 5% CH	*86.6±0.7*	*0.069*	*120.0±4.6*	*0.233*
10mM PC+ 5%PG	*86.8±0.3*	*0.041*	*89.4±2.8*	*0.068*
10mM PC+ 5% PG+ 5%CH	*85.6±0.3*	*0.047*	*89.9±2.2*	*0.051*

Table 5-1c				
	without TRP_3		with TRP_3 (L/P=50)	
Lipid comp	Zav/nm	PI	Zav/nm	PI
10mM DMPC	*87.7±0.2*	*0.066*	*91.9±0.8*	*0.08*
10mM PC+ 5% CH	*86.6±0.7*	*0.069*	*92.8±0.0*	*0.092*
10mM PC+ 5%PG	*86.8±0.3*	*0.041*	*88.3±0.9*	*0.048*
10mM PC+ 5% PG+ 5%CH	*85.6±0.3*	*0.047*	*88.5±1.6*	*0.044*

Table 5-2. DLS results of size distribution of DMPC liposomes before (a) and after (b) interaction with a 10μM indolicidin. The intensity column relates the percentage of liposomes constituting a certain size.

TABLE 5-2(a) DMPC			**TABLE 5-2(b) DMPC-INDO**	
Size(nm)	Intensity		Size(nm)	Intensity
5.1	0		5.1	0
6.6	0		6.6	0
8.7	0		8.7	0
11.4	0		11.4	0
14.9	0		14.9	0
19.5	0		19.5	0
25.6	0		25.6	0
33.5	0		33.5	0
43.9	1.4		43.9	1.2
57.6	10.7		57.6	10.9
75.4	26.2		75.4	26.4
98.8	36.3		98.8	35.3
129.5	25		129.5	23
169.7	0.4		169.7	0
222.3	0		222.3	0
291.3	0		291.3	0
381.6	0		381.6	3.3
500	0		500	0

Peak Analysis by intensity Table 5-2(a)			
Peak	Area	Mean	Width
1	100	95.5	74.5

Peak Analysis by intensity Table 5-2(b)			
Peak	Area	Mean	Width
1	96.7	94.5	73.4
2	3.3	381.6	104.4

Table 5-3. DLS results of size distribution of DMPC/CH liposomes before (a) and after (b) interaction with a 10μM indolicidin.

Table 5-3 (a) DMPC-5%CH			**Table 5-3 (b) DMPC-5%CH-INDO**	
Size(nm)	Intensity		Size(nm)	Intensity
5.1	0		5.1	0
6.6	0		6.6	0
8.7	0		8.7	0
11.4	0		11.4	0
14.9	0		14.9	0
19.5	0		19.5	0
25.6	0		25.6	0
33.5	0		33.5	0.8
43.9	1.7		43.9	2.8
57.6	11		57.6	6.2
75.4	25.8		75.4	10.9
98.8	35.3		98.8	15.8
129.5	24.7		129.5	19.2
169.7	1.5		169.7	19.3
222.3	0		222.3	15.3
291.3	0		291.3	8
381.6	0		381.6	1.7
500	0		500	0

Peak Analysis by intensity Table 5-3(a)			
Peak	Area	Mean	Width
1	100	95.9	76

Peak Analysis by intensity Table 5-3(b)			
Peak	Area	Mean	Width
1	100	150.4	205.1

Table 5-4. DLS results of size distribution of DMPC/PG liposomes before (a) and after (b) interaction with a 10μM indolicidin.

Table 5-4(a) DMPC-5%PG	
Size(nm)	Intensity
5.1	0
6.6	0
8.7	0
11.4	0
14.9	0
19.5	0
25.6	0
33.5	0
43.9	3.7
57.6	13.1
75.4	25.2
98.8	31.7
129.5	22.6
169.7	3.6
222.3	0
291.3	0
381.6	0
500	0

Table 5-4(b) DMPC-5%PG-INDO	
Size(nm)	Intensity
5.1	0
6.6	0
8.7	0
11.4	0
14.9	0
19.5	0
25.6	0
33.5	0
43.9	3.2
57.6	12.4
75.4	24.7
98.8	31.7
129.5	23.3
169.7	4.7
222.3	0
291.3	0
381.6	0
500	0

Peak Analysis by intensity Table 5-4(a)			
Peak	Area	Mean	Width
1	100	95	82.2

Peak Analysis by intensity Table 5-4(b)			
Peak	Area	Mean	Width
1	100	96.7	83

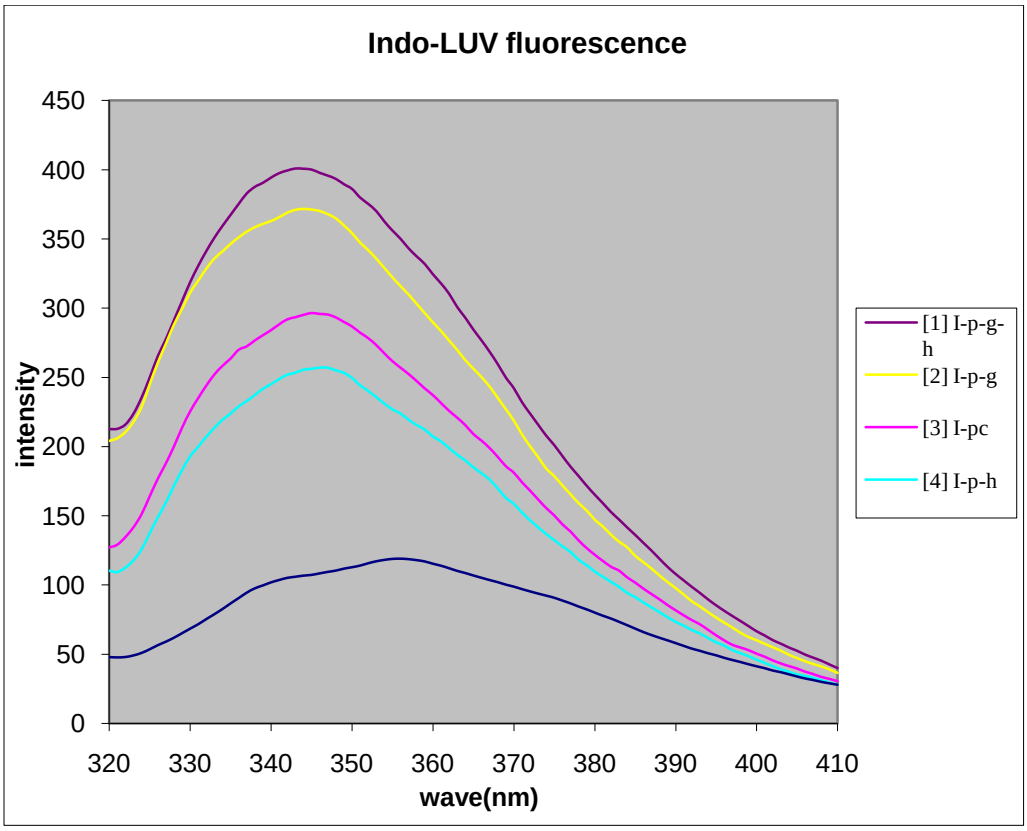

Figure 5-1. Fluoresence emission spectra of 10μM indolicidin incubated in 1mM liposome solution (L/P=100) and in 10mM HEPES buffer. The excitation wavelength was 294nm and emission was monitored at 320-410nm. Spectral lines belong to (top to bottom): [1]-DMPC/PG/CH, [2]-DMPC/PG, [3]-DMPC, [4]-DMPC/CH, [5]-10mM HEPES buffer.

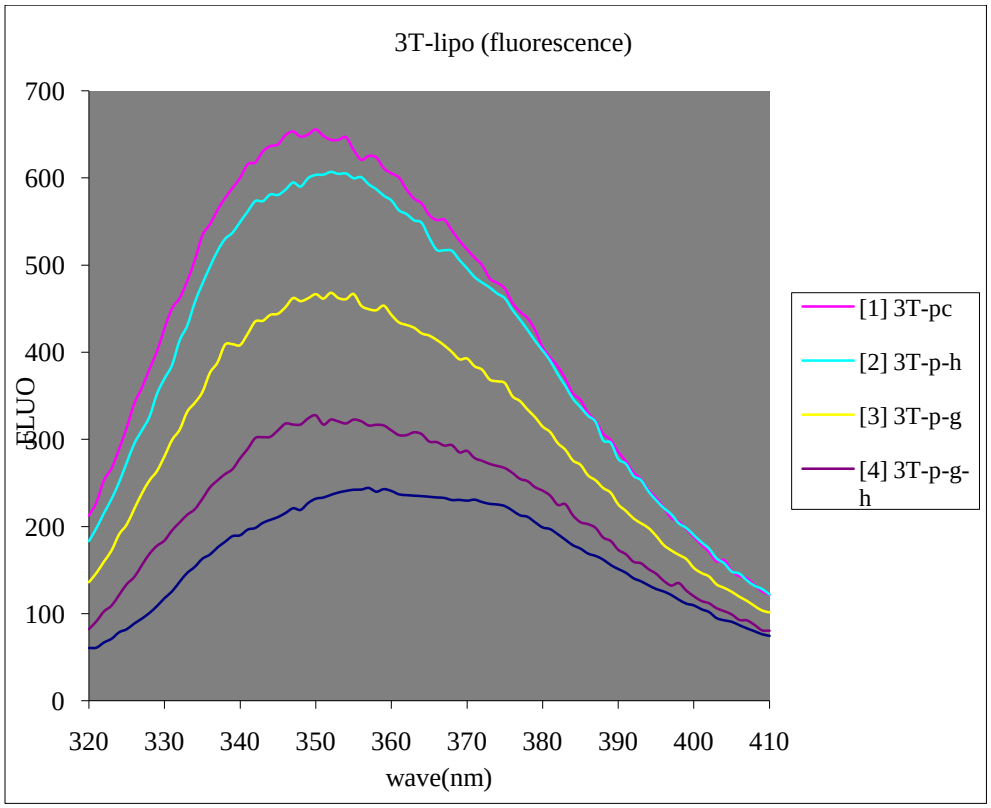

Figure 5-2. Fluoresence emission spectra of 10μM 3-TRP peptide, incubated in 0.5mM liposome solution (L/P=50) and in 10mM HEPES buffer. The excitation wavelength was 297nm and emission was monitored at 320-410nm. Spectral lines belong to (top to bottom): [1]-DMPC, [2]-DMPC/CH, [3]-DMPC/PG, [4]-DMPC/PG/CH, [5]-10mM HEPES buffer.

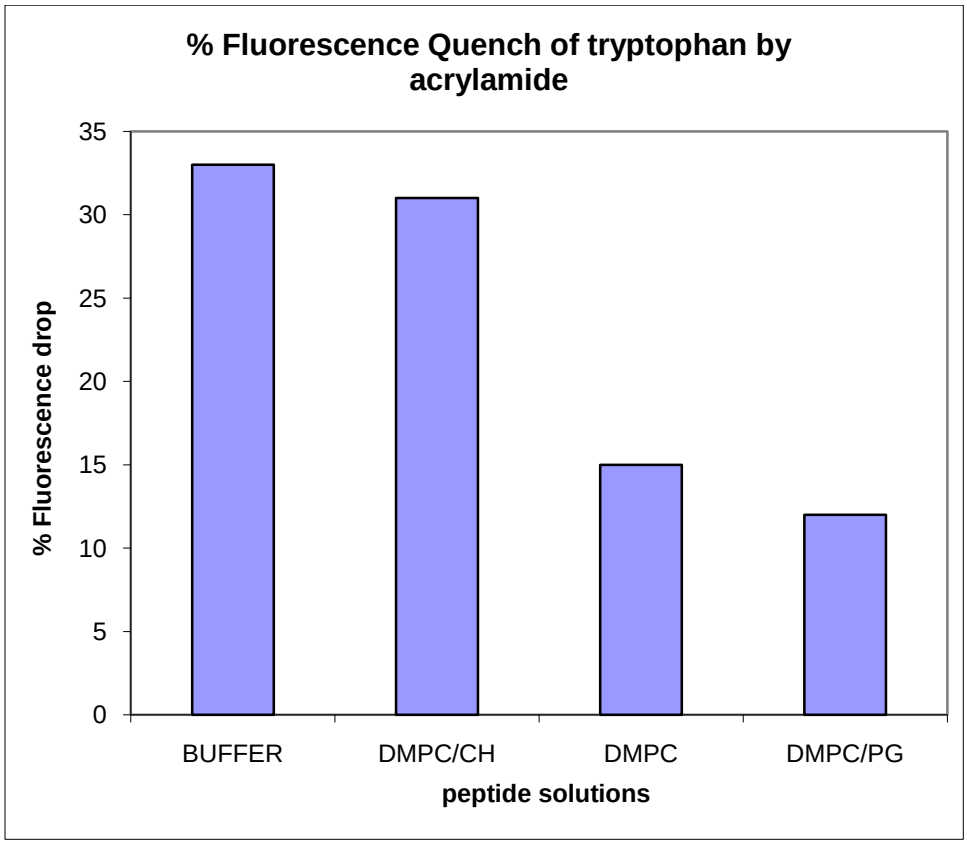

Figure 5-3. Percent innate tryptophan fluorescence (of indolicidin) quenched when acrylamide is added into indolicidin solution with Hepes buffer and different liposome solutions (DMPC/CH, DMPC and DMPC/PG). Percent fluorescence drop (Y-axis) versus tryptophan's environment (lipid or buffer) on X-axis. The %F drop is related to (F_0/F) in Stern-Volmer equation (Equation 1)

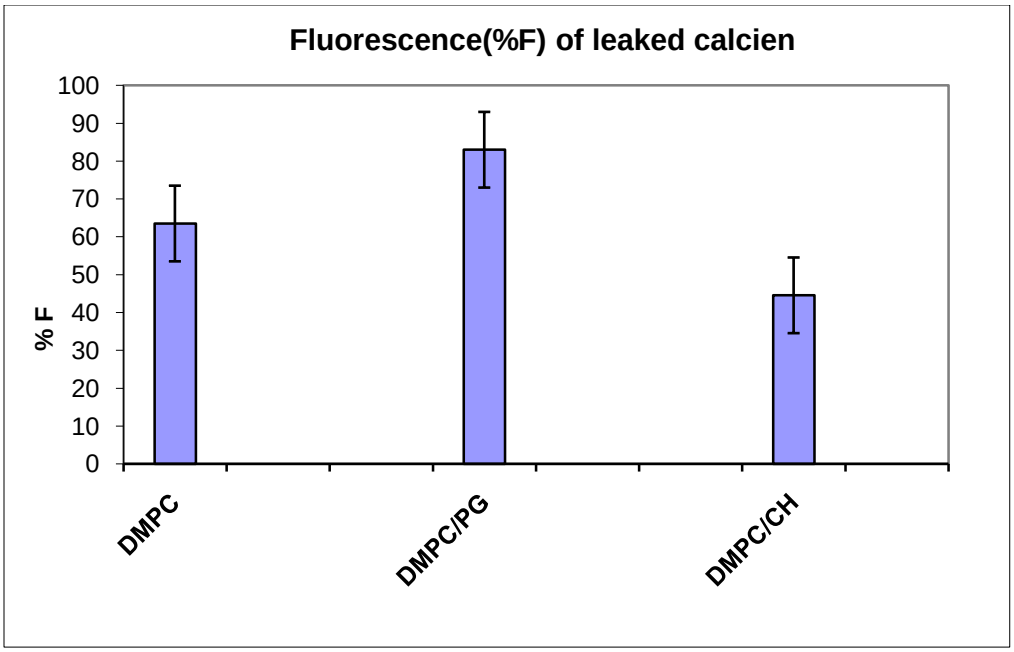

Figure 5-4. Percent Fluorescence (%F) of the leaked calcein dye due to indolicidin perturbation on the liposome membrane. Average %F: DMPC=64%, DMPC/PG=83%, and DMPC/CH=45%.

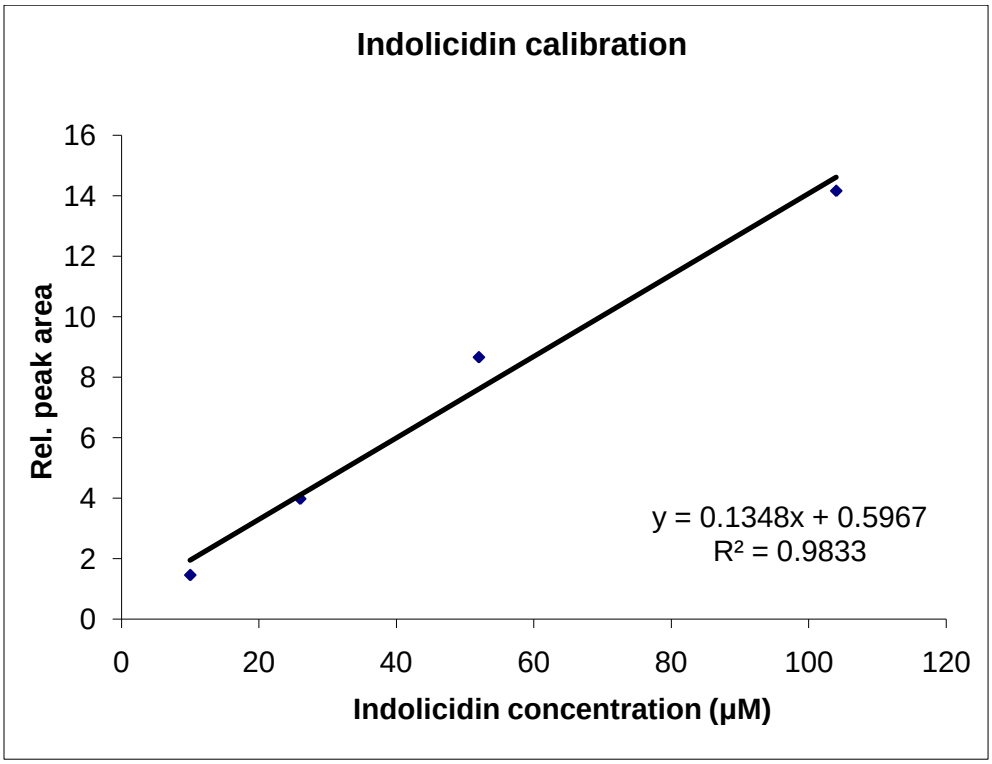

Figure 5-5. Indolicidin calibration curve, peptide is dissolved in 10mM Hepes buffer pH=7.3. Capillary zone electrophoresis was run on 20mM Phosphate buffer at pH 2.5 in 75µm bare fused silica capillary. CZE run at 25kV and UV detection at 214nm. The relative peak area is the ratio of the indolicidin to the internal standard peak area, and the internal standard a 0.001% aminobenzylamine solution.

(A)

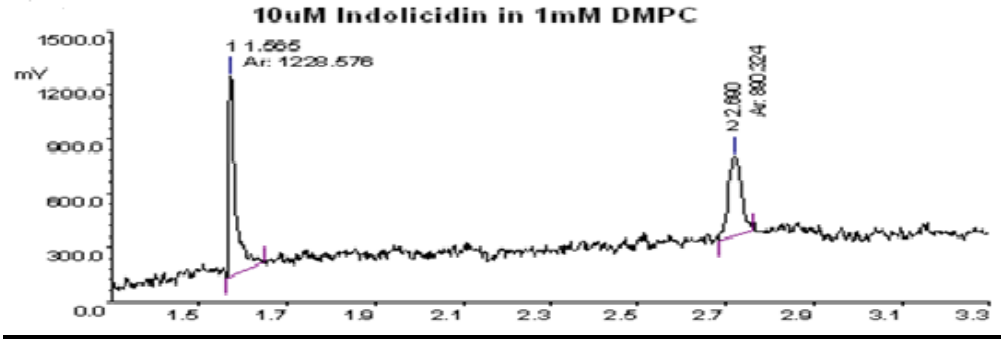

Peak	RT	Area	Rel. peak area (peak2/peak1)
1	1.565	1228.576	**0.725**
2	2.69	890.324	

(B)

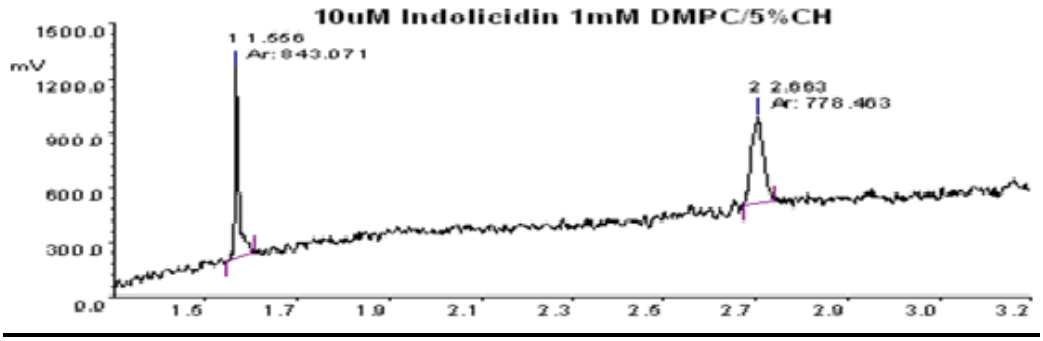

Peak	RT	Area	Rel. peak area (peak2/peak1)
1	1.556	843.071	**0.923**
2	2.663	778.463	

Figure 5-6. CZE of 10µM indolicidin incubated with (A) 1mM DMPC liposomes and (B) 1mM DMPC/5%CH liposomes. Peak 1 is (0.01%v/v) amino benzylamine and peak 2 is indolicidin. CZE is run on 20mM phosphate buffer @ pH2.5 in 75µm bare fused capillary. CZE run at 25kV and UV detection at 214nm

(A)

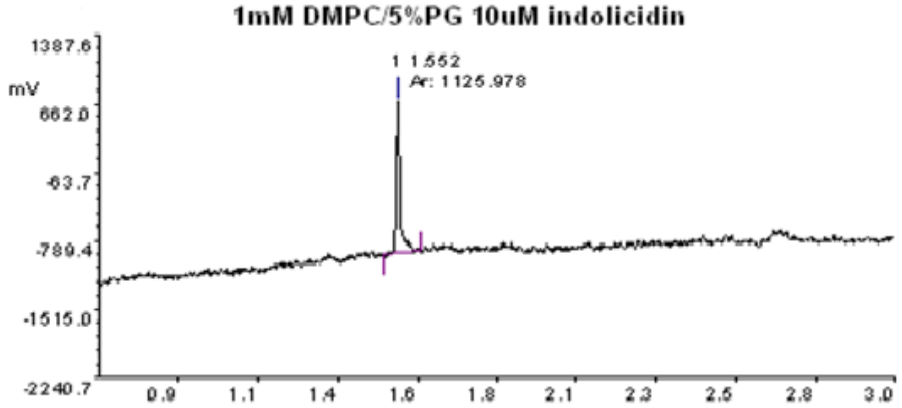

Peak	RT	Area
1	1.552	1125.978

(B)

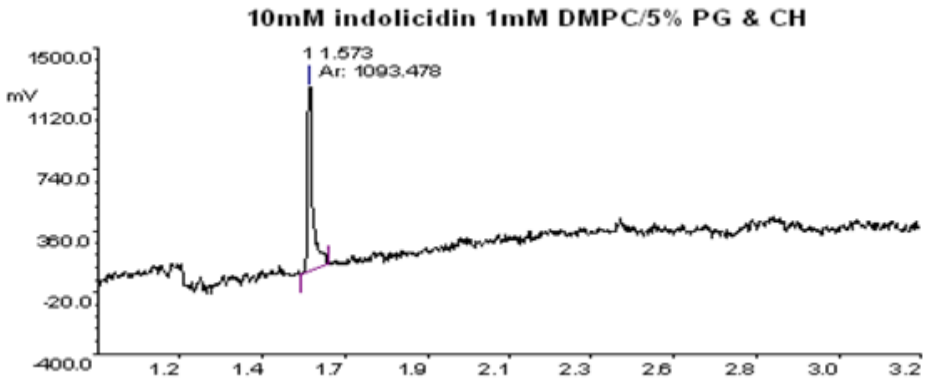

Peak	RT	Area
1	1.573	1093.478

Figure 5-7. CZE of 10μM indolicidin incubated with (A) 1mM DMPC/5% PG liposomes and (B) 1mM DMPC/5%PG & CH liposomes. Peak 1 is (0.01%v/v) amino benzylamine. CZE conditions same as in Figure 5-6.

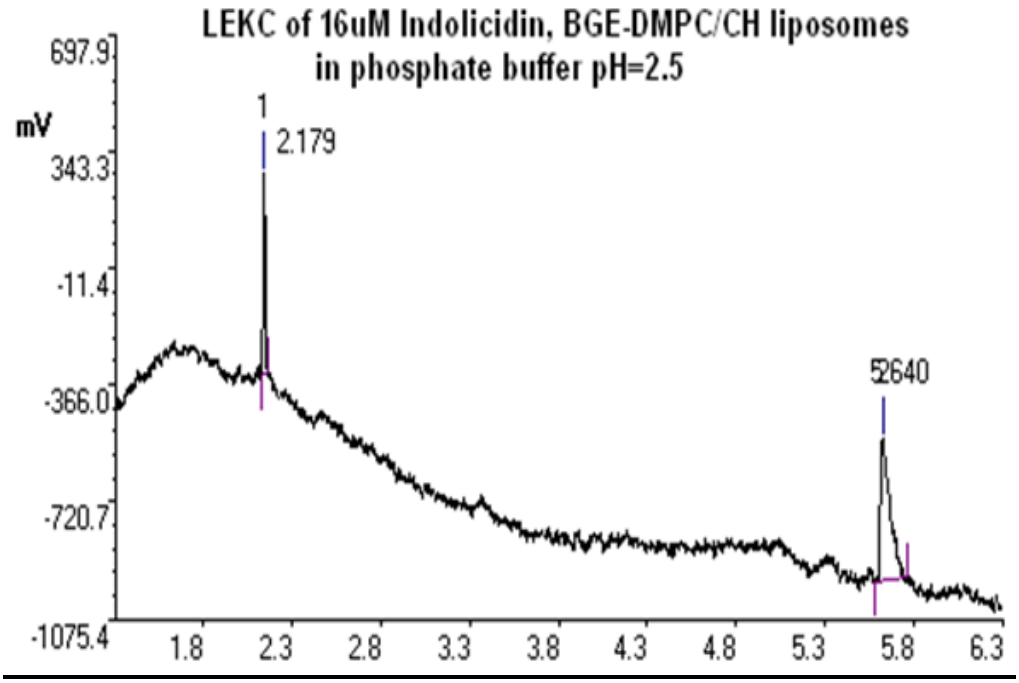

Peak	RT	Area
1	2.179	500.611
2	5.64	1618.116

Figure 5-8. LEKC of 16µM indolicidin, Buffer- 20mM phosphate buffer pH 2.5 with 10mM DMPC/CH (55:45) liposomes. Peak 1 (2.179min) is amino benzylamine internal standard and peak 2 (5.640min) is indolicidin. LEKC was performed in 75µm bare fused silica capillary at 25kV and UV detection at 214nm.

Reference List

[1] Lohner, K. Development of Novel Antimicrobial Agents: Emerging Strategies, Springer-Verlag, New York, 2001.

[2] R.E.Hancock and R.Lehrer, Cationic peptides: a new source of antibiotics, Trends Biotechnol. 16 (1998) 82-88.

[3] R.E.Hancock and D.S.Chapple, Peptide antibiotics, Antimicrob.Agents Chemother. 43 (1999) 1317-1323.

[4] M.Dathe and T.Wieprecht, Structural features of helical antimicrobial peptides: their potential to modulate activity on model membranes and biological cells, Biochim.Biophys.Acta 1462 (1999) 71-87.

[5] M.Zasloff, Antimicrobial peptides of multicellular organisms, Nature 415 (2002) 389-395.

[6] Y.Shai, Mode of action of membrane active antimicrobial peptides, Biopolymers 66 (2002) 236-248.

[7] M.R.Yeaman and N.Y.Yount, Mechanisms of antimicrobial peptide action and resistance, Pharmacol.Rev. 55 (2003) 27-55.

[8] Zhao, H. Mode of Action of Antimicrobial Peptides. 2003. Helsinki, Norway, University of Helsinki, Institute of Biomedicine, Biochemistry, Faculty of Medicine.

[9] K.Farsad and C.P.De, Mechanisms of membrane deformation 1, Curr.Opin.Cell Biol. 15 (2003) 372-381.

[10] R.M.Epand, Do proteins facilitate the formation of cholesterol-rich domains?
1, Biochim.Biophys.Acta 1666 (2004) 227-238.

[11] N.Papo and Y.Shai, Can we predict biological activity of antimicrobial peptides from their interactions with model phospholipid membranes, Peptides 24 (2003) 1693-1703.

[12] R.M.Epand and R.F.Epand, Liposomes as models for antimicrobial peptides, Methods Enzymol. 372 (2003) 124-133.

[13] O.Toke, Antimicrobial peptides: new candidates in the figureht against bacterial infections, Biopolymers 80 (2005) 717-735.

[14] R.M.Epand and H.J.Vogel, Diversity of antimicrobial peptides and their mechanisms of action, Biochim.Biophys.Acta 1462 (1999) 11-28.

[15] L.Tomasinsig and M.Zanetti, The cathelicidins-structure, function and evolution, Curr.Protein Pept.Sci. 6 (2005) 23-34.

[16] M.E.Selsted, M.J.Novotny, W.L.Morris, Y.Q.Tang, W.Smith, and J.S.Cullor, Indolicidin, a novel bactericidal tridecapeptide amide from neutrophils, J Biol.Chem 267 (1992) 4292-4295.

[17] C.L.Friedrich, A.Rozek, A.Patrzykat, and R.E.Hancock, Structure and mechanism of action of an indolicidin peptide derivative with improved activity against gram-positive bacteria, J Biol.Chem 276 (2001) 24015-24022.

[18] W.C.Wimley and S.H.White, Experimentally determined hydrophobicity scale for proteins at membrane interfaces, Nat.Struct.Biol. 3 (1996) 842-848.

[19] C.M.Deber and N.K.Goto, Folding proteins into membranes, Nat.Struct.Biol. 3 (1996) 815-818.

[20] C.Subbalakshmi, V.Krishnakumari, R.Nagaraj, and N.Sitaram, Requirements for antibacterial and hemolytic activities in the bovine neutrophil derived 13-residue peptide indolicidin, FEBS Lett. 395 (1996) 48-52.

[21] T.J.Falla, D.N.Karunaratne, and R.E.Hancock, Mode of action of the antimicrobial peptide indolicidin, J Biol.Chem 271 (1996) 19298-19303.

[22] D.J.Schibli, R.F.Epand, H.J.Vogel, and R.M.Epand, Tryptophan-rich antimicrobial peptides: comparative properties and membrane interactions, Biochem.Cell Biol. 80 (2002) 667-677.

[23] H.Zhao, J.P.Mattila, J.M.Holopainen, and P.K.Kinnunen, Comparison of the membrane association of two antimicrobial peptides, magainin 2 and indolicidin, Biophys.J 81 (2001) 2979-2991.

[24] T.H.Ha, C.H.Kim, J.S.Park, and K.Kim, Interaction of Indolicidin with Model Lipid Bilayer: Quartz Crystal Microbalance and Atomic Force Microscopy Study, Langmuir 16 (2000) 871-875.

[25] C.H.Hsu, C.Chen, M.L.Jou, A.Y.Lee, Y.C.Lin, Y.P.Yu, W.T.Huang, and S.H.Wu, Structural and DNA-binding studies on the bovine antimicrobial peptide, indolicidin: evidence for multiple conformations involved in binding to membranes and DNA, Nucleic Acids Res. 33 (2005) 4053-4064.

[26] A.Rozek, C.L.Friedrich, and R.E.Hancock, Structure of the bovine antimicrobial peptide indolicidin bound to dodecylphosphocholine and sodium dodecyl sulfate micelles, Biochemistry 39 (2000) 15765-15774.

[27] T.J.Falla and R.E.Hancock, Improved activity of a synthetic indolicidin analog, Antimicrob.Agents Chemother. 41 (1997) 771-775.

[28] A.S.Ladokhin, M.E.Selsted, and S.H.White, Bilayer interactions of indolicidin, a small antimicrobial peptide rich in tryptophan, proline, and basic amino acids, Biophys.J 72 (1997) 794-805.

[29] M.Wu, E.Maier, R.Benz, and R.E.Hancock, Mechanism of interaction of different classes of cationic antimicrobial peptides with planar bilayers and with the cytoplasmic membrane of Escherichia coli, Biochemistry 38 (1999) 7235-7242.

[30] M.K.Bahng, N.J.Cho, J.S.Park, and K.Kim, Interaction of Indolicidin with Model Lipid Bilayers: FTIR-ATR Spectroscopic Study, Langmuir 14 (1998) 463-470.

[31] D.G.Lee, H.K.Kim, S.A.Kim, Y.Park, S.C.Park, S.H.Jang, and K.S.Hahm, Fungicidal effect of indolicidin and its interaction with phospholipid membranes, Biochem.Biophys.Res.Commun. 305 (2003) 305-310.

[32] P.Stano, S.Bufali, A.S.Domazou, and P.L.Luisi, Effect of tryptophan oligopeptides on the size distribution of POPC liposomes: a dynamic light scattering and turbidimetric study, J Liposome Res. 15 (2005) 29-47.

[33] J.R.Lakowicz, Solvent and enviromental effects, Principles of Fluorescence Spectroscopy, Springer, Berlin, 2003, pp. 205-235.

[34] C.Kayalar and N.Duzgunes, Membrane action of colicin E1: detection by the release of carboxyfluorescein and calcein from liposomes, Biochim.Biophys.Acta 860 (1986) 51-56.

[35] L.Zhang, A.Rozek, and R.E.Hancock, Interaction of cationic antimicrobial peptides with model membranes, J Biol.Chem 276 (2001) 35714-35722.

[36] N.Duzgunes, L.A.Bagatolli, P.Meers, R.M.Straubinger, Fluorescence methods in liposome research, In: Torchilin, V. P. and Weissig, V. (Eds.), Liposomes: Practical approach, Oxford University Press, London, 2003, pp. 105-147.

[37] S.M.Dalla and G.Menestrina, Liposomes in the study of pore-forming toxins, Methods Enzymol. 372 (2003) 99-124.

[38] A.Kitamura, T.Kiyota, M.Tomohiro, A.Umeda, S.Lee, T.Inoue, and G.Sugihara, Morphological behavior of acidic and neutral liposomes induced by basic amphiphilic alpha-helical peptides with systematically varied hydrophobic-hydrophilic balance, Biophys.J 76 (1999) 1457-1468.

[39] V.D.Trivedi, C.Yu, B.Veeramuthu, S.Francis, and D.K.Chang, Fusion induced aggregation of model vesicles studied by dynamic and static light scattering, Chem Phys Lipids 107 (2000) 99-106.

[40] H.Sasaki, S.Fukuzawa, J.Kikuchi, and K.Tachibana, Cholesterol Doping Induced Enhanced Stability of Bicelles, Langmuir 19 (2003) 9841-9844.

[41] J.K.Towns, Regnier, and F.E., Impact of polycation adsorption on efficiency and electroosmotically driven transport in capillary electrophoresis, Analytical chemistry 64 (1992) 2473-2478.

[42] R.M.McCormick, Capillary zone electrophoretic separation of peptides and proteins using low pH buffers in modified silica capillaries, Anal.Chem 60 (1988) 2322-2328.

[43] N.Matsubara and S.Terabe, Separation of closely related peptides by capillary electrophoresis with a nonionic surfactant, Chromatographia 34 (1992) 493-496.

[44] K.F.Greve, W.Nashabeh, and B.L.Karger, Use of zwitterionic detergents for the separation of closely related peptides by capillary electrophoresis, J Chromatogr.A 680 (1994) 15-24.

[45] Y.Zhang, R.Zhang, S.Hjerten, and P.Lundahl, Liposome capillary electrophoresis for analysis of interactions between lipid bilayers and solutes, Electrophoresis 16 (1995) 1519-1523.

[46] Y.Zhang, S.Aimoto, L.Lu, Q.Yang, and P.Lundahl, Immobilized liposome chromatography for analysis of interactions between lipid bilayers and peptides, Anal.Biochem. 229 (1995) 291-298.

[47] J.O.Mills and L.A.Holland, Membrane-mediated capillary electrophoresis: interaction of cationic peptides with bicelles, Electrophoresis 25 (2004) 1237-1242.

[48] D.Corradini, G.Mancini, and C.Bello, Liposome Capillary Electrophoresis of Peptides and Proteins, Chromatographia 60 (2004) S125-S132.

[49] V.Kasicka, Recent developments in capillary electrophoresis and capillary electrochromatography of peptides, Electrophoresis 27 (2006) 142-175.

[50] B.F.Marques and J.W.Schneider, Sequence-specific binding of DNA to liposomes containing di-alkyl peptide nucleic acid (PNA) amphiphiles, Langmuir 21 (2005) 2488-2494.

[51] M.Gayton-Ely, T.J.Pappas, and L.A.Holland, Probing affinity via capillary electrophoresis: advances in 2003-2004, Anal.Bioanal.Chem 382 (2005) 570-580.

[52] A.L.Den Hertog, H.W.Wong Fong Sang, R.Kraayenhof, J.G.Bolscher, H.W.Van't, E.C.Veerman, and A.V.Nieuw Amerongen, Interactions of histatin 5 and histatin 5-derived peptides with liposome membranes: surface effects, translocation and permeabilization, Biochem.J 379 (2004) 665-672.

[53] C.A.Buser and S.McLaughlin, Ultracentrifugation technique for measuring the binding of peptides and proteins to sucrose-loaded phospholipid vesicles, Methods Mol.Biol. 84 (1998) 267-281.

[54] M.J.Hope, R.Nayer, L.D.Mayer, P.R.Cullis, Reduction of liposome size and preparation of unilamellar vesicles by extrusion techniques, In: Gregoriadis, G. (Ed.), Liposome Technology: liposome preparation and related techniques, CRC Press Inc., Boca Raton, FL, 1993, pp. 123-139.

[55] Malvern instruments. Dynamic Light Scattering: An Introduction in 30 Minutes. http://www.malvern.com/common/downloads/campaign/MRK656-01.pdf . 2009.

[56] K.Bryl, S.Kedzierska, M.Laskowska, and A.Taylor, Membrane fusion by proline-rich Rz1 lipoprotein, the bacteriophage lambda Rz1 gene product, Eur.J Biochem. 267 (2000) 794-799.

[57] R.S.Phadke, S.Srivastava, and G.Govil, Peptide induced polymorphism in model membranes, j biosciences 15 (1990) 153-157.

[58] J.A.Killian and K.B.de, The influence of proteins and peptides on the phase properties of lipids, Chem Phys Lipids 40 (1986) 259-284.

[59] J.E.Shaw, J.R.Alattia, J.E.Verity, G.G.Prive, and C.M.Yip, Mechanisms of antimicrobial peptide action: studies of indolicidin assembly at model membrane interfaces by in situ atomic force microscopy, J Struct.Biol. 154 (2006) 42-58.

[60] H.Tournois and K.B.de, Polymorphic phospholipid phase transitions as tools to understand peptide-lipid interactions, Chem Phys Lipids 57 (1991) 327-340.

[61] B.B.Bonev, R.J.Gilbert, P.W.Andrew, O.Byron, and A.Watts, Structural analysis of the protein/lipid complexes associated with pore formation by the bacterial toxin pneumolysin, J Biol.Chem 276 (2001) 5714-5719.

[62] P.R.Cullis, P.W.van Dijck, K.B.de, and G.J.de, Effects of cholesterol on the properties of equimolar mixtures of synthetic phosphatidylethanolamine and phosphatidylcholine. A 31P NMR and differential scanning calorimetry study, Biochim.Biophys.Acta 513 (1978) 21-30.

[63] S.M.Gruner, P.R.Cullis, M.J.Hope, and C.P.Tilcock, Lipid polymorphism: the molecular basis of nonbilayer phases, Annu.Rev.Biophys.Biophys.Chem 14 (1985) 211-238.

[64] A.L.Bailey, M.A.Monck, and P.R.Cullis, pH-induced destabilization of lipid bilayers by a lipopeptide derived from influenza hemagglutinin, Biochim.Biophys.Acta 1324 (1997) 232-244.

[65] M.Palmer, Cholesterol and the activity of bacterial toxins, FEMS Microbiol.Lett. 238 (2004) 281-289.

[66] M.B.Strom, O.Rekdal, and J.S.Svendsen, Antimicrobial activity of short arginine- and tryptophan-rich peptides, J Pept.Sci. 8 (2002) 431-437.

[67] C.Subbalakshmi, E.Bikshapathy, N.Sitaram, and R.Nagaraj, Antibacterial and hemolytic activities of single tryptophan analogs of indolicidin, Biochem.Biophys.Res.Commun. 274 (2000) 714-716.

[68] P.Staubitz, A.Peschel, W.F.Nieuwenhuizen, M.Otto, F.Gotz, G.Jung, and R.W.Jack, Structure-function relationships in the tryptophan-rich, antimicrobial peptide indolicidin, J Pept.Sci. 7 (2001) 552-564.

[69] J.A.Killian, I.Salemink, M.R.de Planque, G.Lindblom, R.E.Koeppe, and D.V.Greathouse, Induction of nonbilayer structures in diacylphosphatidylcholine model membranes by transmembrane alpha-helical peptides: importance of hydrophobic mismatch and proposed role of tryptophans, Biochemistry 35 (1996) 1037-1045.

[70] M.B.Strom, O.Rekdal, and J.S.Svendsen, The effects of charge and lipophilicity on the antibacterial activity of undecapeptides derived from bovine lactoferricin, J Pept.Sci. 8 (2002) 36-43.

[71] A.Chattopadhyay and H.Raghuraman, Application of fluorescence spectroscopy to membrane protein structure and dynamics, curr sci 87 (2004) 175-180.

[72] A.S.Ladokhin, S.Jayasinghe, and S.H.White, How to measure and analyze tryptophan fluorescence in membranes properly, and why bother?, Anal.Biochem. 285 (2000) 235-245.

[73] D.I.Chan, E.J.Prenner, and H.J.Vogel, Tryptophan- and arginine-rich antimicrobial peptides: structures and mechanisms of action, Biochim.Biophys.Acta 1758 (2006) 1184-1202.

[74] M.Dathe, H.Nikolenko, J.Meyer, M.Beyermann, and M.Bienert, Optimization of the antimicrobial activity of magainin peptides by modification of charge, FEBS Lett. 501 (2001) 146-150.

[75] S.Y.Wei, J.M.Wu, Y.Y.Kuo, H.L.Chen, B.S.Yip, S.R.Tzeng, and J.W.Cheng, Solution structure of a novel tryptophan-rich peptide with bidirectional antimicrobial activity, J Bacteriol. 188 (2006) 328-334.

[76] H.Raghuraman and A.Chattopadhyay, Interaction of melittin with membrane cholesterol: a fluorescence approach, Biophys.J 87 (2004) 2419-2432.

[77] J.R.El, K.Edwards, and M.Lafleur, Characterization of permeability and morphological perturbations induced by nisin on phosphatidylcholine membranes, Biophys.J 77 (1999) 842-852.

[78] C.D.Stubbs and S.J.Slater, Fluorescence techniques for probing water penetration into lipid bilayers, Journal of Fluorescence 5 (1999) 19-28.

[79] R.E.Jacobs and S.H.White, The nature of the hydrophobic binding of small peptides at the bilayer interface: implications for the insertion of transbilayer helices, Biochemistry 28 (1989) 3421-3437.

[80] H.Raghuraman and A.Chattopadhyay, Cholesterol inhibits the lytic activity of melittin in erythrocytes, Chem Phys Lipids 134 (2005) 183-189.

Chapter 6

Future trends

In each of the previous chapters in this thesis we have tried to show different application of marker encapsulated liposomes in the areas of immunoassays, membrane characterization, and peptide-membrane and drug-membrane interaction studies. Their resemblance to real membranes provides liposomes with an enormous potential in a number of applications in the areas mentioned above including encapsulation/delivery of drugs and invitro/in vivo delivery of imaging probes. Based on the liposome applications discussed earlier, here we propose a further study on development of applicable methods in the areas of drug-membrane interaction, specifically in high throughput drug screening, and in homogeneous immunoassay with fluorophore liposomes using sensitive high resolution techniques like CE-LIF, DLS and fluorescence, beside others.

Valid information regarding a drug molecule's passive absorption into membranes is important in determining its ability to transverse cell membranes, which eventually determines its bioavailability. In addition, this information is vital in order to minimize the high attrition rate in early drug development stage, due to poor permeability and pharmacokinetics, which has been recognized as one of the leading causes of failure [1]. From Lipinski Rule of Five it is known that drug like compounds that strongly interact with lipid membrane have a higher permeability and bioavailability; therefore, it is important to constantly look for high throughput methods/models that can help predict the passive absorption of a large

number of potential drug molecules into biological membranes, during the early stages of drug development [2;3]. Permeability studies based on octanol/water partitioning, equilibrium dialysis, column chromatography, and pH-metric titration are all laborious, low throughput, and usually provide poor statistical correlation due to their inadequate mimicry of real biological membranes. Accordingly, dye encapsulated liposomes on multi-well plates can be used to quickly screen the membrane activity of a large number of drug-like compounds by monitoring the fluorescence intensity of the leaked dye, after short drug-liposome incubation. In chapter three of this thesis, we showed the effect of a beta-blocker drug, propranolol, on the permeability of zwitterionic liposomes made from phosphatidylcholine and cholesterol. The extent of liposome's (membrane) perturbation by propranolol was expressed by the fluorescence intensity of the leaked dye. This liposome fluorescence method can be extended and used to determine the membrane activity and permeability of a large number of potential drug compounds that are generated by combinatorial chemistry in pharmaceutical industries during lead generation phase. Two important parameters, the concentration of liposome bound drug and the extent of its membrane perturbation from the fluorescence of the leaked dye, can be determined simultaneously (and rapidly) for a batch of compounds by using a liposome based CE-LIF screening assay. The format of the assay can be either on a conventional capillary or a microchip electrophoresis and both of these formats can be automated to analyze multiple samples from deep well plates in short run times. Because of sensitivity and other desirable qualities, capillary and microchip electrophoresis, with LIF detection, are the best

suited flow based techniques, for liposome-based high throughput screening (HTS) of drug-membrane interactions. Other non-flow based analytical techniques, using solid supported lipid membranes, and fluorescent liposomes, have been proposed and used as a quick membrane mimicking assays to determine the permeability of drug-like compounds in HTS environment using colorimetric and fluorescence detection [4-6]. Artificial membrane based assays can be made from a variety of lipids in order to mimic different types of real membranes that provide insight to diverse biological activities occurring on membrane surfaces. These drug-membrane interaction assays using artificial membranes are more efficient, rugged and reliable than cell based assays, since they don't require sterile culture facility and are not restricted by narrow pH and other physiological requirements. In addition to permeability and related membrane behavior of small drug-like compounds, fluorophore liposomes can be used to study the membrane property of bigger membranophillic molecules like hormones, peptides and proteins [7].

The other successful application of marker encapsulated liposomes has been in signal amplification in the area of immunoassays, since they can accommodate a large number of marker molecules in their internal compartment and receptor molecules on their wide surface area [8;9]. In Chapter 4 of this dissertation we showed how biotin and DNP attached carboxyfluorescein-liposomes were used to successfully analyze avidin and anti-DNP antibodies in a homogenous assay using fluorescence and CE-LIF techniques. This immunoassay application using contact sensitive DOPE liposomes can be further expanded to analyze real world antibody, or

antigen, samples in solution, after immobilizing either of the antigen or antibody molecules on the liposome surface. Most commonly, the PE moiety in DPPE is linked to the antigen, or antibody, which is used to detect and analyze its conjugate analyte in a sample. The linker functional group for most proteins is their amino acids, a thiol group in Fab´ fragments or a hydroxyl group in glycolipids and glycoproteins. For an antibody, a thiol linker is created by first performing a pepsin digestion which yields Fab´ dimers followed by reduction with dithiothreitol (DTT); this step generates thiol-terminated Fab´ monomer fragments. Then, following removal of DTT, the Fab´ fragments are mixed with the liposome vesicles resulting in a stable thioether cross-linkage [10;11]. In our study, the Biotin and DNP moieties were covalently attached to the DOPE lipid head group and used as receptors for the detection of avidin and anti-DNP antibody in solution.

Detection in this liposome immuno-lysis assay (LILA) relies on the self-lysis of the liposomes, after antigen-antibody binding, and the ensuing release of the encapsulated marker, which is then measured and related to the analyte concentration. The sample matrix and the liposome lysis debris might introduce a potential signal interference, or inhibition, effect during conventional (in a test-tube/cuvette) test methods. So to enhance the quality of fluorescence detection, it is necessary to isolate/separate the released marker, from the interference, in liposome lysis assays. From these measurements, reliable qualitative and quantitative relationships can be made about the antigen-antibody complex created on the liposome surface. This is possible if the chemical interferences in the sample matrix are resolved from the marker molecules during analysis and prior to detection.

Accordingly, capillary electrophoresis with laser-induced fluorescence (CE-LIF) is the most fitting hyphenated technique for liposome immune lysis assay since the CE offers the highest resolution, speed, automation capability, and LIF is the most sensitive online detector that easily interfaces with CE. In addition, CE-LIF requires little or no sample preparation, consumes a very small sample (or reagent) and yet it can provide sensitivity and selectivity that is better or comparable to conventional fluorescence techniques like ELISA [12].

In an alternative assay format, intact (non-lysis) marker-encapsulated-antigen-attached liposomes can also be used as labeling agents to detect antibody analytes on CE-LIF with a high sensitivity. The liposomes for this application can be made from a thicker membrane forming lipids, like DSPC (C18), distearoylglycerophosphocholine, and cholesterol, in order to keep the liposome intact with the marker inside during the entire assay process. The lipid composition of the liposome has to be optimized to provide a strong leak resistant membrane and the encapsulated marker needs to be membrane impermeant, with desirable fluorescence qualities. This type of liposome immunoassay is based on the CE separation of the liposome reacted antibody (analyte) from the free unreacted liposome (label) to determine the concentration of the antibody in a sample using LIF detection. The assay can be either competitive or non-competitive. The thousands of marker molecules inside the liposome will increase the sensitivity of the assay by multiple folds than a conventional single fluorescein labeling technique and the high CE resolution allows the simultaneous measurement of an internal standard and other compounds of interest in the assay, or

sample, during the same run. In Recent years, a new class of fluorescent reporters called quantum dots have been successfully encapsulated inside liposomes, as an alternative to organic dyes, for immuno assay applications [13; 14]. Quantum dots are semi conductor nano-particle probes that offer up to 20 times brighter signal, than organic dyes, because of higher quantum yield.

Reference List

[1] L.Di and E.H.Kerns, Profiling drug-like properties in discovery research, Curr.Opin.Chem.Biol. 7 (2003) 402-408.

[2] C.A.Lipinski, Drug-like properties and the causes of poor solubility and poor permeability, J.Pharmacol.Toxicol.Methods 44 (2000) 235-249.

[3] C.A.Lipinski, F.Lombardo, B.W.Dominy, and P.J.Feeney, Experimental and computational approaches to estimate solubility and permeability in drug discovery and development settings, Adv.Drug Deliv.Rev. 46 (2001) 3-26.

[4] A.Loidl-Stahlhofen, A.Eckert, T.Hartmann, and M.Schottner, Solid-supported lipid membranes as a tool for determination of membrane affinity: high-throughput screening of a physicochemical parameter, J.Pharm.Sci. 90 (2001) 599-606.

[5] M.Przybylo, T.Borowik, and M.Langner, Application of liposome based sensors in high-throughput screening systems 2, Comb.Chem.High Throughput.Screen. 10 (2007) 441-450.

[6] S.Pihlasalo, M.Hara, P.Hanninen, J.P.Slotte, J.Peltonen, and H.Harma, Liposome-based homogeneous luminescence resonance energy transfer, Anal.Biochem. 384 (2009) 231-237.

[7] X.Liu, Q.Yang, C.Nakamura, and J.Miyake, Avidin-biotin-immobilized liposome column for chromatographic fluorescence on-line analysis of solute-membrane interactions, J.Chromatogr.B Biomed.Sci.Appl. 750 (2001) 51-60.

[8] H.A.Rongen, A.Bult, and W.P.van Bennekom, Liposomes and immunoassays, J.Immunol.Methods 204 (1997) 105-133.

[9] K.A.Edwards and A.J.Baeumner, Liposomes in analyses, Talanta 68 (2006) 1421-1431.

[10] G.T.Hermanson, Preparation of Liposome Conjugates and Derivatives, Bioconjugate Techniques, Elsevier, Amesterdam, The Netherlands, 2008, pp. 858-960.

[11] L.Nobs, F.Buchegger, R.Gurny, and E.Allemann, Current methods for attaching targeting ligands to liposomes and nanoparticles, J.Pharm.Sci. 93 (2004) 1980-1992.

[12] A.C.Moser and D.S.Hage, Capillary electrophoresis-based immunoassays: principles and quantitative applications, Electrophoresis 29 (2008) 3279-3295.

[13] C.S. Chen, J. Yao, R.A. Durst, Liposome encapsulation of fluorescent nanoparticles: Quantum dots and silica nanoparticles, Journal of Nanoparticle Research 8 (2006) 1033-1038.

[14] G.Y. Shan, D. Li, L.Y. Feng, X.G. Kong, Y.C. Liu, Y.B. Bai, T.J. Li, J.Z. Sun, Encapsulation of CdSe/ZnSe Quantum Dots by Liposome Complexes, Chinese Journal of Chemistry 23 (2005) 1688-1692.